Durham University

Durham E-Theses

Studies on Bis(imido) molybdenum complexes containing unsaturated hydrocarbon ligands

Whittle, Brenda

How to cite:

Whittle, Brenda (1993) *Studies on Bis(imido) molybdenum complexes containing unsaturated hydrocarbon ligands*, Durham theses, Durham University. Available at Durham E-Theses Online: http://etheses.dur.ac.uk/5497/

Use policy

The full-text may be used and/or reproduced, and given to third parties in any format or medium, without prior permission or charge, for personal research or study, educational, or not-for-profit purposes provided that:

- a full bibliographic reference is made to the original source
- a link is made to the metadata record in Durham E-Theses
- the full-text is not changed in any way

The full-text must not be sold in any format or medium without the formal permission of the copyright holders.

Please consult the full Durham E-Theses policy for further details.

Academic Support Office, The Palatine Centre, Durham University, Stockton Road, Durham, DH1 3LE
e-mail: e-theses.admin@durham.ac.uk Tel: +44 0191 334 6107
http://etheses.dur.ac.uk

Studies on Bis(imido) Molybdenum Complexes Containing Unsaturated Hydrocarbon Ligands.

by

Brenda Whittle, B.Sc. (Dunelm).

University of Durham.

A thesis submitted in part fulfilment of the requirements for the degree of Master of Science at the University of Durham.

September 1993.

The copyright of this thesis rests with the author. No quotation from it should be published without his prior written consent and information derived from it should be acknowledged.

15 JUN 1994

Statement of Copyright.

The Copyright of this thesis rests with the author. No quotation from it may be published without her prior written consent and information from it should be acknowledged.

Declaration.

The work described in this thesis was carried out in the Department of Chemistry at the University of Durham between October 1992 and September 1993. All the work is my own, unless stated to the contrary and it has not been submitted previously for a degree at this or any other University.

Acknowledgements.

First thanks must be extended to my supervisor, Dr. Vernon C. Gibson, for his help and advice during my year as a member of his research group. There lies a remarkable ability to encourage and inspire, matched with a valuable sense of perspective.

I am also grateful to Prof. J.A.K. Howard and Roy Copley for the time spent solving my crystal structure. I am equally grateful to the rest of Durham's crystallographers for the time and patience they spent explaining their subject to me.

The NMR service has been invaluable. Mention must be made of Dr. Alan Kenwright's ability to explain the inexplicable, and to produce an amusing acronym for every occasion. Thanks also to Julia Say for acquiring those last minute spectra so promptly.

On a more personal note something special ought to be done for my fellow inhabitants of Lab. 19: Phil, Ed, Matt, Leela, Martyn and Mike. It's been fun and frolics all the way, and never a quiet moment with Leela around. Phil Dyer has been a great help throughout, and thanks especially for the help with proof reading; that also goes for Ed, who spent many valuable Pub hours sitting in the office reading this thesis. My final words of thanks go to Simon, for always being there with a hug, and to Neil, for making life at number 49 so very entertaining.

This thesis is dedicated to my Mum and Dad
- you don't have to read any further than this page...

"Swans sing before they die - 'twere no bad thing should certain persons die before they sing" *Samuel Taylor Coleridge.*

Abstract.

This thesis describes the synthesis and characterisation of molybdenum bis(imido) complexes containing unsaturated hydrocarbon ligands. A principal objective of the work was to examine the effect of various imido substituents on the coordination number of the complex and the orientations adopted by olefin and acetylene ligands.

Chapter One highlights areas of transition metal chemistry relevant to the thesis, with particular emphasis on the psuedo-isolobal analogy between cyclopentadienyl and imido ligands,

A convenient one-pot synthesis of molybdenum bis(imido) complexes of the type $Mo(NR)(NR')Cl_2$.DME (R=R'=1-adamantyl, 2-t-BuC_6H_4; R=2,6-i-$Pr_2C_6H_3$, R'=t-Bu) is described in Chapter Two. Mo(N-1-adamantyl)(O)Cl_2.DME has been synthesised, and its structure determined by single crystal X-ray diffraction.

The preparation of olefin complexes $Mo(NR)(NR')(C_2H_4)(PMe_3)_n$ (R=R'=1-adamantyl, n=1; R=R'=2-t-BuC_6H_4, n=2; R=2,6-i-$Pr_2C_6H_3$, R'=t-Bu, n=1) is outlined in Chapter Three. Structural information derived from NMR data has allowed comparison with metallocene-like olefin adducts.

Chapter Four describes the synthesis of complexes containing σ-bound phenyl ligands ($Mo(NR)(NR')(\sigma\text{-}C_6H_5)(PMe_3)$ (R=R'=1-adamantyl, 2-t-BuC_6H_4; R=2,6-i-$Pr_2C_6H_3$, R'=t-Bu)) as potential precursors to benzyne complexes.

Chapter Five describes the preparation of diphenylacetylene complexes $Mo(NR)(NR')(PhC{\equiv}CPh)(PMe_3)$, structural information derived from NMR data allows comparison with previously known metallocene-like acetylene complexes.

Full experimental details for Chapters Two to Five are given in Chapter Six.

Brenda Whittle, September 1993.

Abbreviations.

L	General 2-electron donor ligand.
X	General 1-electron donor ligand.
E	Oxo or imido ligand.
R	General alkyl group.
Cp	Cyclopentadienyl (C_5H_5).
Cp*	Pentamethylcyclopentadienyl (C_5Me_5).
NR	General imido ligand.
NAr	2,6-diisopropylphenylimido ligand.
THF	Tetrahydrofuran.
DME	Dimethoxyethane.
TMS	Trimethylsilyl group.
Ad	1-adamantyl group.
NAd	1-adamantylimido ligand.
NMR	Nuclear Magnetic Resonance.
NOE	Nuclear Overhauser Effect.
HETCOR	Heteronuclear Correlation.
COSY	Correlation Spectroscopy.
IR	Infrared.
G.C.	Gas Chromatography.
M.O.	Molecular orbital.
HOMO	Highest occupied molecular orbital.
LUMO	Lowest unoccupied molecular orbital.

CONTENTS.

Chapter One		Transition Metal Imido Complexes.	page
	1.1	Introduction.	1
	1.2	Bonding Modes of the Imido Ligand.	1
	1.3	Uses of Imido Complexes.	4
	1.4	The Isolobal Relationship Between Imido and η^5-Cyclopentadienyl Ligands.	6
	1.5	References.	11
Chapter Two		Synthesis of Six Coordinate d^0 Molybdenum Bis(imido) complexes.	
	2.1	Synthesis of Transition Metal Imido Complexes.	14
	2.2	Synthesis of $Mo(N\text{-}2\text{-}t\text{-}BuC_6H_4)_2Cl_2.DME$.	20
	2.3	Synthesis of $Mo(NAd)_2Cl_2.DME$.	21
	2.4	Synthesis of $Mo(NAr)(N\text{-}t\text{-}Bu)Cl_2.DME$.	22
	2.5	Synthesis of $Mo(NAd)(O)Cl_2.DME$.	23
	2.6	Bonding in Octahedral Bis(imido) Complexes.	28
	2.7	References.	33
Chapter Three		Synthesis of d^2 Molybdenum Bis(imido) Olefin Adducts.	
	3.1	Metallocene-like Olefin Adducts.	36
	3.2	Molybdenum Bis(imido) Ethylene Adducts.	41
		3.2.1 Reaction of $Mo(NR)_2Cl_2.DME$ with Grignard Reagents.	
		3.2.2 Synthesis of $Mo(NAd)_2(PMe_3)(C_2H_4)$.	
		3.2.3 Synthesis of $Mo(N\text{-}2\text{-}t\text{-}BuC_6H_4)_2(PMe_3)_2(C_2H_4)$.	

3.2.4 Synthesis of $Mo(NAr)(N\text{-}t\text{-}Bu)(PMe_3)(C_2H_4)$.

3.3 Molybdenum Bis(imido) Propene Complexes. 51

3.4 Magnesium Reduction of $Mo(NR)_2Cl_2.DME$. 52

3.5 Summary. 55

3.6 References. 56

Chapter Four Molybdenum Bis(imido) Di(phenyl) Complexes.

4.1 Introduction. 57

4.2 Synthesis of $Mo(N\text{-}2\text{-}t\text{-}BuC_6H_4)_2(Ph)_2(PMe_3)$. 62

4.3 Synthesis of $Mo(NAr)(N\text{-}t\text{-}Bu)(Ph)_2(PMe_3)$. 64

4.4 Summary. 67

4.5 References. 67

Chapter Five Molybdenum Bis(imido) Acetylene Adducts.

5.1 Metallocene-like Acetylene Complexes. 69

5.2 Synthesis of $Mo(NAd)_2(PMe_3)(PhC{\equiv}CPh)$. 76

5.3 Synthesis of $Mo(NAr)(N\text{-}t\text{-}Bu)(PMe_3)(PhC{\equiv}CPh)$. 78

5.4 Synthesis of $Mo(N\text{-}2\text{-}t\text{-}BuC_6H_4)_2(PMe_3)(PhC{\equiv}CPh)$. 82

5.5 Summary. 84

5.6 References. 85

Chapter Six Experimental.

6.1 General. 86

6.2 Experimental Details To Chapter Two. 87

6.2.1 Preparation of $Mo(NAd)_2Cl_2.DME$.

6.2.2 Preparation of $Mo(N\text{-}2\text{-}t\text{-}BuC_6H_4)_2Cl_2.DME$.

6.2.3 Preparation of $Mo(NAr)(N\text{-}t\text{-}Bu)Cl_2.DME$.

6.2.4 Preparation and Structural Determination of $Mo(NAd)(O)Cl_2.DME$.

6.3 Experimental Details To Chapter Three. 92

6.3.1 Preparation of $Mo(NAd)_2(PMe_3)(C_2H_4)$.

6.3.2 Preparation of $Mo(N\text{-}2\text{-}tBuC_6H_4)_2(PMe_3)_2(C_2H_4)$.

6.3.3 Preparation of $Mo(NAr)(N\text{-}t\text{-}Bu)(PMe_3)(C_2H_4)$.

6.3.4 Magnesium Reductions.

6.4 Experimental Details To Chapter Four. 98

6.4.1 Preparation of $Mo(N\text{-}2\text{-}t\text{-}BuC_6H_4)_2(Ph)_2(PMe_3)$.

6.4.2 Preparation of $Mo(NAr)(N\text{-}t\text{-}Bu)(Ph)_2(PMe_3)$.

6.5 Experimental Details To Chapter Five. 101

6.5.1 Preparation of $Mo(NAd)_2(PMe_3)(PhC{\equiv}CPh)$.

6.5.2 Preparation of $Mo(NAr)(N\text{-}t\text{-}Bu)(PMe_3)(PhC{\equiv}CPh)$.

6.5.3 Preparation of $Mo(N\text{-}2\text{-}t\text{-}BuC_6H_4)_2(PMe_3)(PhC{\equiv}CPh)$.

6.6 References. 106

Appendices.

Appendix 1: Crystal Data and Parameters for $Mo(NAd)(O)Cl_2.DME$.

Appendix 2: Induction Course, October 1992.

Lecture Courses Attended in the Department of Chemistry.

Research Colloquia and Lectures Organised in the Department of Chemistry During 1992-1993.

CHAPTER ONE.

Transition Metal Imido Complexes.

1.1 Introduction.

This thesis is concerned with some chemistry of complexes in which two imido (NR) ligands are multiply bound to a molybdenum metal centre.

Transition metal-imido species play a key role in a range of chemical processes, acting as homogeneous and heterogeneous catalysts for a variety of industrially significant reactions such as ammoxidation, olefin metathesis and ring opening metathesis polymerisations (ROMP). Recently, interest has arisen in the pseudo-isolobal relationship between the η-cyclopentadienyl (Cp) and imido (NR) ligands; this has stimulated a comparison of reactivities of Group 4 bent metallocene complexes, Group 5 half-sandwich imido complexes and Group 6 bis(imido) complexes. In this chapter, the nature of the imido ligand will be discussed along with their applications and in particular, the basis of the metallocene analogy.

1.2 Bonding Modes of Imido Ligands.

Metal complexes have been characterised that contain imido ligands bonding to the metal in a variety of forms, acting as a terminal or bridging ligand[1]. The five established bonding modes are outlined in Fig. 1.1. The discussion here will be limited to the terminal linear and terminal bent arrangements (a) and (b) relevant to the complexes described in this thesis.

UNIV DUNELM

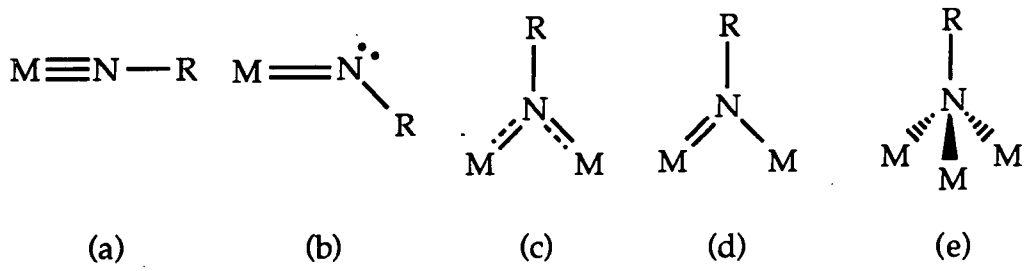

Figure 1.1

The imido ligand may be viewed[2] as a closed shell dianion (NR^{2-}), isoelectronic with O^{2-}. Examination of the frontier orbitals for the NR^{2-} fragment shows them to consist of one filled σ-symmetry and two filled π-symmetry (essentially p-type) orbitals; these may interact with metal orbitals of appropriate symmetry, forming a metal-ligand triple bond (Fig. 1.2). Productive π-bonding requires empty metal d-orbitals; thus these ligands are able to stabilise highly oxidised transition metals[3]. Indeed, imido ligands are most usually found in complexes with electropositive and low d-electron count early transition metals. In a neutral formalism, each π-symmetry orbital is considered to accommodate one electron, the imido ligand is able to donate four electrons to the metal[2], behaving as an "LX_2" ligand and forming a metal ligand triple bond.

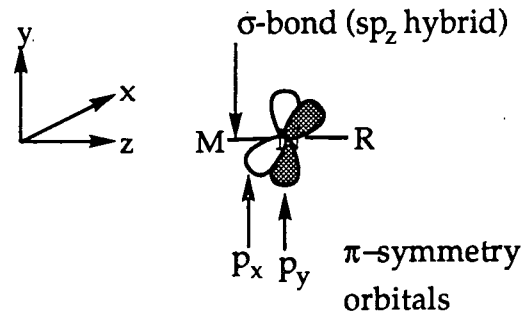

Figure 1.2

The most commonly observed terminal imido ligands occur in a nearly linear geometry (Fig. 1.1(a)). The linear M-N-R unit implies sp hybridisation at nitrogen and all four electrons are donated to the metal

forming a M-N triple bond[1]. Substantial bending of the M-N-R unit (Fig. 1.1(b)) with the M-N-R angle <140°, is associated with the localisation of a lone pair of electrons on nitrogen, and thus donation of only two electrons to the metal forming a M-N double bond[2]. This latter arrangement is expected when donation of all four electrons would result in the electron count for the complex exceeding 18 electrons[1,2]. In orbital terms this would occur when there is no π-symmetry metal orbital available to interact with the second imido π-orbital, either because the d orbitals are filled or through competition with other π-bonding ligands.

To date there is only one example of a structurally characterised complex containing a bent imido ligand (Fig. 1.3), this is the bis(imido) diethyldithiocarbamate species[4] $Mo(NPh)_2(S_2CNEt_2)_2$. It is described as having one bent imido unit bound to the metal by a double bond and linear imido unit bound to the metal by a triple bond.

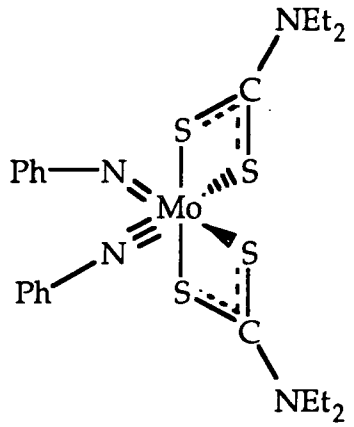

Figure 1.3

More recently, doubt has arisen regarding the validity of using the M-N-C bond angle of the imido group as an indicator of M-N bond order. The formally 20 electron complex $Os(NAr)_3$ and the related $Os(NAr)_2(PMe_2Ph)_2$ have been shown to contain exclusively linear

imido ligands[5]. It has been proposed that one π-symmetry electron pair remains in a ligand based non-bonding molecular orbital, since no symmetry matched orbital exists on the metal. The 20 electron complexes $Cp_2Zr(N\text{-}t\text{-}Bu)(THF)$[6] and $Cp^*_2Ta(NPh)(H)$[7] lend further support to the belief that the linearity of the imido group does not necessarily indicate a metal-nitrogen triple bond with the imido ligand donating four electrons to the metal.

In complexes containing more than one imido ligand, competition for π-bonding orbitals will occur as there are insufficient metal d-orbitals of π-symmetry available for each ligand to form triple bonds to the metal[2]. Instead of one ligand adjusting by bending and donating fewer electrons to the metal, the π-bonding is delocalised and intermediate bond orders exist for both multiply bound units. Thus, the metal-nitrogen distances are, on average, longer in bis and tris(imido) complexes than in mono-imido complexes. Such competitive π-bonding is discussed in section 2.6, where the bonding in octahedral complexes of the general formula $Mo(NR)_2Cl_2.DME$ is rationalised. Complexes containing multiple imido ligands are less common than those containing multiple terminal oxo ligands, the oxo ligand being more able to tolerate the increase in electron density on the ligand associated with a lower metal-ligand bond order, as the oxo ligand is a less strong π donor[2].

1.3 Uses of Imido Complexes.

Imido complexes have been proposed as key surface intermediates in the heterogeneous ammoxidation of propylene[8]. A molybdenum allyl(imido) complex has been produced[9] as a model for one of the key steps. Tungsten (VI) (allyl)imido complexes have been synthesised under mild conditions as homogeneous models for the process (Fig. 1.4).

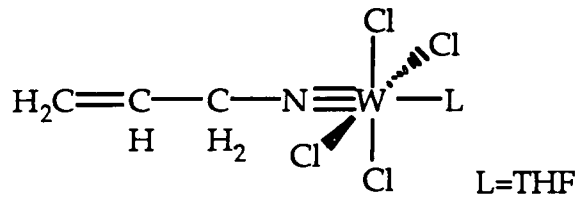

Figure 1.4

The C-N bond forming step from the proposed mechanism has also been modelled with a homogeneous chromium bis(imido) complex[10].

Sharpless demonstrated the use of the osmium imido complex $Os(N\text{-}t\text{-}Bu)(O)_3$ to effect the cis vicinal oxyamination of olefins[11] (Eqn. 1.1). Diamination[12] results from reaction of bis-, tris- and tetraimido complexes with olefins.

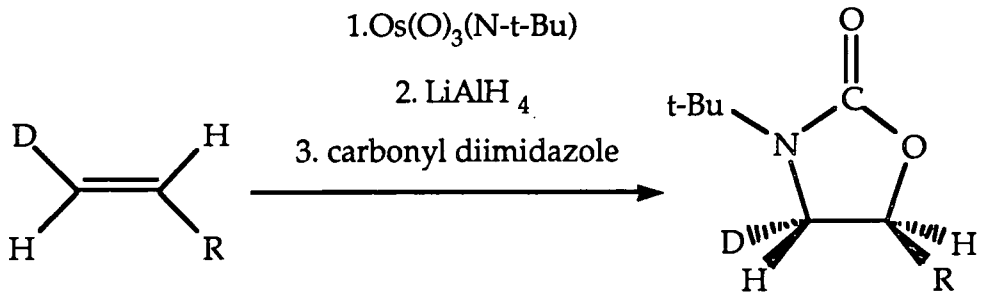

Equation 1.1

Well characterised imido complexes of the type $M(NAr)(CHR)(OR')_2$ (M=W, Mo) have received considerable interest recently[13] resulting from their activity as living ring opening metathesis polymerisation (ROMP) catalysts for mono- and polycyclic olefins (Eqn. 1.2).

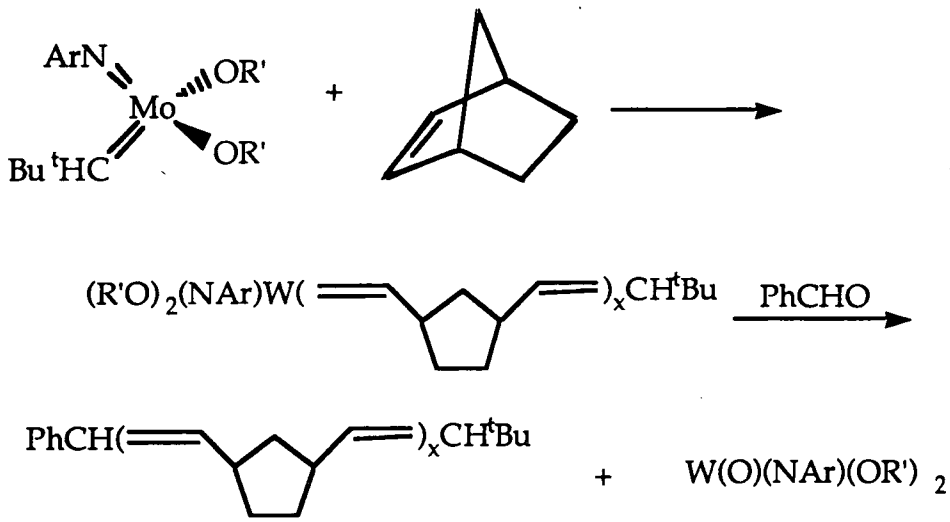

Equation 1.2

The four coordinate complexes based on molybdenum have proved particularly successful with regard to the ROMP of funtionalised monomers. Feast, Gibson and Schrock have investigated the rôle of the ancillary ligands and the synthesis of highly tactic, stereoregular polymers has recently been reported[14].

1.4 The Isolobal Relationship Between Group 4 Bent Metallocene and Group 6 Bis(imido) Complexes.

From simple molecular orbital considerations of the π-molecular orbitals of the cyclopentadienyl ligand[15] it can be shown that, like the imido ligand, it has one σ- and two π-symmetry orbitals available for possible interaction with the metal orbitals. It must be noted, however, that a Cp ligand also possesses two empty orbitals of δ-symmetry which are available for bonding with any suitable filled metal orbitals, although such δ-symmetry interactions are expected to be substantially weaker than π-interactions.

Investigations on the bonding of bent metallocenes of the general formula Cp_2ML_n (n=1-3) using extended Hückel MO methods[16] show that on bending back the cyclopentadienyl rings, three new highly directional orbitals are obtained oriented in the plane perpendicular to the $Cp_{(centroid)}$-metal-$Cp_{(centroid)}$ plane (Fig. 1.5). It is these three orbitals which are used to bind additional ligands in this plane. Many examples of bent metallocene complexes of the Group 4 metals that adopt this geometry are documented.

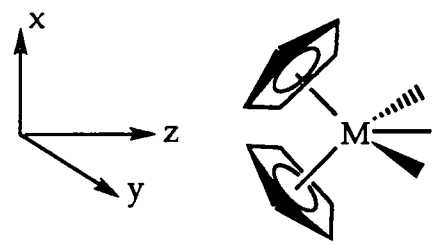

Figure 1.5

The similarities between the MOs of the cyclopentadienyl ligand and imido ligand led to the application of Fenske-Hall calculations[17] to both cyclopentadienyl and imido containing fragments, and demonstrated that there are close similarities between their frontier orbitals.

Since the imido ligand formally contributes one fewer electron than the Cp ligand it was further suggested[18] that the half-sandwich imido complexes of the Group 5 metals may be regarded as pseudo-isolobal and valence isoelectronic with complexes of the Group 4 bent metallocenes. This relationship may be extended to cover the Group 6 metal complexes containing the bis(imido) fragment (Fig 1.6).

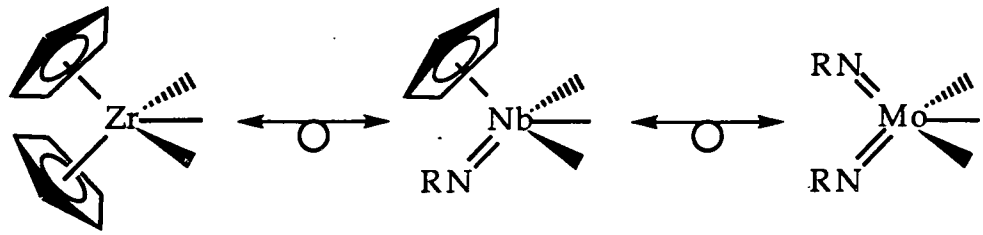

Figure 1.6

A range of d^2 molybdenum bis(imido) complexes[19] of the type $Mo(NR)_2LL'$ have been produced containing a variety of phosphine, olefin and acetylene ligands, many of which are structurally analogous to pseudo-tetrahedral d^2 bent metallocene complexes containing the "Cp_2M" fragment. By regarding the "$Mo(NR)_2$" fragment as isoelectronic and isolobal with the "Cp_2M" fragment the orientation of the additional ligands may be rationalised.

This structural analogy has also been pointed out by Schrock[20] for some tungsten (IV) bis(imido) complexes. In $W(NAr)_2(PMe_2Ph)_2(\eta^2\text{-}OCMe_2)$ the W, P, O, and C atoms lie close to a plane perpendicular to the N-W-N angle[21].

SCF-Xα-SW analysis[21] of the "$M(NH)_2$" fragment shows the frontier orbitals to bear a close resemblance to those of the "Cp_2M" fragment described by Lauher and Hoffmann (Fig. 1.5 above). Fenske-Hall studies show similar results.

Further Fenske-Hall studies[22] on the hypothetical complex $Mo(NH)_2(PH_3)(C_2H_4)$ show that by adopting a geometry (Fig. 1.7) in which the ethylene, phosphine and metal lie in a plane perpendicular to the N-Mo-N plane optimisation of stabilising interactions between the metal and the ethylene π^* orbital results. It is further suggested that interaction between the phosphine and the ethylene π^* orbitals may

further stabilise this geometry. A recent structural determination of the complex $Mo(N\text{-}t\text{-}Bu)_2(PMe_3)(C_3H_6)$ has provided further support for this analogy.

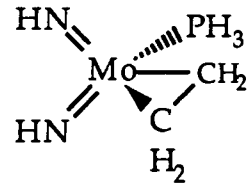

Figure 1.7

It is interesting that an alternative five coordinate geometry ($M(NR)_2L_3$) is possible in the Group 6 bis(imido) system, giving 20 electron complexes; this has no parallel in Group 4 bent metallocenes or Group 5 half-sandwich imido complexes. Since a cyclopentadienyl ligand binds to the metal with five atoms and an imido with one, it is likely that the bis(imido) unit affords less steric protection at the metal centre, allowing a third ligand to bind to the metal in the plane perpendicular to the N-M-N plane. Fenske-Hall calculations[22] have shown that the energy and composition of the molecular orbitals of the "$Mo(NH)_2$" fragment vary little as the N-Mo-N angle varies in the range 120-150°. This is likely to be a source of increased flexibility in the system, allowing the N-M-N angle to be reduced creating extra space to facilitate the coordination of a third ligand in the plane perpendicular to the N-M-N plane.

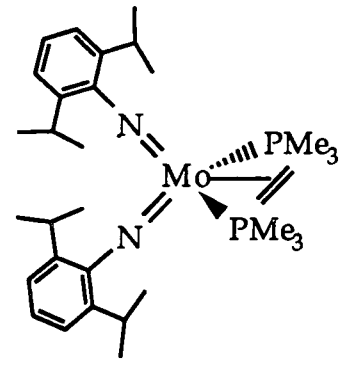

Figure 1.8

Schrock recently reported the synthesis[20, 21] of $W(NAr)_2(PMe_2Ph)_2L$ ($L=\eta^2-C_2H_4$, $\eta^2-C_2H_2$), and $Mo(NAr)_2(PMe_3)_2(C_2H_4)$ has been synthesised and its structure (Fig. 1.8) determined by X-ray methods within this group[19]; the ethylene, two phosphines and molybdenum lie in a plane perpendicular to the N-Mo-N plane. This orientation of the olefin ligand has been rationalised using Fenske-Hall MO calculations[22]. By binding in the plane, two stabilising metal-ethylene π^* orbital interactions are optimised; these result in a stabilising transfer of electron density from the metal to the ligand in this 20 electron system. Were the ethylene rotated out of the plane through 90° to bind in a less crowded orientation, these interactions would not be possible.

Thus, many complexes containing the "$M(NR)_2$" (M=Mo, W) fragment are frequently structurally analogous to "MCp_2" (M=Ti, Zr, Hf) complexes. However an alternative, non-metallocene like behaviour is possible in bis(imido) complexes due to the increased flexibility of the imido group, an effect related to the alkyl or aryl substituent. A principle objective of this thesis was to examine the effect of various imido substituents on the coordination number of the complex and the orientations adopted by olefin and acetylene ligands.

In Chapter Two a range of synthetic routes to transition metal-imido complexes will be outlined. A convenient large scale, one-pot entry into molybdenum bis(imido) complexes has been exploited. This type of complex has been used to synthesise the bis(imido) complexes described in the remainder of the thesis.

Chapter Three discusses a range of Group 4 bent metallocene olefin adducts. A variety of molybdenum bis(imido) olefin adducts have been synthesised, their structure and reactivity compared to that of well documented Group 4 bent metallocene and to the more recent examples of Group 5 half-sandwich imido olefin adducts.

Group 4 bent metallocene and Group 5 half-sandwich imido complexes that contain simple σ- bound aryl ligands are described in Chapter Four. Two bis(imido) molybdenum complexes containing σ-bound phenyl ligands have been synthesised, and are compared with previously known analogues.

In Chapter Five, complexes of Group 4 bent metallocene and Group 5 half-sandwich imido fragments containing acetylene ligands have been outlined. A series of molybdenum bis(imido) diphenylacetylene complexes have been synthesised which appear to exhibit metallocene-like geometries.

1.5 References.

1. W.A. Nugent, B.L. Haymore, *Coord. Chem. Rev.*, 1980, 31, 123.

2. W.A. Nugent, J.M. Mayer, "Metal Ligand Multiple Bonds.", Wiley, New York, 1988.

3. J.M. Mayer, *Comments Inorg. Chem.*, 1988, 8, 125.

4 B.L. Haymore, E.A. Maatta, R.A.D. Wentwoth, *J. Am. Chem. Soc.*, 1979, 101, 2063.

5. J.T. Anhaus, T.P. Kee, M.H. Schofield, R.R. Schrock, *J. Am. Chem. Soc.*, 1990, 112, 1642.

6. P.J. Walsh, F.J. Hollander, R.G. Bergman, *J. Am. Chem. Soc.*, 1988, 110, 8729.

7. G. Parkin, A. van Asselt, D.J. Leahy, L. Whinney, N.G. Hua, R.W. Quan, L. M. Henling, W.P. Schaefer, B.D. Santarierso, J.E. Bercaw, *Inorg. Chem.*, 1992, 31, 82.

8. J.D. Burrington, R.K. Grasselli, *J. Catal.*, 1979, 59, 79.

9. E.A. Maatta, Y. Du, *J. Am. Chem. Soc.*, 1988, 110, 8249.

10. D.M.-T Chan, W.A. Nugent, *Inorg. Chem.*, 1985, 24, 1422.

11. D.W. Patrick, L.K. Truesdale, B.A. Biller, K.B. Sharpless, *J. Org. Chem.*,1978, 43, 2628.

12. A.O. Chong, K. Oshima, K.B. Sharpless, *J. Am. Chem. Soc.*, 1977, 99, 3420.

13. R.R. Schrock, *Acc. Chem. Res.*, 1990, 23, 158; W.J. Feast, V.C. Gibson, "Olefin Metathesis" in "The Chemistry of the Metal Carbon Bond", volume 5, Wiley, New York, 1989.

14. E.L. Marshall, Thesis, 1992.

15. R.H. Crabtree, "The Organometallic Chemistry of the Transition Metals.", Wiley, New York, 1988.

16. J.W. Lauher, R. Hoffmann, *J. Am. Chem. Soc.*, 1976, 98, 1729.

17. D.N. Williams, J.P. Mitchell, A.D. Poole, U. Siemeling, W. Clegg, D.C.R. Hockless, P.A. O'Neil, V.C. Gibson, *J. Chem. Soc., Dalton Trans.*,1992, 739.

18. V.C. Gibson, paper presented at the "Third International Conference on the Chemistry of the Early Transition Metals." Sussex, July, 1992; P.W Dyer, V.C. Gibson, W. Clegg, *J. Chem. Soc., Chem. Commun.*, submitted.

19. P.W Dyer, Thesis, 1993; P.W. Dyer, V.C. Gibson, J.A.K. Howard, B. Whittle, C. Wilson, *J. Chem. Soc., Chem. Commun.*, 1992, 1666.

20. D.S. Williams, M.H. Schofield, J.T. Anhaus, R.R. Schrock, *J. Am. Chem. Soc.*, 1990, 112, 6728.

21 D.S. Williams, M.H. Schofield, R.R. Schrock, *Organometallics* in press.

22 C.E. Housecroft, L.C. Parlett to V.C. Gibson, private communication, May 1992.

CHAPTER TWO.

Synthesis of Six Coordinate Molybdenum Bis(imido) Complexes.

2.1 Synthesis of Transition Metal Imido Complexes.

Many organoimido complexes of the early transition metals are known, and the methodology for producing them covers a range of reactions. Of these approaches many parallel reactions for the synthesis of other multiply bonded ligands such as terminal oxos, alkylidenes and alkylidynes. These methods are thoroughly discussed in "Metal Ligand Multiple Bonds" by Nugent and Mayer[1], but those which are particularly applicable to the production of organoimido complexes are outlined below.

From amines and N-silylated amines: cleavage of α-hydrogen or α-silicon.

Treatment of metal chloride or metal oxo species with amines or N-silylated amines sometimes results in the formation of an imido ligand[1]. The reaction follows the general form of equation 2.1

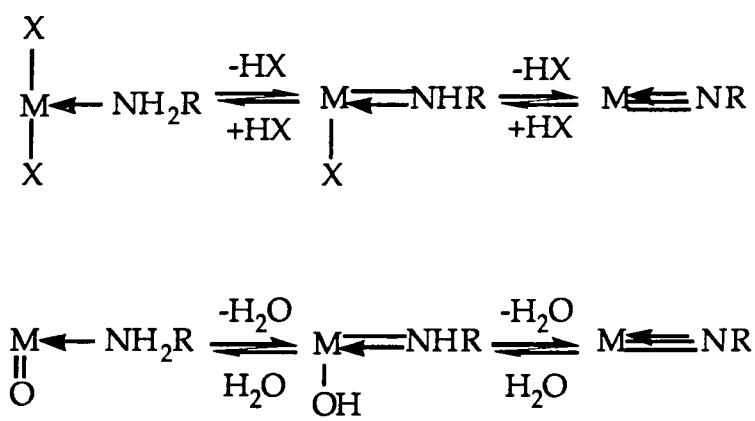

Equation 2.1

If the imido ligand precursor is an amine clearly the reaction will proceed via proton or H atom transfer with loss of hydrogen halide, or loss of water. Such a reaction can be promoted by several factors:

i) raising the oxidation state of the metal, to favour multiple bond formation

ii) using a more basic leaving group X

iii) using an external base such as additional or excess amine in the reaction, in order to mop up eliminated HCl.

If a silylated amine (NH(TMS)R or $N(TMS)_2R$) is used then loss of chlorotrimethylsilane or hexamethyldisiloxane will result in the formation of an imido ligand. Such a reaction is often preferable to α-deprotonation owing to the relatively mild reactivity of side products such as TMSCl and TMS_2O. It is also favoured by the strength of silicon-oxygen and silicon-chlorine bonds. An example of such a reaction pioneered in our group[2] is given below (Eqn. 2.2).

$$CpMCl_4 + NHR(TMS) \longrightarrow CpM(NR)Cl_2 + HCl + (TMS)Cl$$

Equation 2.2 (M=Nb, Ta)

From alkali metal amides by dealkylation: cleavage of α-carbon

This route is not widely used, however one of the first organoimido complexes was made by dealkylation of lithium diethylamide with tantalum pentachloride[3] (Eqn. 2.3).

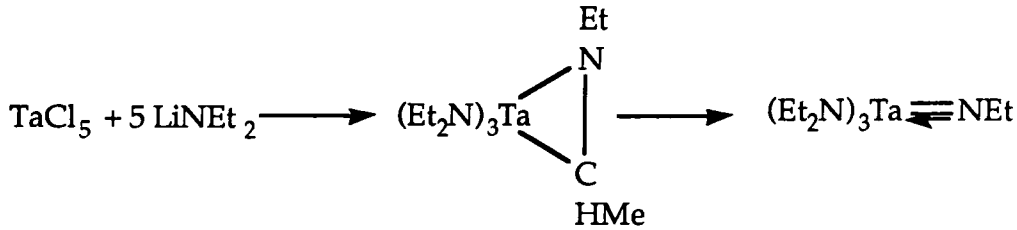

Equation 2.3

Cleavage of an electronegative group on the nitrogen.

Though not a widely used series of reactions, this description does cover the decomposition of azides to give imido or nitrido ligands[1]. The loss of dinitrogen provides a large driving force for the reaction and

facilitates product isolation. The type of azides used are RN_3 (R= TMS, C_6H_5, *p* -MeC_6H_4, C_2H_5). An example is the synthesis of the unusual six coordinate mixed oxo-imido complex[4] below (Eqn 2.4) by reaction of trimethylsilylazide with molybdenum (v) oxytrichloride.

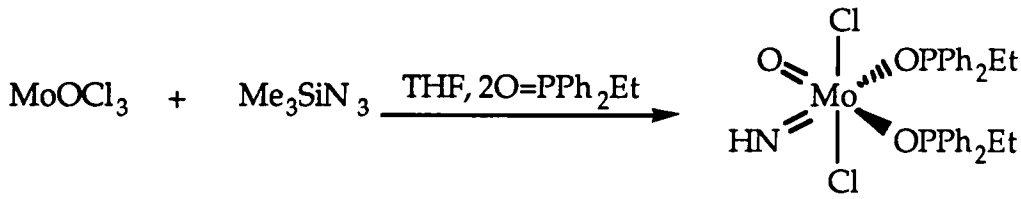

Equation 2.4

Wittig like [2+2] replacement of an existing multiply bonded ligand.

This type of reaction is a common way to interconvert a variety of multiply bonded ligands, it is illustated in equation 2.5 below.

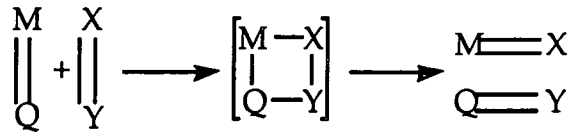

Equation 2.5

Shown to be a very versatile route into organoimido complexes, the metathetical mechanism is similar to that encountered in the catalytic metathesis of olefins by metal alkylidenes and in the ring opening metathesis polymerizations of cyclic olefins. It has been exploited to generate a wide range of metal organoimido complexes from metal oxos, metal alkylidenes and metal alkylidynes by reaction with aryl and alkylisocyanates (RNC=O) or aryl and alkylphosphinimines (R_3P=NR); a powerful driving force comes from the formation of side products with very strong bonds e.g. carbon dioxide or trialkylphosphine oxides. Other potentially useful reagents are aryl and alkylsulfinilamines (ArNSO) and aryl formamides (ArNHCH=NAr). Support for this metathesis-like reaction pathway comes from the isolation of a

cyclometallacarbamate[5] from the reaction of $Cp_2Mo(O)$ with phenylisocyanate; loss of carbon dioxide does not occur.

This metathesis-type route has been used in this research group for the synthesis of four coordinate molybdenum oxo-imido complexes[6] (Eqn. 2.6).

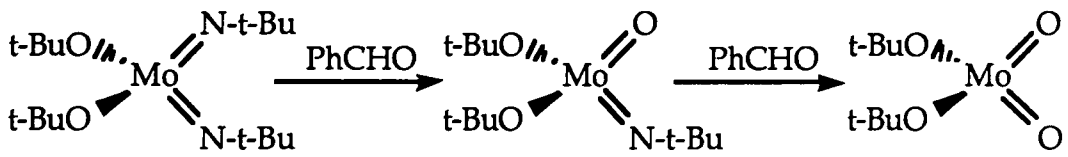

Equation 2.6

This is related to the synthesis[7] of osmium monooxide trisimido species from osmium tetraoxide published by Sharpless (eqn 2.7):

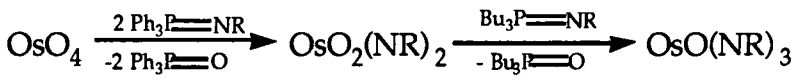

Equation 2.7

Further examples involve inter-metal exchange of multiply bonded ligands[6] (Eqn. 2.8):

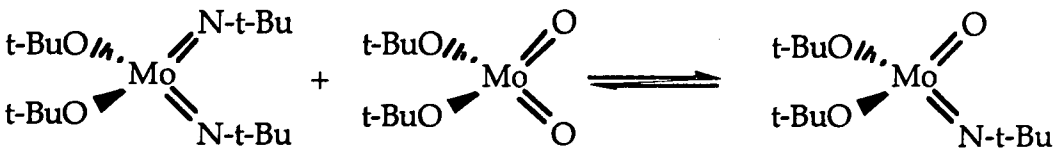

Equation 2.8

While the reactions above can be exploited to lead to a wide variety of imido ligands, they do not provide easy access to metal bis(imido) fragments. Preparative routes to these compounds are less well developed, and while they sometimes use similar synthetic reagents, they frequently involve multi-step procedures.

This point is illustrated by considering the synthetic routes to a range of bis(imido) compounds, some of which are similar to the $Mo(NR)_2Cl_2$.DME compounds discussed subsequently in this section.

Bis(Imido) complexes.

A range of bis(imido) complexes have been synthesised by the reaction of a mono(imido) complex with an N-silylated amine (eqn 2.9). The reaction steps are shown below[8].

$$[Cl_4W{=}O]_2 \xrightarrow{RN{=}CO} [Cl_4W{=}NR]_2 \xrightarrow{(TMS)NHR'}$$

$$[WCl_2(NR)(NR')(NH_2R')]_2 \xrightarrow{bipy} WCl_2(NR)(NR').bipy$$

Equation 2.9

Conversion of a dioxo complex to a bis(imido) complex[9] has also been applied (eqn. 2.10).

$$[Cl_4MoO] \xrightarrow{(TMS)_2O} [MoO_2Cl_2] \xrightarrow{bipy} [MoO_2Cl_2.bipy]$$

$$\xrightarrow{NHR(TMS)} [Mo(NR)_2Cl_2.bipy]$$

Equation 2.10

One route which is relatively simple involves an intermediate bridged imido-amino complex[10] (eqn.2.11).

$$[WCl_6] \xrightarrow{>4NHtBu(TMS)} [WCl_2(NtBu)_2(H_2NtBu)]_x \xrightarrow{bipy} [W(NtBu)_2Cl_2.bipy]$$

Equation 2.11

These strategies have been combined to provide a range of routes to the compound $W(N\text{-}2,6\text{-}iPrC_6H_4)_2Cl_2$.DME.

All the quoted examples are laborious, multi-step synthetic routes. In 1992, Schrock published[11] a simple, one step, high-yielding route to complexes of general formula $Mo(NR)_2Cl_2.DME$ from ammonium dimolybdate and using readily available reagents (eqn 2.12). An analogous route to rhenium (VII) bis- and tris(imido) complexes from ammonium dirhenate or rhenium heptoxide was also developed[12], however attempts to extend these reactions to tungstates failed.

$$(NH_4)_2Mo_2O_7 + 4RNH_2 + 8NEt_3 + 14TMSCl \xrightarrow[\text{dme}]{65°C,\ 6\text{-}10h}$$
$$2Mo(NR)_2Cl_2.dme + 8NEt_3HCl + 7(TMS)_2O + 2NH_4Cl$$

Equation 2.12

The reagents are combined under nitrogen using dimethoxyethane as a solvent, and heated together. In the work-up, the ammonium salts are removed as a precipitate by filtration, and volatiles removed from the filtrate in vacuo; the reaction product is obtained in pure form in high yields.

It is proposed that the reaction proceeds via attack of the amine[11] at the metal centre followed by proton transfer to an oxo ligand (directly or via the external bases present) giving the imido ligand and water. The water produced is consumed by the chlorotrimethylsilane to give hexamethyldisiloxane and hydrogen chloride which is converted into the triethylammonium hydrochloride salt. An alternative possibility is chlorination of the oxoanion by TMSCl to give an oxochloro species which then reacts with the amine. This is also consistent with the order of addition of the reagents.

A variation of this route (eqn 2.13) has been developed in Durham[13] using anhydrous sodium molybdate, and adjusting the quantities of other reagents accordingly.

$$Na_2MoO_4 + 2RNH_2 + 4NEt_3 + 8TMSCl \xrightarrow[dme]{65\text{-}75°C,\ 24h} Mo(NR)_2Cl_2.dme + 4(TMS)_2O + 2NaCl + 4NEt_3HCl$$

Equation 2.13

The reaction is believed to proceed via a related pathway to that above, and the work-up of the product is identical. This modification frequently gives an analytically pure product in improved yield. This is the synthesis employed to make the $Mo(NR)_2Cl_2$.DME compounds below used as starting materials for the remaining compounds in this thesis.

2.2 $Mo(N\text{-}2\text{-}tBuC_6H_4)_2Cl_2$.DME

The 2-t-butylphenylimido group was chosen for comparative purposes with established derivatives containing the 2,6-diisopropylimido ligand. The asymmetrical ring substitution pattern and the steric demands of the t-butyl group may result in orientation preferences, which are potentially observable by NMR.

The compound was made using the reaction outlined above. After work-up, dark red solid $Mo(N\text{-}2\text{-}t\text{-}BuC_6H_4)_2Cl_2$.DME was isolated in 98% yield based on sodium molybdate. ^1H nmr analysis shows good agreement with the published data for this compound; C, H and N elemental analysis are consistent with the desired product. The nmr data for the compound shows identical imido ligands at room temperature, with no apparent restriction of rotation about the $N\text{-}C_{ipso}$ bond.

2.3 $Mo(N\text{-}1\text{-}adamantyl)_2Cl_2$.DME.

The choice of the adamantylimido ligand was made to allow comparison between derivatives of this and of known metallocene-like

bis(t-butylimido)molybdenum compounds. Structurally the adamantyl group and the t-butyl group are quite similar. The cage of the adamantyl structure effectively ties back the ligand, making it "egg-shaped" in comparison to the "football shaped" t-butyl group. Beyond this it was anticipated that adamantylimido derivatives would be more crystalline than the frequently oily t-butylimido derivatives. Sketches of the two ligands are given below, and the labelling scheme adopted for the adamantylimido groups with respect to NMR assignments is shown.

$Mo(NAd)_2Cl_2$.DME was made by the same experimental procedure outlined above. Yellow solid Mo(N-1-adamantyl)$_2Cl_2$.DME was obtained in 61% yield based on sodium molybdate. Proton nmr and C,H,N analysis shows the compound to be pure. Again, due to rotation about the N-C bond the imido ligand substituents are identical.

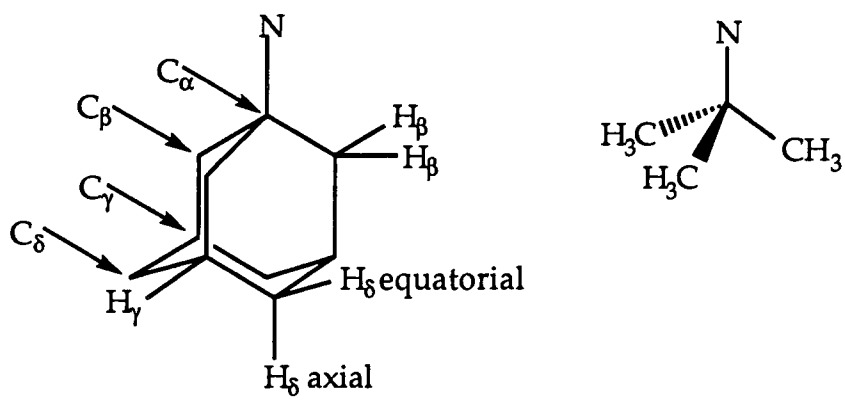

Figure 2.1

It is noted that all of the β-hydrogens are equivalent, as are the three γ-hydrogens; δ-hydrogens occur in two slightly different environments, axial and equatorial and therefore their NMR resonances are split by geminal coupling to give doublet of doublet resonances. None of the adamantyl protons exhibit significant vicinal coupling owing to the dihedral angle of 60°, which according to a Karplus correlation for vicinal coupling is expected to give a very small coupling constant. Thus

the proton nmr spectrum for the adamantyl ligand comprises of broad singlets for H_β and H_γ (δ 2.24 ppm and 1.97 ppm in C_6D_6) and a doublet of doublet resonance at δ 1.49 ppm for the two H_δ protons. Further it is noted that the shift for C_α in the ^{13}C spectrum is at 73.1ppm (C_6D_6), this figure is comparable with that in the t-butyl analogue at 71.7 ppm (C_6D_6).

2.4 Mo(N-2,6-iPr$_2$C$_6$H$_3$)(N-t-Bu)Cl$_2$.DME.

This compound was made in order to draw comparisons between its derivatives and the metallocene-like bis(t-butylimido) compounds and the non-metallocene like bis(2,6-diisopropylphenylimido) compounds which are already known. Beyond this, the prochiral metal centre may invoke orientation preferances in derivatives, and provides an extra handle for NMR investigations. A sample of this compound was made jointly by Mr P.W. Dyer, Dr E.L. Marshall and the author using the same experimental procedure save for using a mixture of the two amines.

A 1: 1 mixture of 2,6-diisopropylaniline and t-butylamine gave on work-up a mixture of products containing 54% Mo(NAr)(NtBu)Cl_2.DME, 18% Mo(NtBu)$_2$$Cl_2$.DME and 28% Mo(NAr)$_2$$Cl_2$.DME. The proportions of the amines were adjusted in an attempt to optimise the formation of the mixed imido species, with little succes. For example, a mix of 0. 8 : 1.2 diisopropylaniline : t-butylamine was used which on work-up gave a mixture of products containing 56% Mo(NAr)(NtBu)Cl_2.DME, 29% Mo(NtBu)$_2$$Cl_2$.DME and 15% Mo(NAr)$_2$$Cl_2$.DME. The product mixture was recrystallised from diethylether to give the desired mixed (imido)complex exclusively.

2.5 Mo(N-1-adamantyl)(O)Cl_2.DME

By using only one molar equivalent of 1-adamantanamine in the reaction used to produce Mo(N-1-adamantyl)$_2$$Cl_2$.DME, a mixture of products is obtained consisting of 60% Mo(N-1-adamantyl)(O)Cl_2.DME and 40% Mo(N-1-adamantyl)$_2$$Cl_2$.DME. Recrystallisation from DME yields pure Mo(N-1-adamantyl)(O)Cl_2.DME as a yellow amorphous compound.

A further attempt to form Mo(N-1-adamantyl)(O)Cl_2.DME by reaction of Mo(N-1-adamantyl)$_2$$Cl_2$.DME with one equivalent of water in diethylether gave on work-up a mixture of 25% Mo(N-1-adamantyl)(O)Cl_2.DME and 75% Mo(N-1-adamantyl)$_2$$Cl_2$.DME. An attempt to make Mo(N-2-tBuC_6H_4)(O)Cl_2.DME by the same method was unsuccessful.

This complex has been characterised by ^1H and ^{13}C nmr and by C,H,N analyses. The infra-red spectrum of the compound shows a characteristic metal oxo stretch at 908cm^{-1}. This value is consistent with other Mo=O stretches in similar compounds; these are recorded in the table below for comparative purposes.

In the infra red spectrum, two Mo=O stretches are expected in dioxo compounds with a cis geometry, due to symmetric and asymmetric modes; in the oxo-imido complex only one Mo=O stretch is expected.

Compound	ν (M=O) cm^{-1}	Reference
$Mo(NAd)(O)Cl_2.DME$	908	This work
$Mo(O)_2Cl_2.DME$	960,920	14
$Mo(O)_2Cl_2.BIPY$	930,908	15
$Mo(O)_2Me_2.BIPY$	934,905	16
$Mo(O)_2(CH_2tBu)_2.BIPY$	922, 890	17
$W(O)_2Cl_2.DME$	976, 933	18
$W(O)(N\text{-}t\text{-}Bu)Cl_2.BIPY$	913	19

Table 2.1

Crystals of Mo(N-1-adamantyl)(O)Cl_2.DME suitable for X-ray analysis were grown from a solution of the compound in DME at -40°C. Data were collected and solved by Mr R.C.B. Copley and Prof. J.A.K. Howard within this department. Several views of the molecule are shown in Figure 2.2 and selected bond distances and angles are presented in Table 2.2.

Bond lengths (Å)		Bond lengths (Å)	
Mo(1) - Cl(1)	2.3979(4)	C(4) - C(7)	1.535(3)
Mo(1) - Cl(2)	2.3928(5)	C(5) - C(8)	1.532(3)
Mo(1) - O(1)	1.708(1)	C(5) - C(10)	1.533(3)
Mo(1) - N(1)	1.719(2)	C(6) - C(8)	1.529(3)
Mo(1) - O(12)	2.346(1)	C(6) - C(9)	1.533(3)
Mo(1) - O(15)	2.356(1)	C(7) - C(9)	1.534(3)
N(1) - C(1)	1.436(2)	C(7) - C(10)	1.534(3)
C(1) - C(2)	1.539(2)	C(11) - O(12)	1.448(2)
C(1) - C(3)	1.545(2)	O(12) - C(13)	1.440(2)
C(1) - C(4)	1.542(2)	C(13) - C(14)	1.502(3)
C(2) - C(5)	1.538(3)	C(14) - O(15)	1.444(2)
C(3) - C(6)	1.532(2)	O(15) - C(16)	1.436(2)

Bond Angles (°)		Bond Angles (°)	
Cl(1) - Mo(1) - Cl(2)	157.88(2)	C(1) - C(3) - C(6)	109.0(1)
Cl(1) - Mo(1) - O(1)	96.04(5)	C(1) - C(4) - C(7)	109.2(1)
Cl(1) - Mo(1) - N(1)	97.14(5)	C(2) - C(5) - C(8)	109.4(2)
Cl(1) - Mo(1) - O(12)	79.04(3)	C(2) - C(5) - C(10)	109.6(2)
Cl(1) - Mo(1) - O(15)	82.74(3)	C(8) - C(5) - C(10)	109.9(2)
Cl(2) - Mo(1) - O(1)	98.48(5)	C(3) - C(6) - C(8)	109.6(2)
Cl(2) - Mo(1) - N(1)	95.28(5)	C(3) - C(6) - C(9)	109.4(2)
Cl(2) - Mo(1) - O(12)	81.54(3)	C(8) - C(6) - C(9)	109.7(2)
Cl(2) - Mo(1) - O(15)	80.81(3)	C(4) - C(7) - C(9)	109.1(2)
O(1) - Mo(1) - O(12)	159.54(6)	C(4) - C(7) - C(10)	109.7(2)
O(1) - Mo(1) - O(15)	89.48(6)	C(9) - C(7) - C(10)	109.8(2)
O(1) - Mo(1) - N(1)	104.45(7)	C(5) - C(8) - C(6)	109.6(2)
N(1) - Mo(1) - O(12)	95.89(6)	C(6) - C(9) - C(7)	109.7(2)
N(1) - Mo(1) - O(15)	165.98(6)	C(5) - C(10) - C(7)	109.3(1)
O(12) - Mo(1) - O(15)	70.27(4)	Mo(1) - O(12) - C(11)	119.9(1)
Mo(1) - N(1) - C(1)	169.2(1)	Mo(1) - O(12) - C(13)	114.4(1)
N(1) - C(1) - C(2)	109.0(2)	C(11) - O(12) - C(13)	110.9(1)
N(1) - C(1) - C(3)	108.3(1)	O(12) - C(13) - C(14)	107.6(1)
N(1) - C(1) - C(4)	110.9(1)	C(13) - C(14) - O(15)	107.1(1)
C(2) - C(1) - C(3)	109.5(1)	Mo(1) - O(15) - C(14)	113.5(1)
C(2) - C(1) - C(4)	109.8(1)	Mo(1) - O(15) - C(16)	120.0(1)
C(3) - C(1) - C(4)	109.4(1)	C(14) - O(15) - C(16)	112.0(1)
C(1) - C(2) - C(5)	109.0(2)		

Table 2.2:*Selected bond lengths (Å) and angles (^{0}) for Mo(N-1-adamantyl)(O)Cl_2.DME.*

The structure (Fig. 2.2) consists of monomeric Mo(N-1-adamantyl)(O)Cl_2.DME in a distorted octahedral geometry, possessing mutually *cis* oxo and imido ligands and *trans* chloride ligands; the chelating DME is bound *trans* to the multiply bonded ligands. The Cl-Mo-Cl angle (157.88(2)°) is strongly distorted from linear and the angle between the oxo and imido ligand (104.45(7)°) is obtuse. As is rationalised in Section 2.6, the multiply bonded ligands are arranged *cis* to maximise the π-bonding interactions with the metal d_π orbitals and minimise π-antibonding. Of the other ligands the chloride is the stronger π-bonding ligand, thus by not binding *trans* to the multiply bonded ligands it avoids competition for orbitals.

Such mixed oxo-imido complexes of the Group 6 metals are uncommon, at the present being limited to two other structurally characterised complexes (Mo(NH)(O)Cl_2.$(OPPh_2Et)_2$[4] and W(N-t-Bu)(O)Cl_2.BIPY [19]). These exist as distorted octahedra which parallel the wide range of structurally characterised complexes $M(E)_2Cl_2.L_2$ (M=W, Mo; E=O, NR; L=base)[4, 10, 19, 20]. Comparison with a range of dioxo molybdenum complexes ($Mo(O)_2Cl_2.L_2$, L_2=DME, BIPY, HMPA, o-phenanthroline, 2 O=PPh_3)[21, 14, 16] suggests that the molybdenum-oxygen bond distance in Mo(N-1-adamantyl)(O)Cl_2.DME (1.708(1)Å) is consistent with a pseudo-triple bond. One octahedral bis(imido) molybdenum (VI) complex has been structurally characterised (Mo(N-t-Bu)(NAr)Cl_2.DME), however, comparison with the general range of molybdenum imido bond lengths in bis(imido) fragments suggests that the observed Mo-N distance in Mo(N-1-adamantyl)(O)Cl_2.DME (1.719(2)Å) is again consistent with a pseudo-triple bond.

Figure 2.2: *The crystal structure of Mo(NAd)(O)Cl_2.DME.*

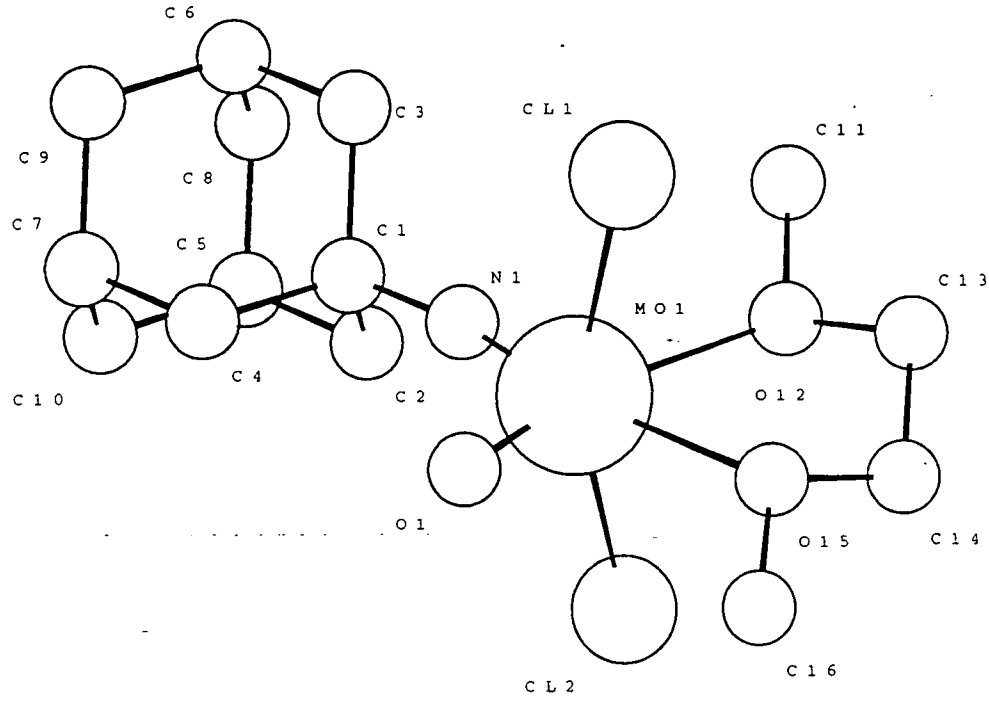

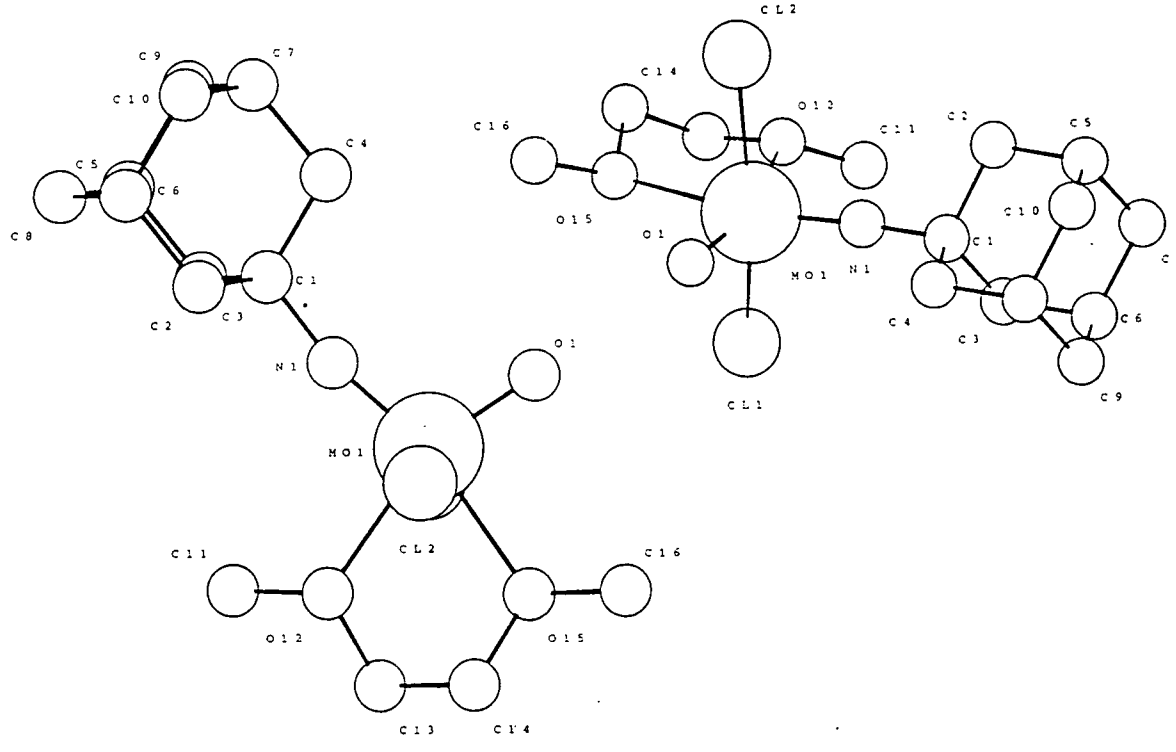

The fact that both the imido and oxo ligands bind to the molybdenum atom with pseudo-triple bonds is interesting, since it might have been expected that the stronger π-bonding imido ligand would dominate over the oxo ligand in the competition for π-bonding with the metal centre. Structurally, this might be expected to manifest itself in a lengthening of the bond and a shortening of the metal-imido bond. Instead it appears that the oxo and imido ligands have a roughly equal share of the three available metal d_π orbitals resulting in both metal ligand multiple bonds being of bond order 2.5. The metal-oxygen bonds of the DME ligand trans to the metal-oxo and metal-imido bonds are quite similar, indicating that the oxo and the imido ligand exhibit similar *trans* influences in this complex. It has previously been shown that the oxo ligand exhibits a stronger *trans* influence than the imido ligand. However, observations to the contrary have also been made; these have been attributed to hydrogen bonding in the lattice reducing the *trans* influence of the oxo ligand below that of the imido ligand.

The bond angle at nitrogen is 169.2° and is within the range expected for a fully π bonding imido ligand donating four electrons to the metal centre. Note however that the level of bending of the imido ligand is no longer taken as being indicative of the bond order, instead this is better indicated by the actual bond length.

2.6 Bonding In Octahedral Bis Imido Complexes.

This section aims to discuss in a simple and qualitative manner some of the factors involved in the π–bonding of a bis-imido or bis-oxo fragment within an octahedral complex. The treatment is simplistic and assumes that the octahedral complex contains two ($\sigma + 2\pi$) ligands and

four purely σ–bonding ligands. For complexes involving halogen ligands this is obviously a gross approximation since their lone pairs are able to be donated to empty metal d_π orbitals[22]. A further approximation is in the assumption of a perfect octahedral geometry; the type of distortion observed in Mo(NAd)(O)Cl_2.DME is usual among these complexes, indeed, calculations[23] have shown that the MoO_2^+ fragment favours a strongly bent geometry. Despite these drawbacks, the model usefully shows the metal-ligand interactions which may occur and rationalises the experimentally observed geometries.

In a model which places the metal at the origin of a set of orthogonal cartesian axes, each of the six ligands forms one σ-bond to the metal, directed along the axis. Combination of the six ligand group orbitals with the six suitable metal orbitals directed along the axes results in the formation of six σ-bonding and six σ^*-antibonding orbitals[22]. The remaining metal orbitals (d_{xy}, d_{yz}, d_{xz}, comprising the t_{2g} set) are directed off axis and are incapable of σ-bonding; they are treated separately for their π-bonding interactions[1].

The ligand orbitals of an imido ligand consist of one σ-symmetry component (essentialy sp hybrid) and two π-symmetry components (essentially p orbitals) (Fig. 2.3) which may interact with the metal t_{2g} set to form π bonds[1].

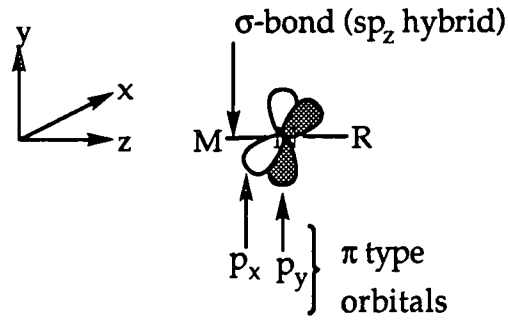

Figure 2.3

The d_π-p_π interactions, arising from the imido group positioned along the z-axis, are shown in figure 2.4.

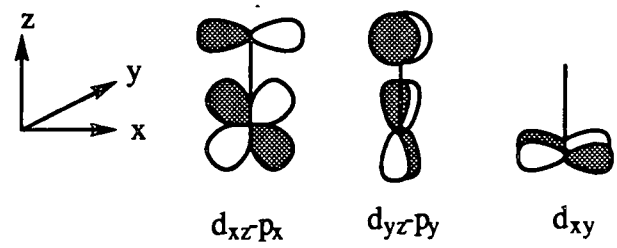

Figure 2.4

The d_{xy} orbital is of the wrong symmetry to interact with any ligand orbitals and so remains non-bonding.

The approach of an oxo or imido (E) ligand along the z-axis perturbs the molecular orbital energy level diagram[1] as shown in figure 2.5. The lowering of the symmetry splits the degeneracy of the t_{2g} and e_g^* levels; two of the t_{2g} levels become involved in π-bonding and, as indicated, the d_{xy} remains non-bonding.

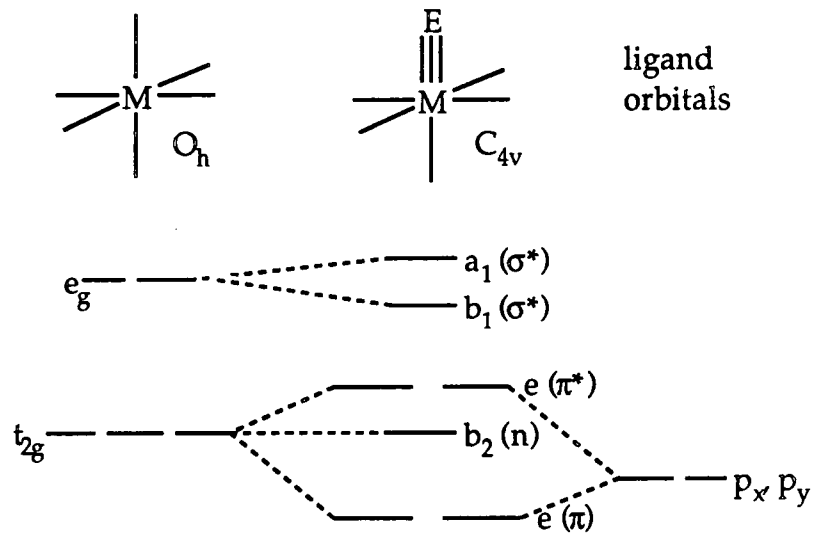

Figure 2.5

If the two π-bonding orbitals resulting from these two interactions are both occupied then two π-bonds result, which in addition to the σ-bond forms a triple bond. Metal-imido interactions are invariably intermediate between double and triple bonds owing to competition for the t_{2g} set of metal orbitals.

In a charge formalism, the π orbitals and the non-bonding orbitals are occupied by the four π electrons of the O^{2-} or NR^{2-} ligand plus any remaining d-electrons on the metal. The twelve σ-bonding electrons occupy the low lying σ-bonding orbitals. Thus we can rationalise the observation that metal-imido and metal-(terminal)oxo complexes are found predominantly for d^0, d^1 and d^2 electron configurations: d^3 and higher configurations results in the population of highly destabilising π^* orbitals[24].

In an octahedral complex with two (E) ligands there will be competition for the three d_π metal orbitals by the four π-symmetry ligand orbitals. The system adopts either a cis- or trans- geometry to maximise the π-bonding interactions and minimise the π^*-antibonding interactions; this is achieved by a balance between sharing one or more d_π orbitals between the two ligands, having a d_π orbital dedicated to a ligand, or having non-bonding d_π orbitals[1].

In a cis geometry the d_π orbitals interact with the p_π orbitals of ligands 1 and 2 as shown in fig. 2.6

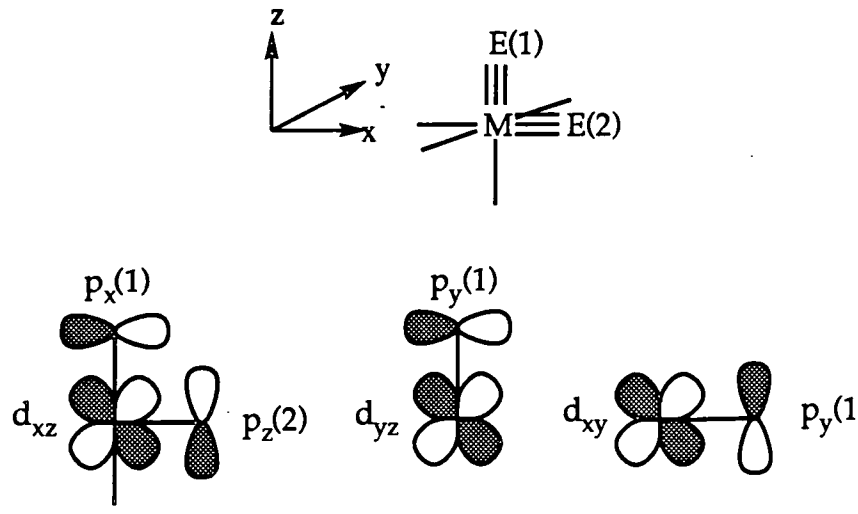

Figure 2.6

Competition by both ligands occurs for interaction with the d_{xz} orbital and the d_{xy} and d_{yz} orbitals are dedicated to one ligand orbital each. This results in the formation of a system of three π-bonding orbitals and three π^*-antibonding orbitals.

In a charge formalism, the two imido ligands are able to donate four π electrons each, however the availability of only three π-bonding orbitals results in each imido being able to donate only three electrons to the metal forming three π bonds. Clearly the metal must be of d^0 electron configuration to tolerate the two ligands in a cis arrangement, any more electrons would populate the highly destabilising π^* levels.

In $Mo(NR)_2Cl_2$.DME and $Mo(NR)(O)Cl_2$.DME the molybdenum is in oxidation state (VI), so has a d^0 configuration. The three π-bonds are delocalised between the metal and the two multiply bound ligands; these together with the σ-bonds result in a total net bond order between the imido or oxo ligands and the metal of 2.5. The structure may usefully be represented (Fig 2.7) as having the second π-bond delocalised over the two multipy bonded ligands.

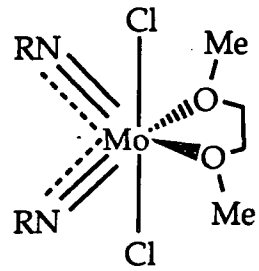

Figure 2.7

In a trans geometry, the d_π orbitals interact with the p_π orbitals of ligands 1 and 2 along the z-axis as shown in fig. 2.8. Competition by both ligands occurs for interaction with the d_{xz} and d_{yz} orbitals; the d_{xy} orbital is non-bonding. The result is a system of two π-bonding, one non-bonding and two π^*-antibonding orbitals[23, 25, 26].

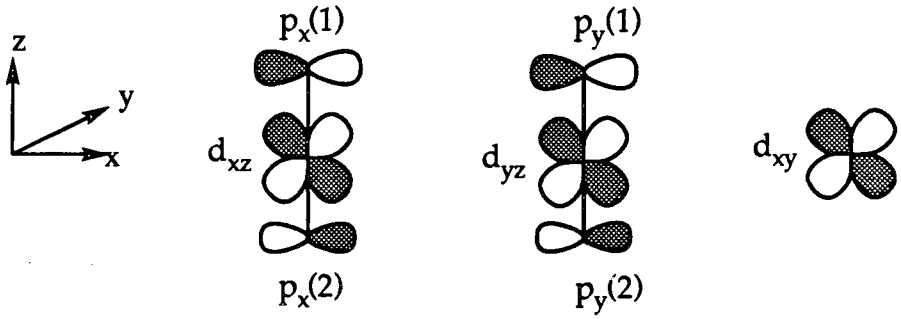

Figure 2.8

In this geometry the two E ligands are able to donate only two π electrons each to the complex because of the competition for the d_π orbitals, giving a total of two π-bonds. With the σ-bonds this results in two metal ligand double bonds. Such complexes are therefore stable with up to two d-electrons which will populate the d_{xy} non-bonding orbital. Species exhibiting such geometries[25] are:

$[ReO_2L_4]^z$ ($L=CN^-$, z=3-; $L=^1/_2$ en or py, z=1+) : Re(v), d^2

With the eight π-electrons this fills the π-bonding and the non-bonding levels. Excited states of this complex show lengthening of the Mo=O bond due to population of the e_g (π^*) level.

From these arguments it can be seen that such dioxo and bis(imido) complexes only form where the metal is highly oxidised. In effect these ligands are very good at stabilising such high oxidation states since productive π -bonding requires the metal orbitals to be empty. If they are filled then population of the highly destabilising π^*-antibonding orbitals results. Thus terminal oxos and imidos of the later transition metals are inaccessible[24].

2.6 References.

1. W.A. Nugent, J.M. Mayer, *"Metal Ligand Multiple Bonds."*, Wiley, New York, 1988.
2. D.N. Williams, J.P. Mitchell, A.D. Poole, U. Siemeling, W. Clegg, D.C.R. Hockless, P.A. O'Neill, V.C. Gibson, *J. Chem. Soc., Dalton Trans.*, 1992, 739.
3. D.C. Bradley, I.M. Thomas, *Can. J. Chem.*, 1962, **40**, 1355.
4. J. Chatt, R. Choukroun, J.R. Dilworth, J. Hyde, P. Vella, J. Zubieta, *Transition Metal Chemistry*, 1979, **4**, 59.
5. P. Jernakoff, G.L.Geoffroy, A.L. Rheingold, S.J. Geib, *J. Chem. Soc., Chem. Commun.*, 1987, 1610.
6. M. Jolly, Thesis, (1993); M. Jolly, J.P. Mitchell, V.C. Gibson, *J. Chem. Soc., Dalton Trans.*, 1992, 1329; M. Jolly, J.P. Mitchell, V.C. Gibson, *J. Chem. Soc., Dalton Trans.*, 1992, 1331.

7. A.O. Chong, K. Oshima, K.B. Sharpless, *J. Am.. Chem. Soc.*, 1977, **99**, 3420.

8. B.R Ashcroft, A.J. Neilson, D.C. Bradley, R.J. Errington, M.B. Hursthouse, R.L. Short, *J. Chem. Soc., Dalton Trans.*, 1987, 2059; D.C. Bradley, R.J. Errington, M.B. Hursthouse, R.L. Short, B.R Ashcroft, G.R. Clark, A.J. Neilson, C.E.F. Rickard, *J. Chem. Soc., Dalton Trans.*, 1987, 2067.

9. W.A. Herrmann, W.R. Thiel, E. Herdtweck, *Chem. Ber.*, 1990, **123**, 271.

10. B.R Ashcroft, D.C. Bradley, G.R. Clark, R.J. Errington, A.J. Neilson, C.E.F. Rickard, *J. Chem. Soc., Chem. Commun.*, 1987, 170.

11. H.H. Fox, K.B. Yap, J. Robbins, S. Cai, R.R. Schrock, *Inorg. Chem.*, 1992, **31**, 2287.

12. R. Toreki, R.R. Schrock, W.M. Davis, *J. Am.. Chem. Soc.*, 1992, 3367.

13. P.W Dyer, V.C. Gibson, J.A.K. Howard, B. Whittle, C. Wilson, *J. Chem. Soc., Chem. Commun.*, 1992, 1666.

14. B. Kamenar, M. Penavic, B. Korpar-Colig, B. Markovic, *Inorg. Chim. Acta.*,1982, **65**, L 245.

15. C.G.Hill, M.H.B. Stiddard, *J. Chem. Soc. (A)*, 1966, 1633.

16. G.N. Schrauzer, L.A. Hughes, N. Strampach, P.R. Robinson, E.O. Schlemper, *Organometallics*, 1982, **1**, 44.

17. G.N. Schrauzer, L.A. Hughes, N. Strampach, F. Ross, D. Ross, E.O. Schlemper, *Organometallics*, 1982, **2**, 481.

18. K. Dreisch, C. Andersson, C. Stalhandske, *Polyhedron*, 1991, **10**, 2417.

19. W. Clegg, R.J. Errington, D.C.R. Hockless, C. Redshaw, *J. Chem. Soc., Dalton Trans.*, 1993, 1965.

20. G.R. Clark, A.J. Neilson, C.E.F. Rickard, *Polyhedron*, 1988, **7**, 117.

21. B. Voissat, P. Khodadad, N. Rodier, *Acta. Cryst. (B)*, 1977, **33**, 3793; B. Voissat, P. Rodier, *Acta. Cryst. (B)*, 1979, **35**, 1979.

22. F.A. Cotton and G. Wilkinson, "Comprehensive Inorganic Chemistry.", 5th Edition, Wiley, New York, 1988.

23. K. Tatsumi, R. Hoffmann, *Inorg. Chem.*, 1980, **19**, 2656.

24. J.M. Mayer, *Comments Inorg. Chem.*, 1988, **8**, 125.

25. J.C. Dobson, K.J. Takeuchi, D.W Pipes, D.A. Geselowitz, T.J. Meyer, *Inorg. Chem.*, 1986, **25**, 2357.

26. J.R. Winkler, H.B.Gray, *Inorg. Chem.*, 1985, **24**, 346.

CHAPTER THREE.

Synthesis of Molydenum Bis(imido) Olefin Adducts.

3.1 Introduction

Transition metals are able to bind and activate a range of hydrocarbon ligands. Complexes containing multiply bonded imido ligands and neutral organic molecules at a single metal centre are of interest because of their relevance to catalytic processes like ammoxidation, amination and oxyamination. Research into complexes of metallocenes with unsaturated organic ligands has also been stimulated by the activity of titanocene and zirconocene alkyl species as Ziegler-Natta catalysts for olefin polymerizations.

The isolobal relationship between such Group 4 metallocenes, Group 5 half-sandwich imido fragments and Group 6 bis(imido) metal fragments has stimulated studies on the latter systems. This section discusses the synthesis of a variety of molybdenum bis(imido) olefin complexes and compares them with other known molybdenum bis(imido) olefin[1] and half-sandwich niobium imido olefin complexes[2] in terms of this isolobal relationship.

Olefin adducts of group 4 metallocenes.

The first stable ethylene adduct of titanocene was reported by Bercaw[3] in 1983 via the reduction of permethyltitanocene dichloride in the presence of ethylene (Eqn. 3.1). A structural determination shows the geometry expected from M.O. calculations[4]; the carbon-carbon double bond length is consistent with significant metallacyclopropane character, indicative of appreciable d_{π}-π^* back-donation. Reaction of this 16 electron titanium (II) adduct with further ethylene leads to a highly reactive 16 electron titanium (IV) metallacyclopentane.

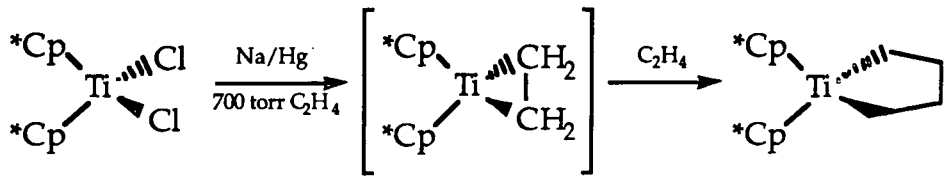

Equation 3.1

The development of $Cp_2Ti(PMe_3)_2$ as a convenient source of titanocene[5] led to the detection at -50°C of the five coordinate 18 electron titanium (II) compound $Cp_2Ti(PMe_3)(\eta^2\text{-}C_2H_4)$ and the metallacyclopentane $Cp_2Ti(C_4H_8)$ (Fig. 3.1) as intermediates in the dimerisation of ethylene.

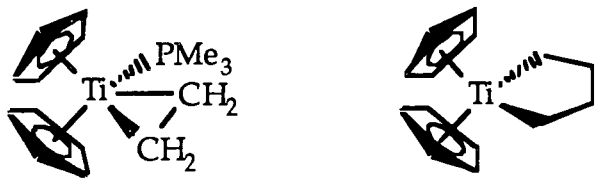

Figure 3.1

Zirconocene olefin adducts are accessible via similar routes: $Cp_2Zr(PMe_3)(\eta\text{-PhHC=CHPh})$ is produced[6] from $Cp_2Zr(PMe_3)_2$ with Z/E-stilbene, and $Cp_2Zr(PMe_3)$(but-1-ene) from the bis(alkyl) species $Cp_2Zr(n\text{-}Bu)_2$ by reaction with trimethylphosphine[7]. The first stable ethylene complex (Fig. 3.2) of zirconocene was $Cp_2Zr(PMe_3)(\eta^2\text{-}C_2H_4)$[8], isolated from the reaction of $Cp_2Zr(PMe_3)_2$ with ethylene under pressure. The metallacyclopentane and polyethylene were also formed.

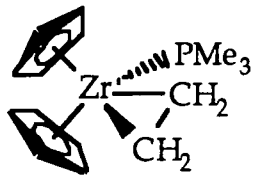

Figure 3.2

Hafnocene olefin adducts are uncommon, the isobutene-phosphine adduct (Eqn. 3.2) being accessible[9] from a mixed bis(alkyl) species.

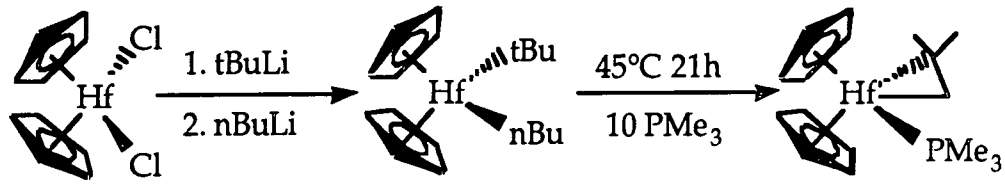

Equation 3.2

An intermediate ethylene adduct has also been trapped in the reaction shown below (Eqn. 3.3).

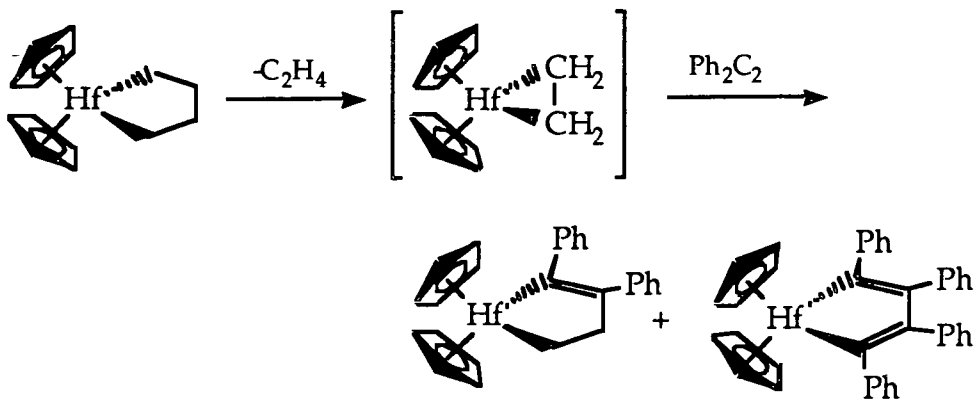

Equation 3.3

These compounds are either three coordinate, 16 electron or four coordinate, 18 electron complexes. The former environment is accessible owing to the less flexible electronic and steric demands of the η^5-cyclopentadienyl rings. Among these, the structurally characterised metallocene olefin complexes show the expected geometry[4], with the olefin and any phosphine lying in the equatorial binding plane.

Olefin Adducts of Group 5 Half-sandwich Imido fragments.

Group 5 half-sandwich imido olefin complexes have been made previously in this group[2] employing similar routes to those discussed above. Reduction of $Cp(NAr)NbCl_2$ with ethylmagnesium chloride in the presence of trimethylphosphine produces[10] $Cp(NAr)Nb(PMe_3)(\eta^2\text{-}C_2H_4)$. Further group 5 complexes of this type have been produced, including some propene adducts (Eqn. 3.4).

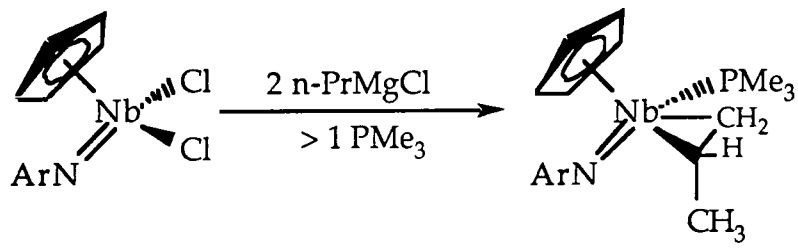

Equation 3.4

The reaction proceeds with generation of propane, this is evidence for the intermediacy of a dialkyl intermediate; subsequent β-hydride elimination gives η^2-bound olefin and loss of alkane. An analogous reaction path has been observed in the formation of a zirconocene butene adduct from a dibutylzirconocene complex[7]. Evidence for the isolobal relationship has been provided by an X-ray structure determination of $Cp(NAr)Nb(PMe_3)(\eta^2\text{-}C_3H_6)$. This molecule exhibits the expected metallocene-like geometry; the carbon-carbon double bond lies in the plane of the metal-phosphine bond. These complexes contain an 18 electron niobium or tantalum (III) centre in a four coordinate pseudo-tetrahedral arrangement.

It is noted that these species, unlike their metallocene analogues, show no tendency to form three coordinate 16 electron $Cp(NAr)Nb(\eta^2\text{-}C_2H_4)$ compounds, nor do they react further with carbon-carbon multiple

bonds to form metallacyclic compounds. In part this is believed to be owing to the lower steric demands of the imido ligand compared with the cyclopentadienyl ligand.

Olefin Adducts of Group 6 Bis(imido) fragments.

Group 6 metal bis(imido) olefin complexes have been targeted since they are isolobal to Group 4 metallocene olefin complexes and Group 5 half-sandwich imido olefin complexes. Tungsten complexes have been formed[11] by reaction of $W(NAr)_2(PMe_2Ph)_2$ (Ar= 2,6-$iPr_2C_6H_3$) with ketones, olefins and acetylenes in ligand substitution rections. The products vary between four coordinate 18 electron compounds of the type $W(NAr)_2(PR_3)L'$ and five coordinate, formally 20 electron, $W(NAr)_2(PR_3)_2L'$ complexes. The structure[12] of $W(NAr)_2(PMe_2Ph)(\eta^2\text{-}O{=}CMe_2)$ shows a pseudo-tetrahedral metallocene-like geometry maximising the π-bonding of the imido ligands. The increased flexibility of the sterically undemanding aryl groups and the flexibility of the imido ligand for π-bonding compared with the cyclopentadienyl ligand allows the formation of the five coordinate $W(NAr)_2(PR_3)_2L'$ complexes.

Studies on the bis(t-butylimido) molybdenum system[1] have shown that the bulky t-butylimido groups help to maintain a four coordinate metallocene-like geometry about the metal. Among the complexes isolated are $Mo(N\text{-}t\text{-}Bu)_2(PMe_3)(C_2H_4)$ and $Mo(N\text{-}t\text{-}Bu)_2(PMe_3)(C_3H_6)$[12], synthesised by reduction of $Mo(N\text{-}t\text{-}Bu)_2Cl_2$.DME with Grignard reagents in the presence of trimethylphosphine.

The propene adduct $Mo(N\text{-}t\text{-}Bu)_2(PMe_3)(C_3H_6)$[12] has been the subject of an X-ray structure determination. The complex adopts a metallocene-like geometry with the metal atom-phosphorus and olefinic bonds lying essentially in a plane orthogonal to the N-M-N plane (Fig.3.3(a)).

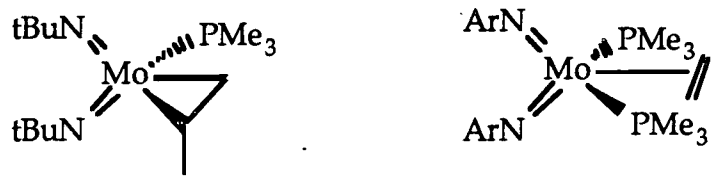

(a) (b)

Figure 3.3

Unpublished studies by Mr P.W. Dyer on $Mo(NAr)_2$ systems[1] led to a structurally characterised (Fig. 3.3(b)) five coordinate trigonal bipyramidal ethylene adduct $Mo(NAr)_2(PMe_3)_2(C_2H_4)$, a complex analogous to a tungsten species produced by Schrock. Increased flexibility in the orientation of the 2,6-diisopropylphenylimido ligands allow access to this five coordinate geometry. Here the carbon-carbon double bond lies in the metal-bis-phosphine plane; this is a crowded position compared with the possible upright geometry. Fenske-Hall calculations[14] show that such a geometry is preferred owing to the ability of the ethylene to participate in d_π-π^* back-bonding from the metal.

3.2 Molybdenum bis(imido) Ethylene compounds.

3.2.1 Reaction of $Mo(NR)_2Cl_2$.DME with Grignard Reagents.

As mentioned earlier, reduction of the six coordinate molybdenum (VI) compounds $Mo(NR)_2Cl_2$.DME with Grignard reagents in the presence of trimethylphosphine provides a synthesis of bis(imido) molybdenum olefin complexes[1].

As in the niobium system[10], two reaction pathways are possible. The likely first step is exchange of DME for trimethylphosphine. Subsequent alkylation may proceed to give a bis(imido)(dialkyl)phosphine complex or a bis(imido)(alkyl)(chloro)(phosphine) species. β-hydride elimination and

loss of alkane or HCl (which is consumed by excess trimethylphospine to give [PMe_3H]Cl) results in the generation of a metal bound olefin. The complex may then coordinate an additional PMe_3 resulting in a five coordinate product.

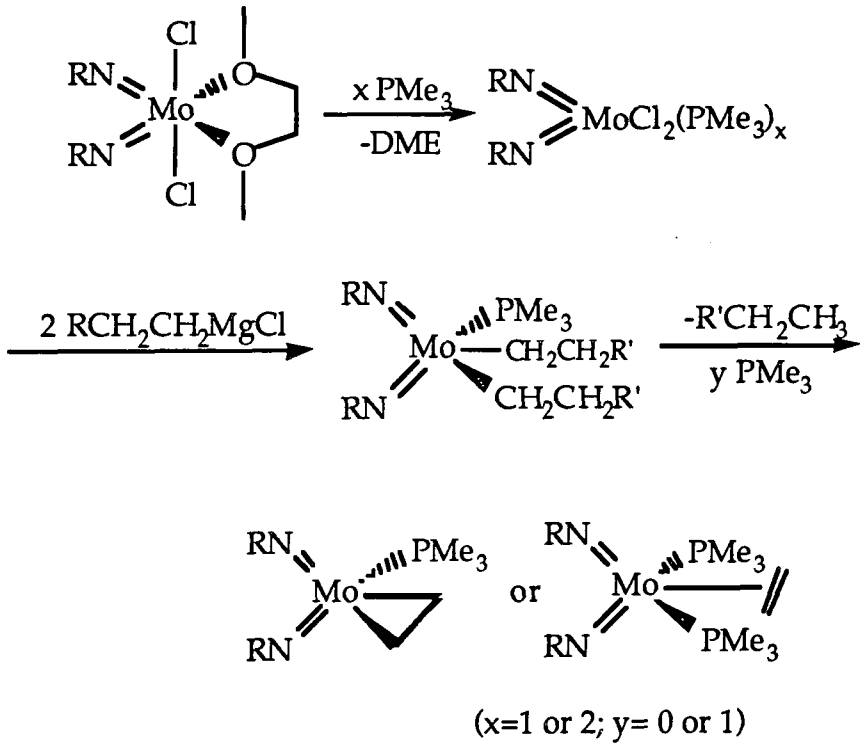

Equation 3.5

Studies on the reaction of $Mo(NAr)_2Cl_2$.DME with n-propylmagnesium chloride by G.C. mass spectrometry have shown that propane is evolved during the reaction and infrared analysis of the inorganic products shows no characteristic P-H stretch from [PMe_3H]Cl. These observations are consistent with the mechanism proceeding via a dialkyl intermediate (Eqn. 3.5). A similar pathway has been observed[7] in the synthesis of (but-1-ene)zirconocene via elimination of butane from di-n-butylzirconocene by reaction with excess trimethylphosphine.

3.2.2 Synthesis of $Mo(NAd)_2(PMe_3)(C_2H_4)$.

Structural similarities exist between the shape of the adamantyl group and the t-butyl group; the latter is a sterically demanding ball-like substituent, whereas the adamantyl group is rather less demanding being somewhat "tied-back". Therefore olefin adducts containing the bis(adamantylimido) fragment were sought in order to allow comparison with the known[1] four coordinate $Mo(N\text{-}t\text{-}Bu)_2(PMe_3)(C_2H_4)$. Reaction of $Mo(NAd)_2Cl_2$.DME with two molar equivalents of ethylmagnesium chloride in the presence of trimethylphosphine is found to give the mono-phosphine complex $Mo(N\text{-adamantyl})_2(PMe_3)(C_2H_4)$. The yield is low, however, owing to difficulties in extraction of the product.

NMR spectra and C,H,N atomic analysis confirm a stoichiometry consistent with $Mo(N\text{-adamantyl})_2(PMe_3)(C_2H_4)$. Both adamantylimido ligands are equivalent by NMR owing to free rotation about the C-N bond. Ethylene proton resonances (Fig. 3.4) are observed as a triplet at δ 2.31 ppm ($^3J_{HH}$=12 Hz) and an additional signal masked by the phosphine proton doublet at δ 1.2 ppm. These are assigned to the different ends of the ethylene ligand; the coincidence of the phosphine and one set of ethylene signals prevented the assignment of the triplet at δ 2.31 ppm by NOE means

The ethylene carbon resonances (Fig. 3.5) are observed as a triplet and a triplet of doublets at δ 21.2 ppm ($^1J_{CH}$=152.4 Hz) and 32.1 ppm ($^1J_{CH}$=149.8 Hz, $^2J_{PC}$=9.5 Hz). Again these may be assigned to the *trans* and *cis* carbons respectively. A two dimensional heteronuclear correlation experiment shows coupling between the appropriate carbon and hydrogen atoms.

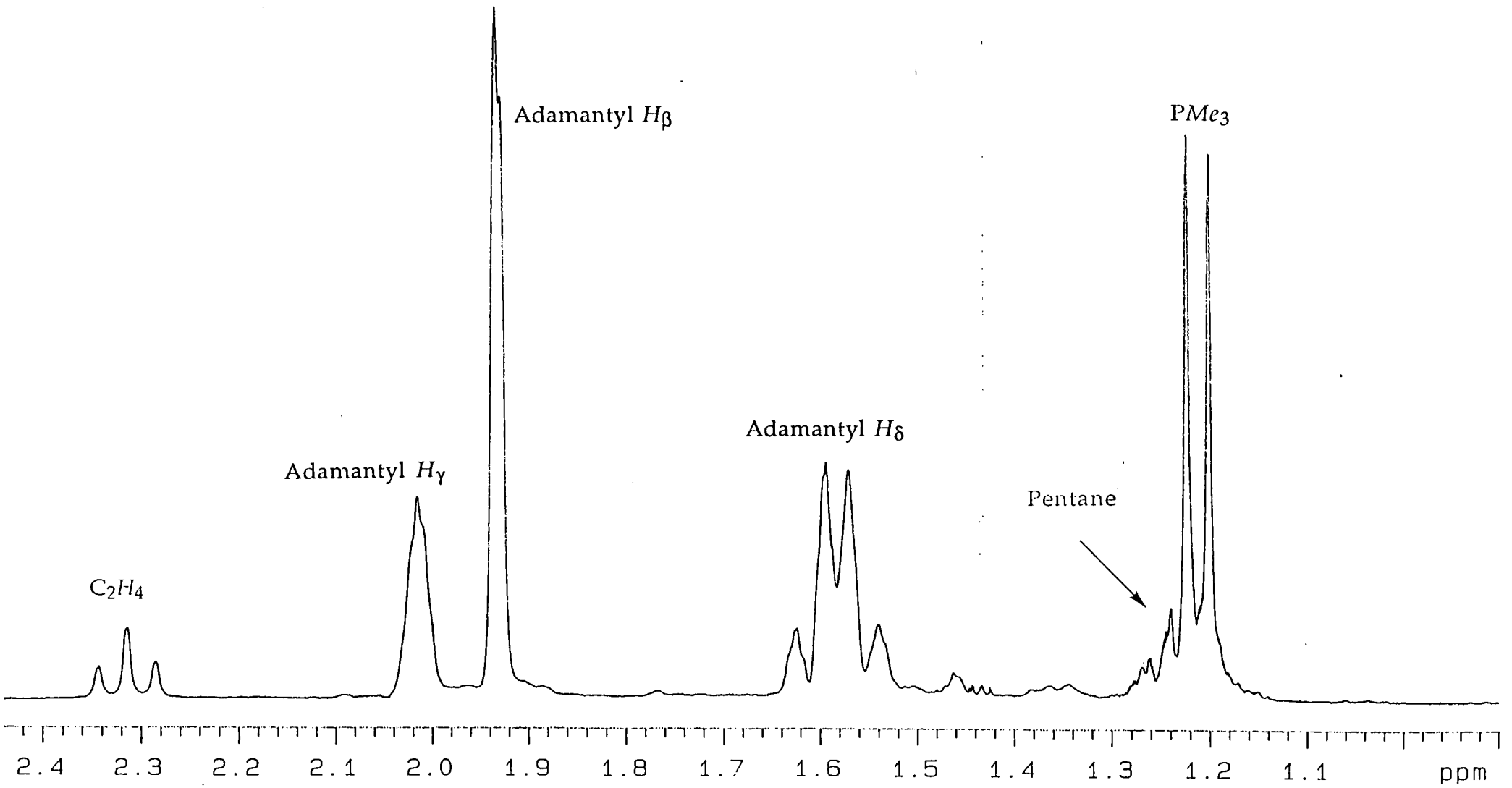

Figure 3.4: ^1H *NMR spectrum of* $Mo(NAd)_2(PMe_3)(C_2H_4)$

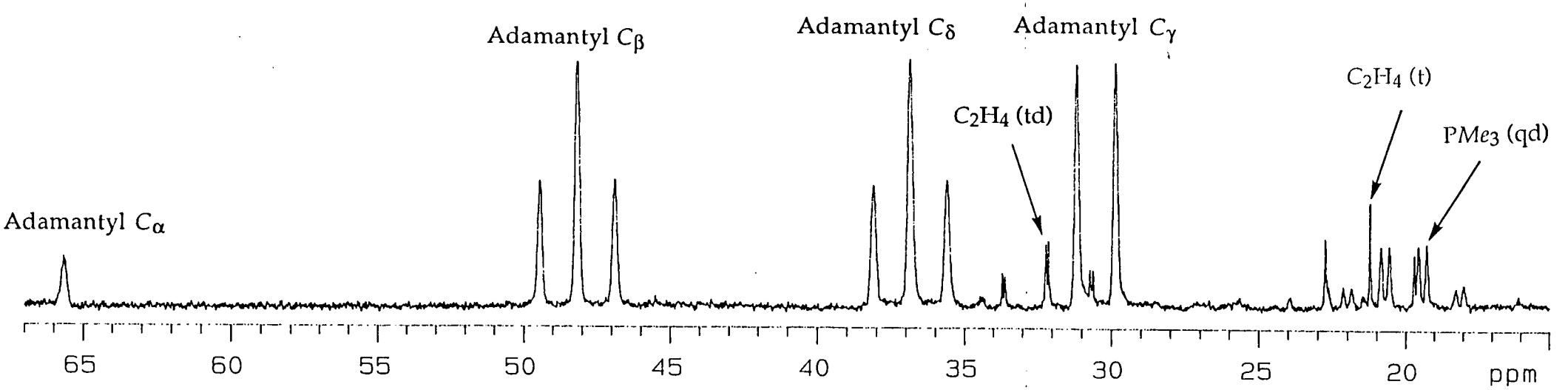

Figure 3.5: ^{13}C *NMR spectrum of* $Mo(NAd)_2(PMe_3)(C_2H_4)$.

These results are compatible with the maintainance of a four coordinate, 18 electron metallocene-like geometry as shown in figure 3.6(a). As anticipated from the similarities between the adamantyl and t-butyl groups close similarities in the ethylene ligands of this compound and those in $Mo(N\text{-}t\text{-}Bu)_2(PMe_3)(C_2H_4)$ (ref 1) are apparent. It is proposed that $Mo(N\text{-}adamantyl)_2(PMe_3)(C_2H_4)$ has a geometry similar to that observed (Fig. 3.6(b)) in the structurally characterised propene adduct[1] $Mo(N\text{-}t\text{-}Bu)_2(PMe_3)(C_3H_6)$.

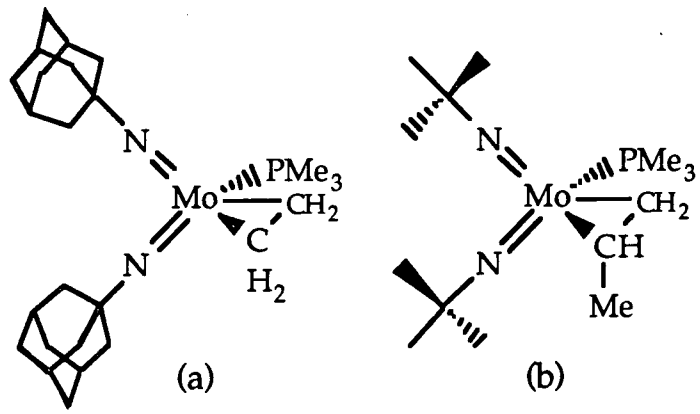

Figure 3.6

3.2.3 Synthesis of $Mo(N\text{-}2\text{-}t\text{-}BuC_6H_4)_2(PMe_3)_2(C_2H_4)$.

Olefin complexes containing the $[Mo(N\text{-}2\text{-}t\text{-}BuC_6H_4)_2]$ fragment were sought to allow comparison with the structurally characterised diisopropylphenylimido derivative $Mo(NAr)_2(PMe_3)_2(C_2H_4)$ (Figure 3.9(a)). It was anticipated that the ethene complex would prove to be a similar five coordinate, non-metallocene-like 20 electron complex.

Dark purple microcrystalline $Mo(N\text{-}2\text{-}t\text{-}BuC_6H_4)_2(PMe_3)_2(C_2H_4)$ is obtained in high yield by reaction of $Mo(N\text{-}2\text{-}t\text{-}BuC_6H_4)_2Cl_2.DME$ with two equivalents of ethylmagnesium chloride in the presence of greater than two equivalents of trimethylphosphine. Recrystallisation from diethyl ether readily affords large crystals. NMR and C,H and N atomic

analyses show the crystals to contain a small quantity of diethyl ether co-crystallised in the lattice; this is not removed by prolonged exposure to vacuum.

Both imido ligand substituents are identical in solution, indicating free rotation about the C_{ipso}-N bond. The t-butyl group provides a useful NMR handle allowing complete assignment of the aromatic protons and carbons by its NOE response and 2-D experiments. At room temperature the ethylene protons appear as a singlet (δ 1.60 ppm) (Fig. 3.7); all are equivalent by the symmetry of the complex, and the olefin is apparently bound symmetrically between the two identical trimethylphosphine ligands. Both trimethylphosphine ligands are equivalent in solution and notably the phosphine methyl proton resonance in this complex is a singlet, possibly arising due to phosphine exchange with free PMe_3. Similarly the phosphine carbon resonances (q, δ 15.6) reveal no coupling to phosphorus. In the carbon NMR spectrum (Fig. 3.8), the *ipso* carbon resonance is at a characteristically low field (δ 156.7 ppm in d_6-benzene). Both ethylene carbons are equivalent and appear as a triplet of doublets at δ 34.5 ppm; the vicinal phosphorus coupling is small (4.2 Hz) compared with that in $Mo(N\text{-adamantyl})_2(PMe_3)(C_2H_4)$ (9.5 Hz) as a result of the change in the torsion angles between the P-Mo and Mo-C bonds. These results point to a highly symmetrical structure analogous to that observed in $Mo(NAr)_2(PMe_3)_2(C_2H_4)$ (Figure 3.9(b))with the olefinic bond lying in the plane of the two metal-phosphorus bonds.

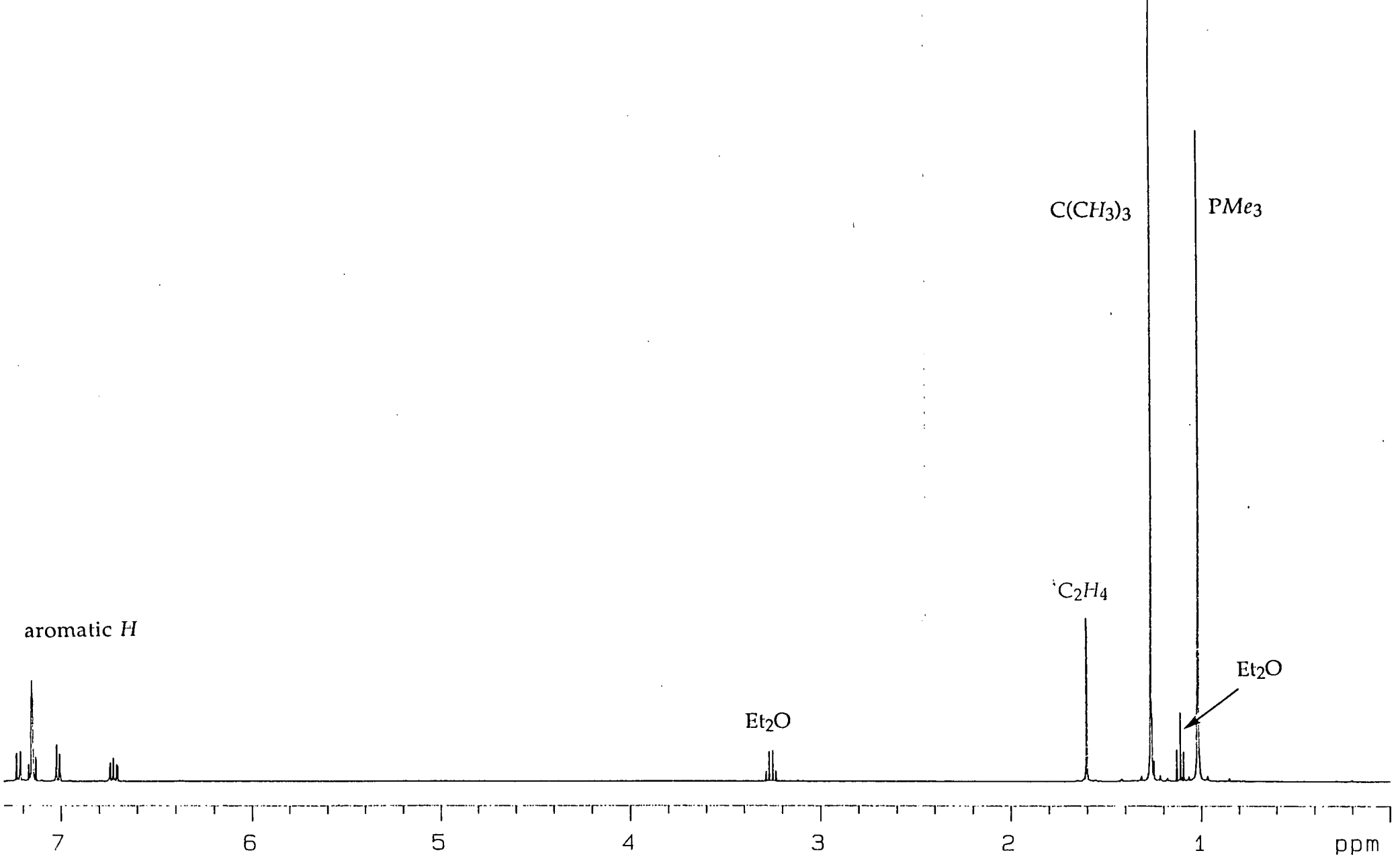

Figure 3.7: ^1H *NMR spectrum of* $Mo(N\text{-}2\text{-}t\text{-}BuC_6H_4)_2(PMe_3)_2(C_2H_4)$.

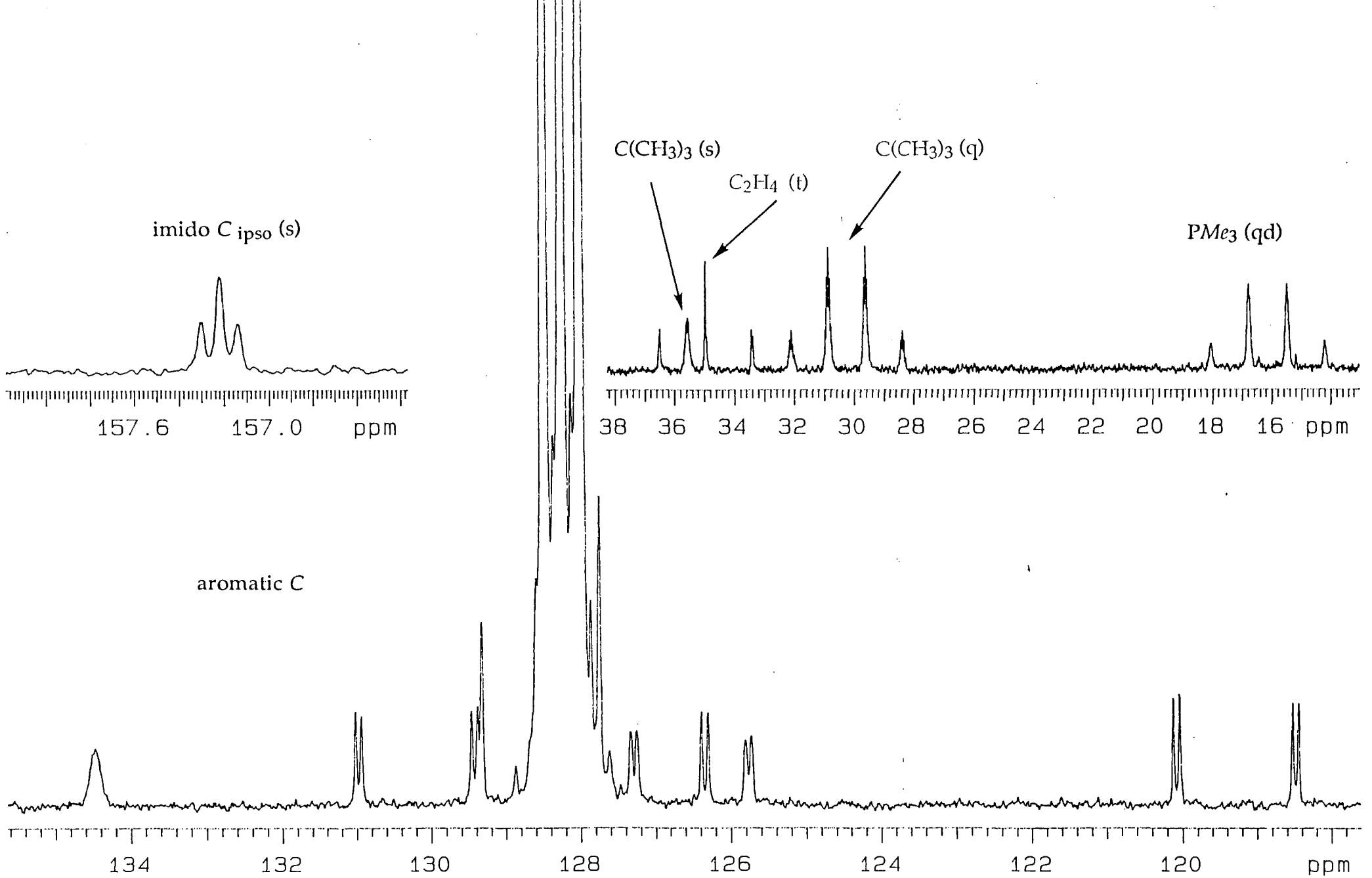

Figure 3.8: ^{13}C *NMR spectrum of* $Mo(N\text{-}2\text{-}t\text{-}BuC_6H_4)_2(PMe_3)_2(C_2H_4)$.

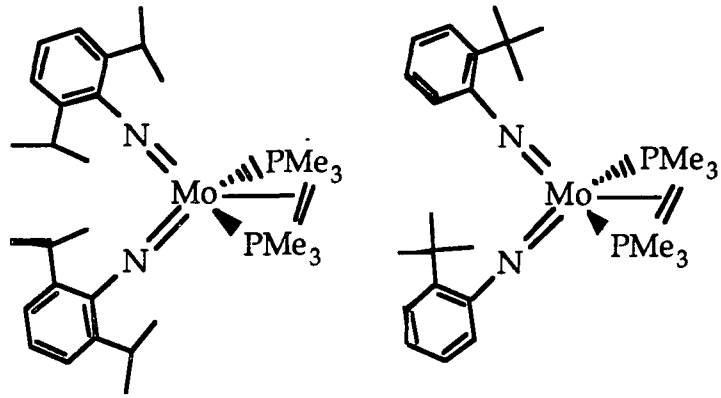

Figure 3.9

The infrared spectrum shows an olefin C=C stretch at 1415 cm^{-1}; this is to low frequency of the ~1640 cm^{-1} in free olefins and is indicative of a significant amount of back-bonding into the ethylene π^* levels thus weakening the olefinic bond.

Fenske-Hall calculations on the interactions of the four coordinate $Mo(NH)_2(PMe_3)_2$ fragment with ethylene[14] indicate that by coordinating with the olefinic bond in the MoP_2 plane, the ethylene is able to participate in d_π–π^* back-bonding. Thus the sterically unfavourable geometry is stabilised relative to the alternative of bonding in the plane of the two phosphine ligands. Additionally, back-bonding into the ethylene π^* orbitals relieves the metal centre of some electron density, this compound being formally a 20 electron species.

3.2.4 Synthesis of $Mo(NAr)(N\text{-}t\text{-}Bu)(PMe_3)(C_2H_4)$.

This complex was prepared in order to compare the behaviour of the mixed imido complex with the four coordinate metallocene like bis(t-butylimido) system and the five coordinate non-metallocene-like bis(arylimido) system.

Reaction of $Mo(NAr)(N\text{-}t\text{-}Bu)Cl_2.DME$ with two equivalents of ethylmagnesium chloride in the presence of greater than two equivalents of trimethylphosphine yielded an oily red solid. ^1H NMR analysis of this showed it to be $Mo(NAr)(N\text{-}t\text{-}Bu)(PMe_3)(C_2H_4)$; attempts to recrystallise this as a solid from a range of solvents were unsuccessful.

Resonances attributable to t-butylimido, arylimido and trimethylphosphine ligands are observed. The $C\underline{H}Me_2$ proton resonances on the aromatic ring appear as a clearly resolved septet; this contrasts with the $C\underline{H}Me_2$ proton resonance in $Mo(NAr)_2(PMe_3)_2(C_2H_4)$ which is unresolved owing to hindered rotation about the $N\text{-}C_{ipso}$ bond. No signals attributable to ethylene protons are observable at room temperature; they are broadened into the baseline by a fluxional process; this contrasts with the bis(t-butylimido) ethene complex which is conformationally rigid on the NMR timescale. Some support for the existence of an ethylene ligand comes from the infrared spectrum of this compound which shows an absorbance at 1415 cm^{-1}, assignable to the C=C stretch. A subsequent experiment (section 5.2) shows that ethylene is displaced by diphenylacetylene in this complex, leading to the presence of free ethylene in the sealed system (by ^1H NMR). This provides conclusive proof for the presence of ethylene in this complex.

Variable temperature proton NMR studies were carried out between -80°C and +70°C in d_8-toluene in order to discern the nature of these fluxional processes. The relevant parts of the spectra obtained are collected in figure 3.10.

At the low temperature limit, the i-Pr doublet (δ 1.32 ppm), the t-Bu singlet (δ 1.36 ppm) and the trimethylphosphine doublet (0.93 ppm) are all apparent. In addition, two poorly resolved triplets are present at δ

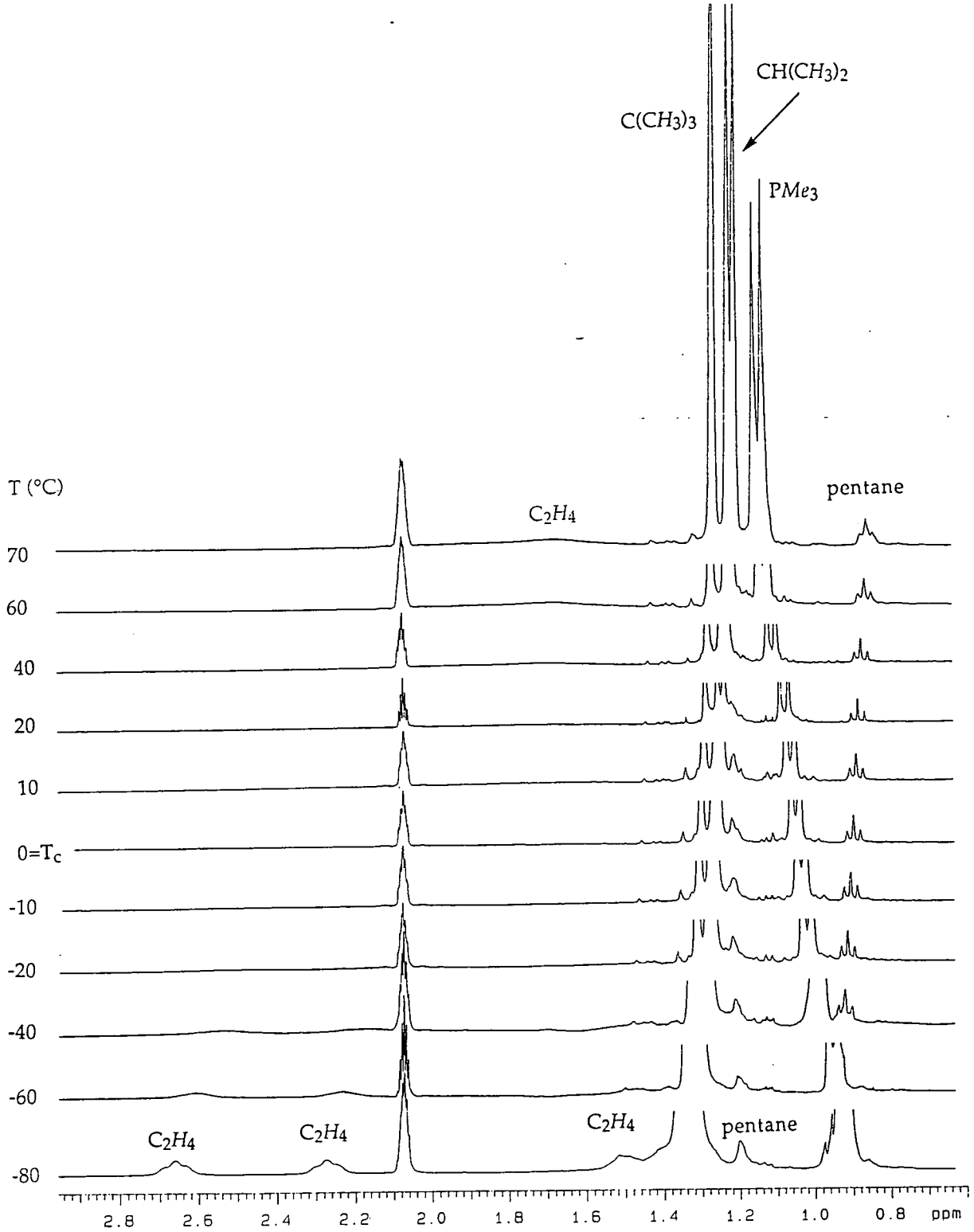

Figure 3.10: *Temperature dependance of* ^1H *NMR spectra of* $Mo(NAr)(N\text{-}t\text{-}Bu)(PMe_3)(C_2H_4)$.

2.66 ppm and 2.38 ppm; these integrate to one proton each. Two other signals are partially hidden under the the i-Pr doublet and the t-Bu singlet (1.52 ppm and ca. 1.3 ppm). The resonance at 1.52 ppm has been confirmed as being coupled to that at 2.66 ppm by a homonuclear decoupling experiment, however, a similar experiment failed to provide comfirmation that the more thoroughly masked signal at 1.3 ppm is associated with the ethylene ligand.

As the temperature increases the chemical shift of the ethylene proton signals moves to high field. This shift would at first sight appear to indicate a longer residence time for the ethylene on the metal at high temperature; the corollary to this is that at low temperature the ethylene spends less time strongly bound to the metal, and as such its protons appear to resonate in an artificially low field, slightly toward that of free ethene. At the high temperature limit (allowing for the change in shifts through solvent effects of ca. 0.25 ppm to high field) they coalesce at the mid point of all four signals (δ 1.7 ppm).

In addition to the ethylene coalescence, the most noticeable feature of the spectrum is the movement of the trimethylphosphine resonance, which in this temperature range moves to low field by ca. 0.25 ppm. This again at first sight would appear to indicate stronger coordination of the phosphine at high temperatures. However a more likely explanation is that the PMe_3 and ethylene ligands are exposed to substantially different localised magnetic fields as the aryl substituent is freed to rotate.

Carbon spectra of Mo(NAr)(N-t-Bu)(PMe_3)(C_2H_4) recorded at room temperature show no signals attributable to the ethylene carbon atoms. The low temperature spectrum does, however, successfully allow two resonances attributable to the ethylene carbon atoms to be located. These

have chemical shifts of 35.6 ppm (d, $^2J_{PC}$=10 Hz) and 27.3 ppm (singlet), values comparable with those observed for $Mo(NAd)_2(PMe_3)(C_2H_4)$; unequal spin-spin coupling between the phosphorus and carbon atoms in the NMR is observed and therefore is consistent with a metallocene like ground state (Fig3.11).

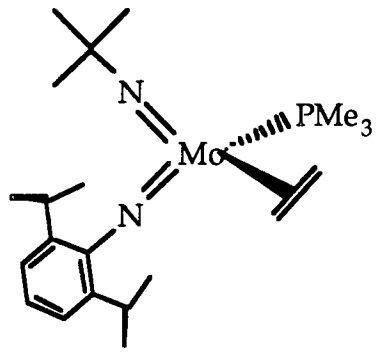

Figure 3.11

It is interesting to note that the ethylene proton resonances coalesce to a broad singlet. Such a coalescence pattern suggests that, at the freely rotating high temperature limit, all the protons of the ethylene are equivalent. In the usual mode of olefin rotation about the metal-olefin bond, it is not possible to fulfil such a condition in this complex because it is chiral. A Newman projection (Fig. 3.12(a)) down the olefin-metal bond demonstrates this point; when the ethylene rotates freely about this bond, two diastereotopic pairs of protons exist: A/A′ and B/B′. Never during such a rotation do the A pair and B pair interchange, thus at the high temperaure limit an AA′BB′ pattern should be observed in the proton NMR spectrum. An example of such behaviour is known[15] in the chiral chromium complex $Cr(CO)(NO)(Cp)(C_2H_4)$ (Fig. 3.12(b)). In the low temperature limit the ethylene protons are all different, their resonances appear as an ABCD pattern; the high temperature limit coalesces to an AA′BB′ pattern from the two pairs of protons. The energy barrier to rotation of the olefin in this complex is 11.4 kcal mol^{-1}. The fact that the

proton resonances in Mo(NAr)(N-t-Bu)(PMe_3)(C_2H_4) coalesce to a singlet indicative of an A_4 system suggests that an additional averaging process must be occuring to exchange the A and B sites. This could either be as a result of rotation about the C-C axis or alternatively, and perhaps more likely via dissociation and re-coordination of the ethylene.

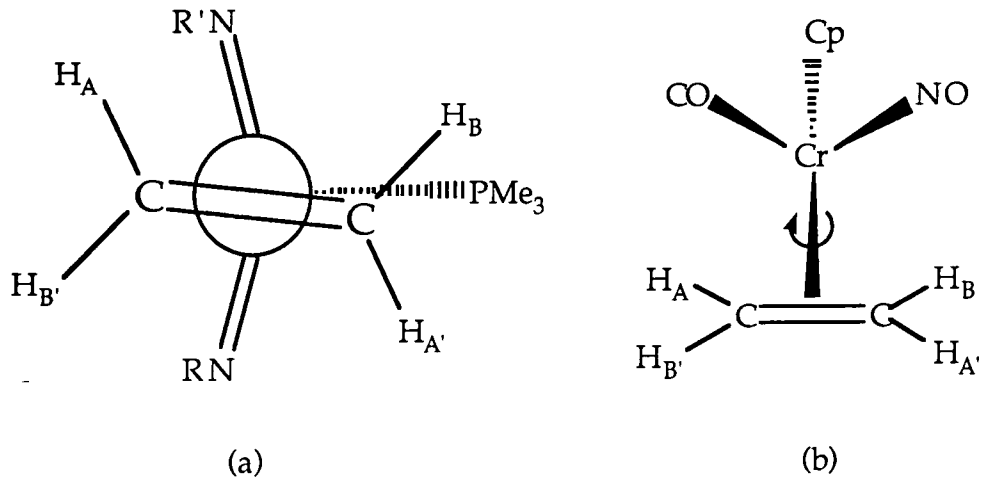

Figure 3.12

The differences in the resonant frequencies of the ethylene protons in Mo(NAr)(N-t-Bu)(PMe_3)(C_2H_4) is approximately 460 Hz; this corresponds[16] (Eqn 3.6 a) to a rate constant, k_c, for olefin rotation of 1030 s^{-1}. The observed coalescence temperature, T_c, is 273K; with k_c this allows calculation (Eqn 3.6 b) of a free energy of activation for olefin rotation in this complex of 12.2 kcal mol^{-1}. This value is near to that observed in the chromium complex mentioned above.

$$k_c = \Delta\nu\, \pi/\sqrt{2} \quad (s^{-1}) \quad \text{(Eqn 3.6 a)}$$

$$\Delta G\dagger = 4.57\, T_c\, (10.32 + \log T_c - \log k_c) \quad (\text{cal mol}^{-1}) \qquad \text{(Eqn 3.6 b)}$$

3.3 Molybdenum bis(imido) propene complexes.

It is known that the bis(t-butylimido) fragment will coordinate propene in a four coordinate metallocene-like environment[13] (Fig. 3.4(b)

above). Reaction of $Mo(NAd)_2Cl_2$.DME with n-PrMgCl and PMe_3 was carried out in an attempt to obtain a compound analogous to the stucturally characterised $Mo(N\text{-}t\text{-}Bu)_2(PMe_3)(C_3H_6)$. The reaction followed the same procedure as the synthesis of ethylene adducts, and after recrystallisation only a small amount of somewhat impure material was obtained. This was analysed by NMR methods (200 MHz ^1H; 100 MHz $^{13}C\{^1H\}$) which supported the formulation $Mo(NAd)_2(PMe_3)(CH_2{=}CHMe)$ (Fig. 3.13). These spectra contain two superimposed sets of signals, particularly apparent from the phosphine and $CH_2{=}CH\mathit{Me}$ protons, and are attributed to two isomers present in differing ratios.

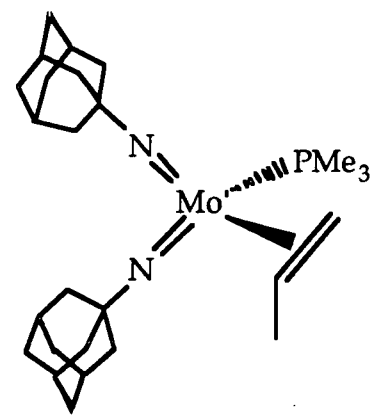

Figure 3.13

The reaction between $Mo(N\text{-}2\text{-}t\text{-}BuC_6H_4)_2Cl_2$.DME with n-PrMgCl and PMe_3 was carried out to allow comparison with the bis(arylimido) system whose propene adduct is unstable to vacuum, affording[1] $Mo(NAr)_2(PMe_3)_2$. During reaction the mixture became intense purple in colour similar to that observed in the synthesis of $Mo(N\text{-}2\text{-}t\text{-}BuC_6H_4)_2(PMe_3)_2(C_2H_4)$. After extraction of the product and drying under vacuum overnight, the solid obtained was dark green in colour. Two recrystallisations yielded a small quantity of dark green crystals. ^1H NMR showed these to be still impure, however it is possible to assign the

complex as $Mo(N\text{-}2\text{-}t\text{-}BuC_6H_4)_2(PMe_3)_2$ (Fig. 3.14). The spectrum shows no sign of any bound propene, and owing to their labile binding, the phosphine proton resonance is particularly broad at room temperature (ca.32 Hz). Levels of impurity in this compound were such that no further analysis was carried out.

Variable NMR studies on this phosphine resonance at 1.06 ppm showed narrowing as temperature was reduced and eventual appearance of a doublet at 1.25 ppm ($^2J_{HH}$=8 Hz). This behaviour suggests that the broadening of the trimethylphophine proton resonance is due to ligand dissociation; at low temperatures this is retarded and the resonance narrows.

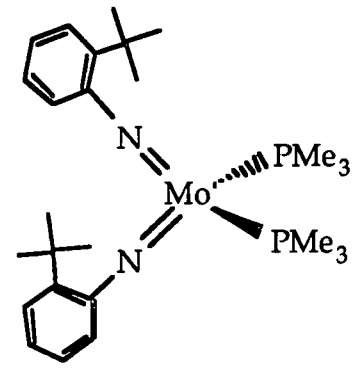

Figure 3.14

3.4 Magnesium reductions of $Mo(NR)_2Cl_2.DME$

Metallocene dichloride complexes and half-sandwich imido niobium dichoride complexes may be reduced in the presence of trimethylphosphine. By analogy $Mo(NR)_2Cl_2.DME$ may be reduced with magnesium metal in the presence of trimethylphosphine[1].

Reduction of $Mo(NAd)_2Cl_2.DME$ with magnesium metal in the presence of PMe_3 was attempted in view of the similarities observed for the ethylene and propene adducts with those of the $Mo(N\text{-}t\text{-}Bu)_2$

fragment. By analogy with the product of the reduction[1] of $Mo(N\text{-}t\text{-}Bu)_2Cl_2.DME$ it was anticipated that the binuclear complex $(NAd)(PMe_3)Mo(\mu\text{-}NAd)_2Mo(NAd)(PMe_3)$ might be formed. Several attempts at this reaction were made, all resulting in unidentifiable products.

$Mo(NAr)_2Cl_2.DME$ may be reduced with magnesium in the presence of trimethylphosphine[1,17] affording synthetically useful $Mo(NAr)_2(PMe_3)_2$. The analogous complex $Mo(N\text{-}2\text{-}t\text{-}BuC_6H_4)_2(PMe_3)_2$ (Fig. 3.14) was produced by ligand dissociation from the propene adduct, thus it was expected to be readily accessible via magnesium reduction.

Reaction of $Mo(N\text{-}2\text{-}t\text{-}BuC_6H_4)_2Cl_2.DME$ with magnesium in the presence of PMe_3 afforded dark green solid in good yield. ^1H NMR analysis shows the complex to be identical to that obtained in the reaction of $Mo(N\text{-}2\text{-}t\text{-}BuC_6H_4)_2Cl_2.DME$ with n-PrMgCl and PMe_3; i.e $Mo(N\text{-}2\text{-}t\text{-}BuC_6H_4)_2(PMe_3)_2$. Again the complex was difficult to purify, and no further analysis was undertaken.

Reactions of $Mo(N\text{-}2\text{-}t\text{-}BuC_6H_4)_2(PMe_3)_2$.

(a) With Ethylene.

Reaction on a 30 mg scale of $Mo(N\text{-}2\text{-}t\text{-}BuC_6H_4)_2(PMe_3)_2$ with excess free ethylene was carried out in benzene, producing a purple solution. ^1H NMR analysis shortly after thawing showed signals identical to those seen for $Mo(N\text{-}2\text{-}t\text{-}BuC_6H_4)_2(PMe_3)_2(C_2H_4)$, with free excess ethylene. The coordination of ethylene occurred quickly and completely.

(b) With propene.

As a parallel with the reaction above, excess free propene was introduced to a benzene solution of $Mo(N\text{-}2\text{-}t\text{-}BuC_6H_4)_2(PMe_3)_2$. The initially green solution became deep purple on thawing, this colour change is identical to that observed in reaction with free ethylene. ^1H NMR analysis shortly after thawing showed a marked change in signals from those of $Mo(N\text{-}2\text{-}t\text{-}BuC_6H_4)_2(PMe_3)_2$.

The phosphine proton resonance changes shift and becomes a sharp singlet, consistent with the cessation of the fluxional processes on coordination of the propene. The t-Bu signals in the proton spectrum are also shifted. Bound propene is apparent as a doublet (CH_2=CH<u>Me</u>) at 1.98 ppm; the remaining propene signals are swamped by the impurities in the $Mo(N\text{-}2\text{-}t\text{-}BuC_6H_4)_2(PMe_3)_2$ starting material. No free phosphine is observed in the spectrum; it is proposed that the reaction has produced $Mo(N\text{-}2\text{-}t\text{-}BuC_6H_4)_2(PMe_3)_2(CH_2{=}CHMe)$ (Fig. 3.15). Levels of impurity were such that no carbon spectra were obtained.

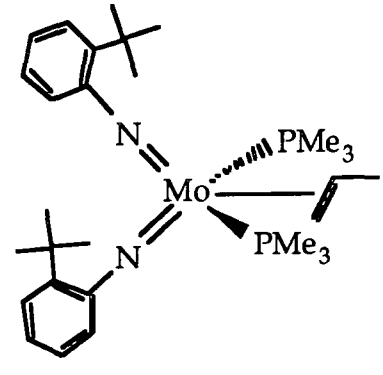

Figure 3.15

3.5.Summary

The $[Mo(N\text{-}2\text{-}t\text{-}BuC_6H_4)_2]$ system shows close comparison with the $[Mo(NAr)_2]$ system studied by Mr P.W. Dyer. The ethylene adduct is a non-metallocene-like five coordinate 20 electron complex. The propene adduct is similar, however exposure to vacuum produces $Mo(N\text{-}2\text{-}t\text{-}BuC_6H_4)_2(PMe_3)_2$ by dissociation of propene. Magnesium reduction affords $Mo(N\text{-}2\text{-}t\text{-}BuC_6H_4)_2(PMe_3)_2$ in good yield. This coordinates gaseous ethylene and propene.

The $[Mo(NAd)_2]$ system is comparable with the $[Mo(N\text{-}t\text{-}Bu)_2]$ system investigated by Mr P.W. Dyer. The ethylene adduct is a metallocene-like four coordinate 18 electron complex. The propene adduct is an analogous metallocene-like four coordinate 18 electron complex.

The Mo(NAr)(N-t-Bu) system is an interesting "half-way house" between metallocene-like and non-metallocene-like behavoir. The ethylene adduct is a fluxional complex. Its ground state is a metallocene-like four coordinate 18 electron complex.

Further studies on the complexes discussed in this section might include exchange reactions replacing olefins with other L-type ligands, or reactions of the four coordinate complex $Mo(N\text{-}2\text{-}t\text{-}BuC_6H_4)_2(PMe_3)_2$ with a variety of other species.

	$Mo(NAd)_2(PMe_3)(C_2H_4)$[a]	$Mo(N\text{-}2\text{-}tBuC_6H_4)_2(PMe_3)_2(C_2H_4)$[a]	$Mo(NAr)(N\text{-}tBu)(PMe_3)(C_2H_4)$	
			ground state[bc]	freely rotating[bc]
C_2H_4 (cis)	2.31 t	1.61 s	2.66 & 2.37	1.7 broad
(trans)	1.24 t		1.50 & 1.3	
C_2H_4 (trans)	21.2 t	34.5 td $^2J_{PC}$=4.2 Hz	27.3	not observed
(cis)	32.1 td $^2J_{PC}$=9.5 Hz		35.5 $^2J_{PC}$=ca.10 Hz	
Imido C(ipso)		156.7 s	153.6	154.2
C(quarternary)	65.6 s		65.0	66.8
Phosphine CH_3	1.21 d	1.02 s	0.92 d	1.16 d
CH_3	20.1 qd	15.9 q	18.3 d	18.5 d

[a] Shifts reported in C_6D_6 as a solvent.
[b] Shifts reported in C_7D_8 as a solvent.
[c] Carbon resonances quoted from proton decoupled spectra.

Table 3.1 *Comparison of selected NMR data for the ethylene complexes synthesised.*

3.6 References.

1. P.W. Dyer, Thesis, 1993.
2. A.D. Poole, Thesis, 1992.
3. S.A Cohen, P.R. Auburn, J.E. Bercaw, *J. Am. Chem. Soc.*, 1983, **105**, 1136.
4. J.W. Lauher, R. Hoffmann, *J. Am. Chem. Soc.*, 1976, **98**, 1729.
5. M.D. Rausch, H.G. Alt, M. Herberhold, U. Thewalt, B. Wolf, *Angew. Chem. Int. Ed. Engl.*, 1985, **24**, 394.
6. T. Takahashi, D.R. Swanson, E.-i. Negishi, *Chem. Lett.*, 1987, 623.
7. S.L. Buchwald, B.T Watson, J.C. Huffmann, *J. Am. Chem. Soc.*, 1987, **109**, 2544.
8. H.G. Alt, C.E Denner, U. Thewalt, M.D. Rausch, *J. Organomet. Chem.*, 1988, **356**, C83.
9. S.L. Buchwald, K.A. Kreutzer, R.A. Fisher, *J. Am. Chem. Soc.*, 1990, **112**, 4600.
10. A.D. Poole, V.C. Gibson, W. Clegg, *J. Chem. Soc., Chem. Commun.*, 1992, 237.
11. D.S. Williams, M.H. Schofield, J.T. Anhaus, R.R. Schrock, *J. Am. Chem. Soc.*, 1990, **112**, 6728.
12. D.S Williams, M.H. Schofield, R.R. Schrock, Organometallics, in press.
13. P.W. Dyer, V.C. Gibson, J.A.K. Howard, B. Whittle, C. Wilson, *J. Chem. Soc., Chem. Commun.*, 1992, 1666.
14. C.E. Houscroft, L.C. Parlett to V.C. Gibson, Private Communication.
15. A.H. Helmut, M. Herberhold, C.G. Kreiter, H. Strack, *J. Organomet. Chem.*, 1974, **77**, 353.
16. William Kemp, "NMR in Chemistry : A Multinuclear Introduction", Macmillan Education Ltd.,1986
17. P.W. Dyer, V.C. Gibson, J.A.K. Howard, C. Wilson, In press.

CHAPTER FOUR.

Molybdenum Bis(imido) Di(phenyl) Complexes.

4.1 Metallocene-like diaryl and benzyne complexes.

An increasing number of mononuclear η^2-benzyne complexes are known[1]. These complexes range from being isolable, structurally characterised species containing discrete η^2-C_6H_4 units to ephemeral intermediates whose existence is demonstrated by their trapping reactions with other compounds. The benzyne ligand possesses two orthogonal π-systems[2], and so can act as a two or four electron donor. When donating two electrons to a metal centre, the aromatic π-system is essentially undisturbed; as a four electron donor the aromatic π-system is disrupted and so the inter-ring carbon distances are perturbed.

Group 4 metallocene benzyne adducts are available from the thermolysis of diaryl precursors. Diaryltitanocenes may be made by reaction of titanocene dichloride with two equivalents of phenyllithium; several studies on the thermolysis and photolysis of these compounds have been carried out[3,4]. As early as 1970, it was suggested that a benzyne intermediate occured in the themolysis reactions of diphenyltitanocene with diphenylacetylene[5] and with carbon dioxide[6] (Scheme 4.1).

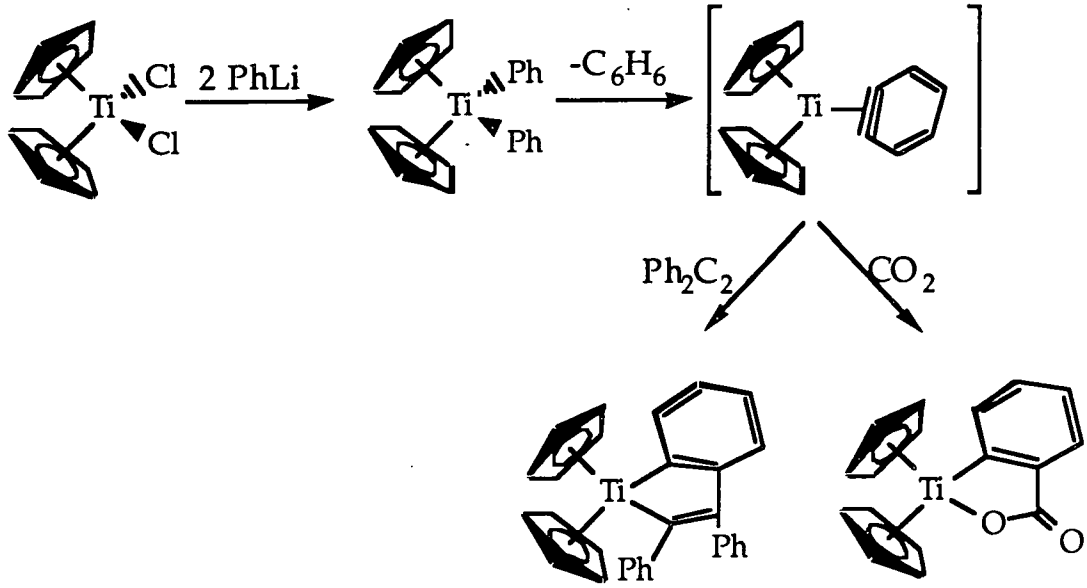

Scheme 4.1

Diarylzirconocenes may be made by the same reaction. These complexes have been shown[7] to undergo successive replacement of σ-aryl ligands by aryl groups from the solvent, and photochemical degradation forms a range of biphenyls via intermediate arynezirconocene complexes. Further studies[8,9] have demonstrated the trapping of a zirconocene benzyne (Eqn. 4.1) with alkenes resulting in the formation of zirconaindans.

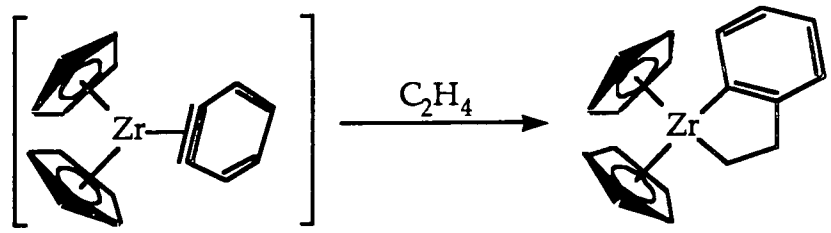

Equation 4.1

The trimethylphosphine adduct has been structurally characterised[10] (Eqn 4.2). This complex was isolated from thermolysis of diphenylzirconocene in the presence of excess trimethylphosphine.

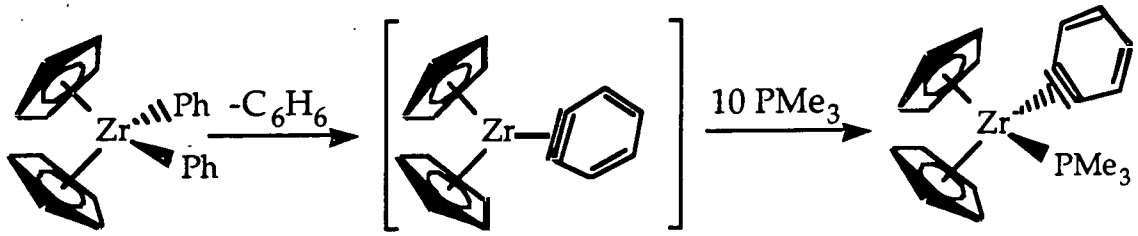

Equation 4.2

This complex, in contrast to $Cp^*TaMe_2(\eta^2\text{-}C_6H_4)$[11], does not show the short-long alternation of single and double bonds indicative of electron donation from the orthogonal π system. Distortion in the coordination of the benzyne is apparent due to crowding by the phosphine. Bond angles within the benzyne indicate minimal ring strain.

A wide range of other methods of trapping benzynes are known, two interesting examples involve the use of elemental selenium[12], or methylenetriphenylphosphorane[13] (Eqns 4.3).

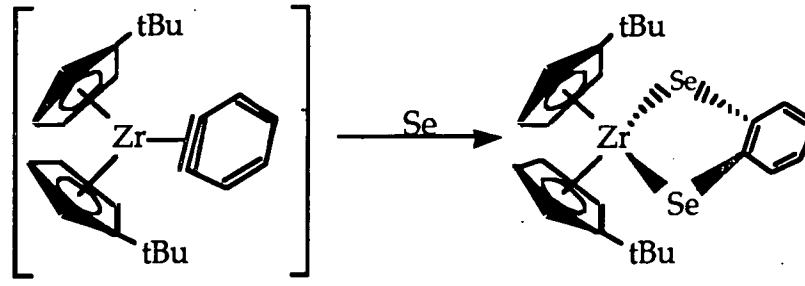

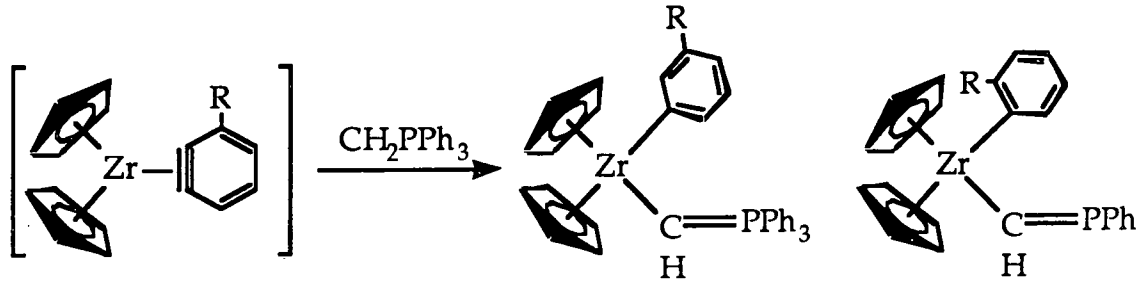

Equations 4.3

Work in this group on group 5 half-sandwich imido systems[14] resulted in the formation of phenyl adducts and the subsequent isolation and structural determination of a benzyne complex[15] (Eqn. 4.4). Notably in this complex the phosphine protons resonate at low frequency, upfield of even free trimethylphosphine. This is attributed to ring current effects associated with the phenyl rings.

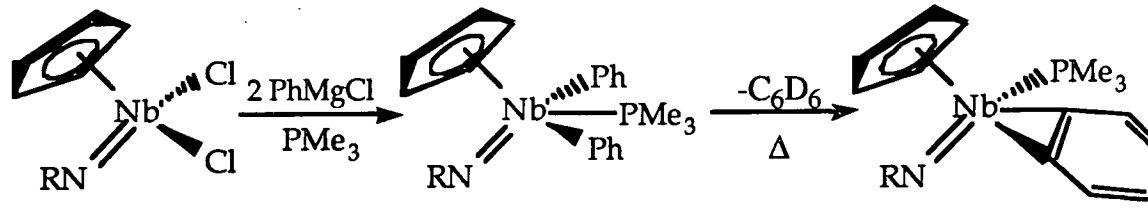

Equation 4.4

Structural determination of this complex highlights remarkable similarities to $Cp_2Zr(\eta^2\text{-}C_6H_4)(PMe_3)$. Indications are that back-bonding into π^* benzyne orbitals is strong and, by virtue of the isolobal relationship, their geometries are similar. This benzyne however is relatively unreactive; no reaction is observed with ethene, carbon monoxide or acetonitrile.

Molybdenum bis(imido)di(phenyl) complexes $[Mo(NR)_2(Ph)_2(PMe_3)]$ have been targeted as potential precursors to molybdenum bis(imido)(η^2-benzyne) complexes of the type $(Mo(NR)_2(\eta^2\text{-}C_6H_4)(PMe_3))$ (Eqn 4.5). Having precedent in group four metallocenes, as highlighted in this introduction, such compounds are potentially useful in coupling reactions.

Synthesis of a range of compounds of molybdenum di(phenyl) complexes of the type $Mo(NR)_2(Ph)_2(PMe_3)$ has been carried out by reduction of $Mo(NR)_2Cl_2$.DME with phenylmagnesium chloride in the presence of trimethylphosphine[16] (Eqn. 4.5). This reaction is ostensibly that used to produce the ethene and propene adducts of Section 3, however, at room temperature, the reaction produces the 18 electron complexes $Mo(NR)_2(Ph)_2(PMe_3)$ with two σ-bound phenyl ligands. Subsequent elimination of benzene if it occurs, requires elevated temperatures (Eqn 4.6). In many cases such thermoysis simply decomposes the product.

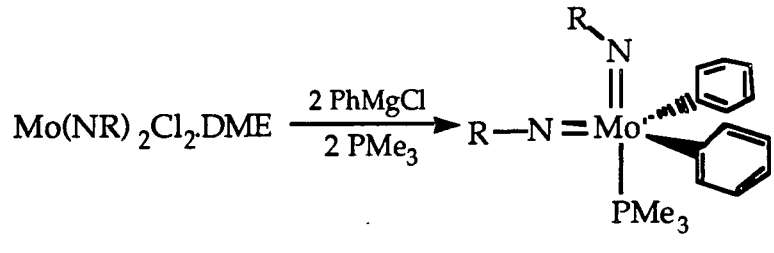

Equation 4.5

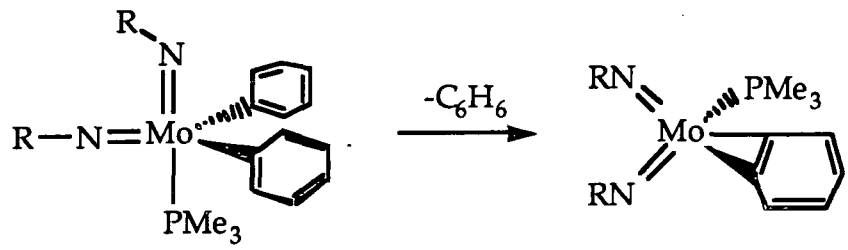

Equation 4.6

The structure of $Mo(NAr)_2(Ph)_2(PMe_3)$[17] reveals a non-metallocene-like distorted trigonal bipyramid. Unexpectedly the imido ligands occupy axial and equatorial sites, bond lengths are consistent with pseudo-triple bonds.

4.2 Synthesis of $Mo(N\text{-}2\text{-}t\text{-}BuC_6H_4)_2(Ph)_2(PMe_3)$.

$Mo(N\text{-}2\text{-}t\text{-}BuC_6H_4)_2Cl_2$.DME was reacted with phenylmagnesium chloride in the presence of trimethylphosphine resulting in the formation of a dark green solid. Recrystallisation from pentane yielded red cubic crystals. NMR studies and elemental (CHN) analyses are consistent with the stoichiometry for $Mo(N\text{-}2\text{-}t\text{-}BuC_6H_4)_2(Ph)_2(PMe_3)$. For the purposes of comparison, relevant NMR shifts for two derivatives are presented in table 4.1.

From the proton spectrum (Fig. 4.1), the imido ligands are equivalent, as are the phenyl groups. As for $CpNb(NAr)(\eta^2\text{-}C_6H_4)(PMe_3)$ the phosphine methyl protons occur at particulary high field (δ 0.60 ppm) as do the carbons (δ 12.6 ppm); this is attributed to ring current effects from the close phenyl ligands. A proton-proton COSY experiment (Fig. 4.2) reveals coupling between the three types of phenyl protons (δ 7.77-7.22-7.09 ppm) and the

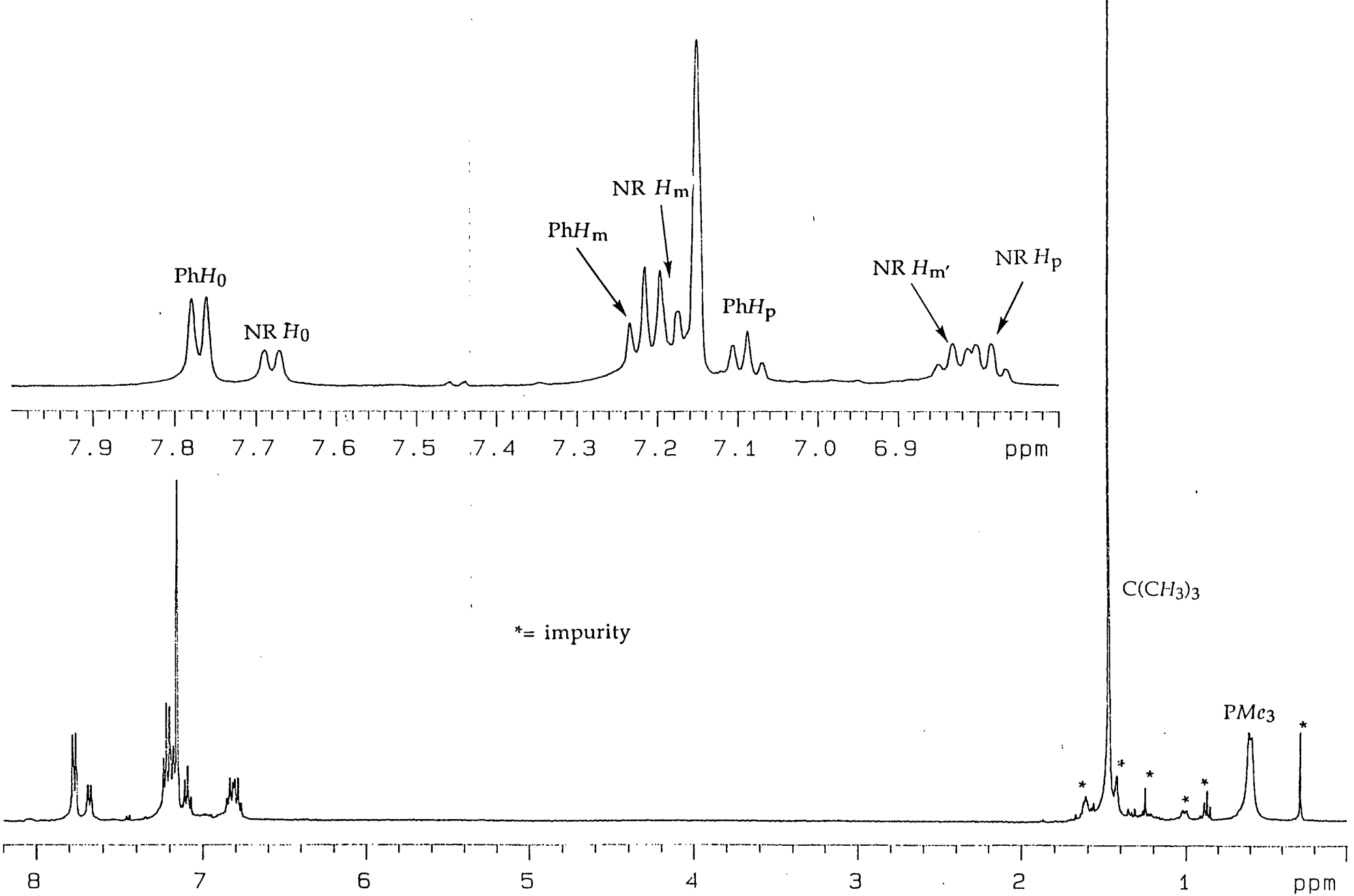

Figure 4.1: ^1H *NMR spectrum of* $Mo(N\text{-}2\text{-}t\text{-}BuC_6H_4)_2(Ph)_2(PMe_3)$.

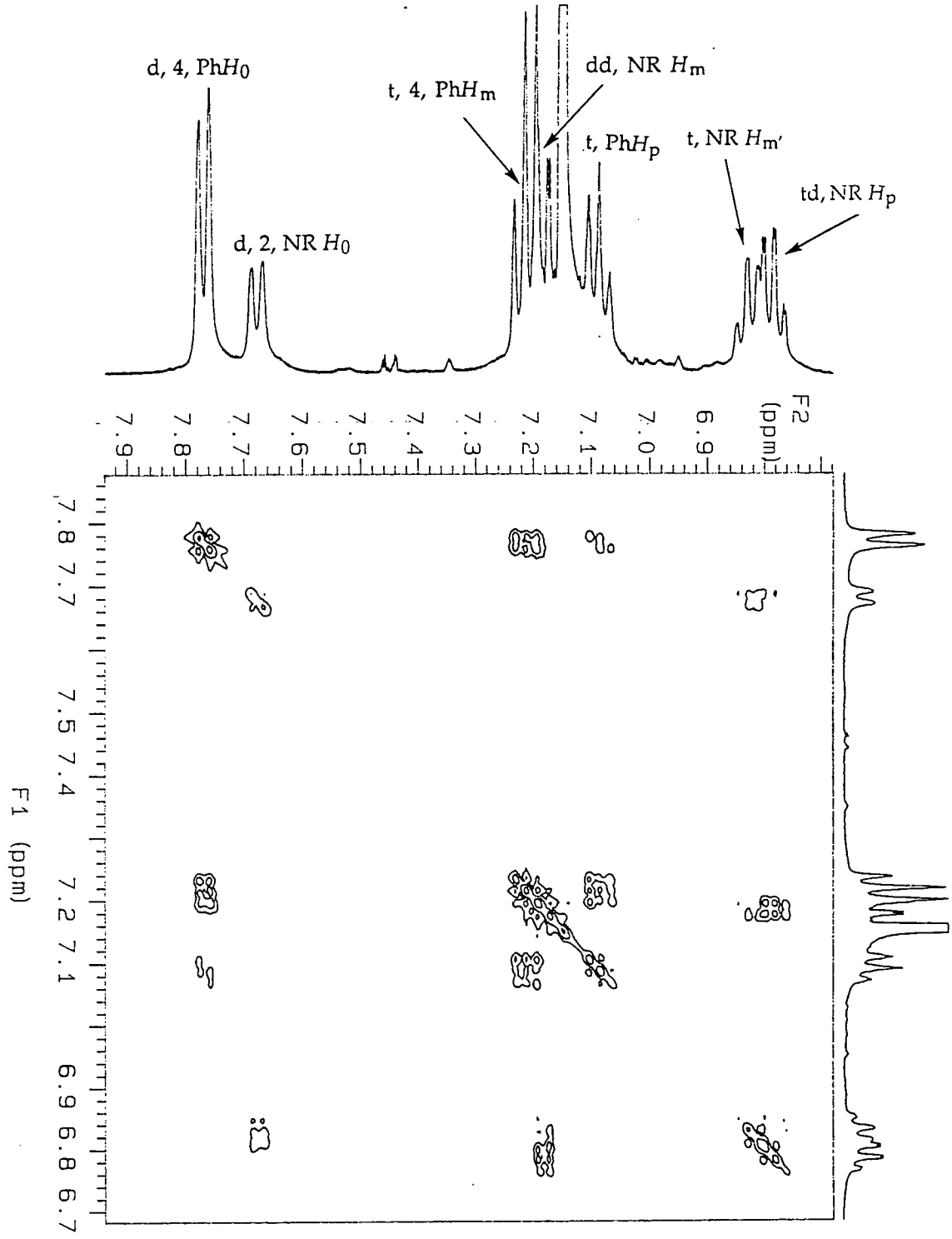

Figure 4.2: ^1H-^1H *COSY spectrum for the aromatic region of* $Mo(N\text{-}2\text{-}t\text{-}BuC_6H_4)_2(Ph)_2(PMe_3)$.

remaining four types of imido substituent aromatic protons (δ 7.68-6.84 & 6.78-7.18 ppm).

In the carbon spectrum, the phenyl ipso carbon resonance is at characteristically high field (δ 174 ppm); this is indicative of substantial deshielding upon binding to the metal. Some of the aromatic carbon resonances are masked by solvent.

The equivalence of the imido and phenyl groups on the NMR timescale suggests that the molecule is highly fluxional in solution, averaging occuring via ligand rotation and possibly also via pseudo-rotation. There is no reason to expect the compound to exist in the solid phase in a geometry different from that observed in $Mo(NAr)_2(Ph)_2(PMe_3)$. All data is consistent with the product being the five coordinate, 18 electron complex shown (Fig. 4.3).

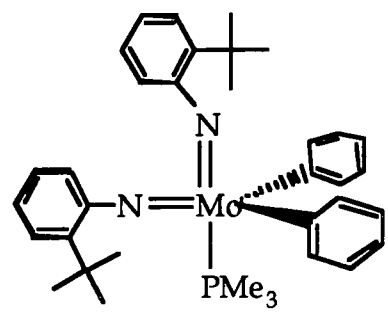

Figure 4.3

A sample of $Mo(N\text{-}2\text{-}t\text{-}BuC_6H_4)_2(Ph)_2(PMe_3)$ was heated to 60°C in d_6-benzene in the hope of forming a benzyne by elimination of benzene. A marked change in the ^1H NMR was observed.

The trimethylphosphine proton resonance moved downfield to 1.12 ppm and the t-butyl signal to 1.36 ppm. The phenyl proton resonances have

changed markedly; those assigned as H_{ortho} have been lost. Signals in the aromatic region are complex, and not clearly indicative of a benzyne ligand. A relatively clean transformation occurred, however it was not possible to identify the products.

4.3 Synthesis of $Mo(N\text{-}t\text{-}Bu)(NAr)(Ph)_2(PMe_3)$.

$Mo(N\text{-}t\text{-}Bu)(NAr)Cl_2.DME$ was reacted with phenylmagnesium chloride in the presence of trimethylphosphine resulting in the formation of a dark brown-yellow solid. Recrystallisation from pentane yielded pink-brown crystalline material. Elemental (CHN) analysis and NMR observations are consistent with the anticipated product $[Mo(N\text{-}t\text{-}Bu)(NAr)(Ph)_2(PMe_3)]$. For comparative purposes some relevant NMR shifts are presented in Table 4.1.

Proton NMR experiments show both phenyl ligands to be equivalent. Both isopropyl groups on the imido ligands are equivalent due to fast rotation about the $N\text{-}C_{ipso}$ bond on the NMR timescale. Again the trimethylphosphine protons and carbons (δ 14.5 ppm) resonate at particularly high field.

The carbon NMR spectra show the phenyl ipso carbon at characteristically low field (δ 174 ppm); this value is similar to that observed in $Mo(N\text{-}2\text{-}t\text{-}BuC_6H_4)_2(Ph)_2(PMe_3)$ above; again is indicative of the metal having a deshielding effect on the phenyl ligands. These spectra for this compound were run in d_{12}-cyclohexane as a solvent, so all aromatic carbons are clearly observed. A sample of this compound run in d_6-benzene showed that this change of solvent had minimal effects on chemical shifts of the carbon atom resonances.

The mass spectrum of this compound gives an envelope centred at m/z 492-502. Since the masses of PMe_3 and C_6H_5 are similar this may correspond to either the daughter fragment [Mo(N-t-Bu)(NAr)$(Ph)_2$] or [Mo(N-t-Bu)(NAr)(η^2-C_6H_4)(PMe_3)]. Theoretical calculations on isotope cluster abundances for [Mo(N-t-Bu)(NAr)$(Ph)_2$] bear a close resemblance to that observed for this fragment. These data are consistent with Mo(N-t-Bu)(NAr)$(Ph)_2$(PMe_3) (Fig. 4.4), analogous to the bis(2-t-butylphenylimido)molybdenum complex obtained above. Again the complex is highly fluxional in solution, showing none of the potential isomers with different imido ligands axial and equatorial. It is possible that the easy interconversions giving rise to this ligand equivalence are due to a Berry-pseudo-rotation mechanism.

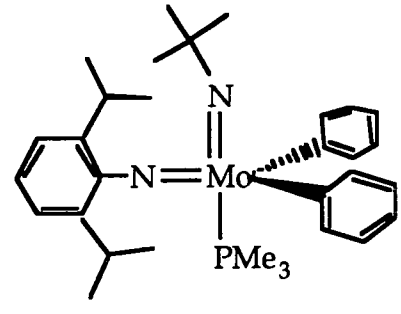

Figure 4.4

Heating a sample of Mo(N-t-Bu)(NAr)$(Ph)_2$(PMe_3) in d_{12}-cyclohexane gave changes in the proton spectrum, again these are consistent with the destruction of the phenyl ligands. The spectrum is complex and compound decomposition is likely.

To allow comparison between the complexes Mo$(NR)_2(Ph)_2$(PMe_3) made, selected NMR data is collected in table 4.1 below.

	$Mo(N\text{-}tBuC_6H_4)_2(Ph)_2(PMe_3)^a$		$Mo(N\text{-}tBu)(NAr)(Ph)_2(PMe_3)^b$	
	^1H	^{13}C	^1H	^{13}C
Phenyl				
ortho	7.77 d	136.7 dm	7.55 d	138.3 d
meta	7.21 t	127.0 dd	7.10 t	127.4 dd
para	7.09 t	125.7 dm	6.98 t	125.4 dt
ipso		174.3 s		174.5 s
Imido				
ipso		155.7 s		153.7 s
4°				72.0 s
Phosphine	0.60 d	12.6 qd	0.80 d	14.5 qd

[a] Shifts quoted in C_6D_6 as a solvent.
[b] Shifts quoted in C_6D_{12} as a solvent.

Table 4.1: *Selected NMR data for the complexes $Mo(NR)_2(Ph)_2(PMe_3)$.*

4.4 Summary.

The two molybdenum bis(imido)di(phenyl) complexes Mo(N-t-Bu)(NAr)$(Ph)_2(PMe_3)$ and $Mo(N\text{-}2\text{-}t\text{-}BuC_6H_4)_2(Ph)_2(PMe_3)$ have been synthesised and characterised; both are five coordinate, eighteen electron complexes. There is no reason to expect them to exist in any geometry other than the distorted trigonal bipyramidal structure observed for $Mo(NAr)_2(Ph)_2(PMe_3)$ (Eqn. 4.6).

Unlike the 2,6-diisopropylphenyl derivative[16] $Mo(NAr)_2(Ph)_2(PMe_3)$, they do not convert to benzyne species, although there is evidence from ^1H NMR experiments that a clean transformation does occur.

4.5 References.

1. S.L Buchwald, R.B. Neisen, *Chem. Rev.*, 1988, **88**, 1047.
2. F.A. Cotton, G. Wilkinson, "Comprehensive Inorganic Chemistry.", 5th edn., Wiley, New York, 1988.
3. C.P. Boekel, J.H. Teuben, H.J. de Liefde Meijer, *J. Organomet. Chem.*, 1975, **102**, 161.
4. C.P. Boekel, J.H. Teuben, H.J. de Liefde Meijer, *J. Organomet. Chem.*, 1974, **81**, 371.
5. J. Dvorak, R.J. O'Brien, W. Santo, *J. Chem. Soc., Chem. Commun.*, 1970, 411.
6. I.S. Kolomnikov, T.S. Lobeeva, V.V. Gorbachevskaya, G.G. Aleksandrov, Y.T. Struckhov, M.E. Vol'Pin, *J. Chem. Soc., Chem. Commun.*, 1971, 972.
7. G. Erker, *J. Organomet. Chem.*, 1977, **134**, 189.
8. K. Kropp, G. Erker, *J. Am. Chem. Soc.*, 1979, **101**, 3659.
9. K. Kropp, G. Erker, *Organometallics*, 1982, **1**, 1247.
10. S.L Buchwald, B.T. Watson, *J. Am. Chem. Soc.*, 1986, **108**, 7411.
11. M.A. Bennet, T.-W. Hambley, N.K. Roberts, G.B. Robertson, *Inorg. Chem.*, 1979, **18**, 1679.
12. B. Gaultheron, G. Tainturier, S. Pouly, F. Theobald, H. Vivier, A. Laarif, *Organometallics*, 1984, **3**, 1495.
13. G. Erker, P. Czisch, R. Mynott, Y-H. Tsay, C. Kruger, *Organometallics*, 1985, **4**, 1310.
14. A.D. Poole, Thesis (1992).

15. J.K. Cockcroft, V.C. Gibson, J.A.K. Howard, A.D. Poole, U. Siemeling, C. Wilson, *J. Chem. Soc., Chem. Commun.*, 1992, 1668.

16. P.W. Dyer, Thesis (1993).

17. P.W. Dyer, V.C. Gibson, J.A.K. Howard, C. Wilson, *J. Organomet. Chem.*, in press.

CHAPTER FIVE.

Molybdenum Bis(imido) Diphenylacetylene Complexes.

5.1 Introduction

These acetylene complexes have precedent in group 4 metallocene complexes[1] and group 5 half sandwich imido complexes[2], a selection of examples are described below.

An acetylene ligand may behave as a four or two electron donor[3], by virtue of its two orthogonal π-systems; in the complexes described below it behaves as a two electron donor. This is confirmed by the observed NMR chemical shifts of the acetylenic carbon atoms; as a 2 electron donor these are in the range δ 110-120 ppm, as a four electron donor shifts are in the range δ 190-210 ppm.

Bent metallocenes are widely known to reductively couple unsaturated organic molecules[1], in the case of acetylenes giving rise to metallacyclopentadienes. These reactions are widely accepted as going via a metallocene acetylene complex as an intermediate. Isolable metallocene complexes containing acetylene ligands are somewhat uncommon, owing to such reductive coupling reactions (Eqn. 5.1).

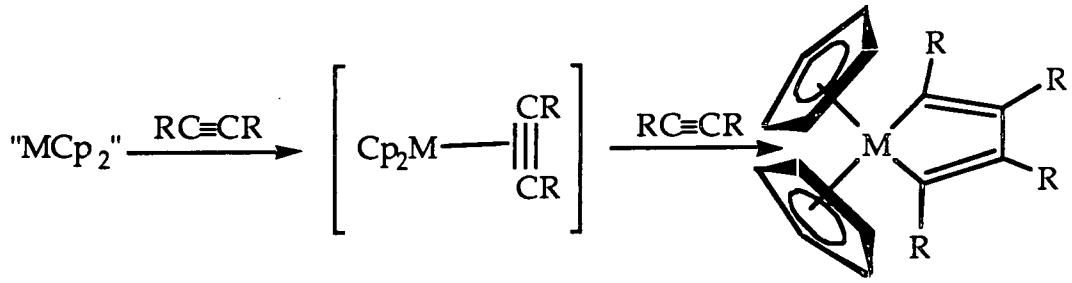

Equation 5.1

For example, comparison is drawn with the use of an ethylene adduct as a starting material. Reaction of permethyltitanocene ethylene(II) with propyne[4] results in reductive coupling of the olefin and acetylene giving a titanacyclopentene (Eqn 5.2).

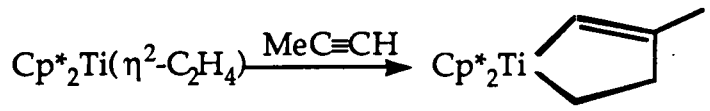

Equation 5.2

With diphenylacetylene, such reductive coupling is inhibited; ligand exchange can occur and results in the formation of an acetylene complex (Eqn 5.3). Infrared spectra show the C≡C stretch to be at 1647 cm^{-1}; this value is low compared with the free acetylene and is indicative of considerable back bonding into the π^* orbitals.

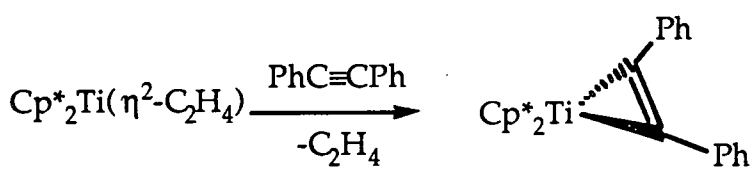

Equation 5.3

A hafnocene isobutene complex[5] also undergoes ligand exchange with one equivalent of acetylene (Eqn 5.6). Excess acetylene produces the hafnacyclopentadiene.

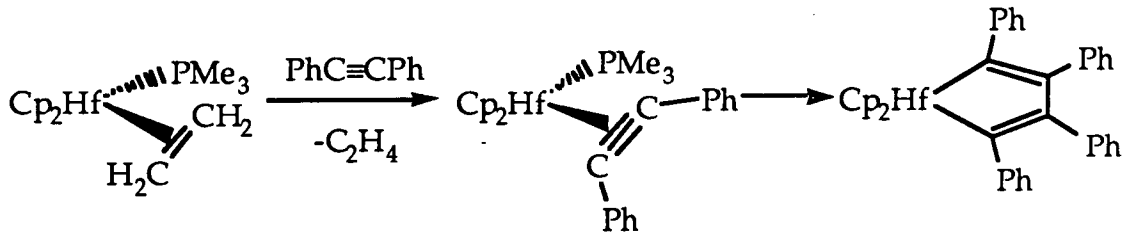

Equation 5.4

Among the structurally characterised metallocene acetylene complexes is $Cp_2Ti(CO)(PhC{\equiv}CPh)$[6]; this is stabilised as a discrete acetylene complex by the carbonyl ligand. The complex (Fig. 5.1) is produced from $Cp_2Ti(CO)_2$ by ligand exchange and shows typical pseudo-tetrahedral geometry; the acetylene and the carbonyl lie in the equatorial plane of the metallocene fragment. Lengthening of the acetylenic bond and bending from linearity of the acetylene substituents reflects a major back-bonding contribution; this is further inferred by the value of $\nu(C{\equiv}C)$ 1780 cm^{-1}. At temperatures >30°C the complex disproportionates to starting material and a titanacyclopentadiene. The complex $Cp_2Ti(CO)(PhC{\equiv}CPh)$ is a highly active hydrogenation catalyst for alkenes and acetylenes.

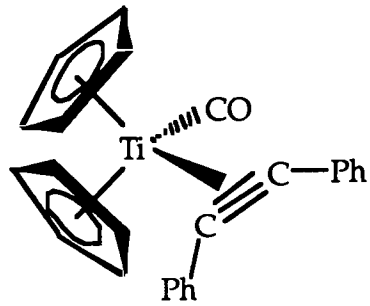

Figure 5.1

The stability of the acetylene complexes may be further enhanced by the introduction of a trimethylphosphine ligand[7] (Fig. 5.2); none of the titanacyclopentadiene is produced.

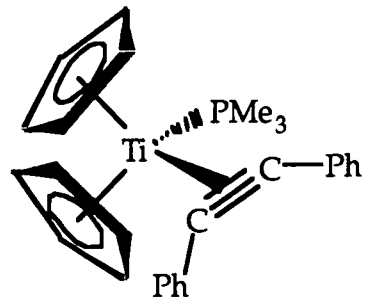

Figure 5.2

Use of $Cp_2Ti(PMe_3)_2$ as a titanocene source has led to the stabilised acetylene complexes $Cp_2Ti(PMe_3)(PhC{\equiv}CPh)$ and $Cp_2Ti(PMe_3)(HC{\equiv}CH)$[8]; these react with excess acetylene to give metallacyclopentadienes[7,9]. While not structurally characterised, the acetylene derivative shows different phosphorus coupling to the acetylenic protons; this is indicative of a geometry analogous to that observed in $Cp_2Ti(CO)(PhC{\equiv}CPh)$ (Fig 5.1) above. An adaptation of this route[10] has led to the zirconocene acetylene complex $Cp_2Zr(PMe_3)(PhC{\equiv}CPh)$, however this has not proved to be a generally useful synthesis.

A more general route to zirconocene complexes of both terminal and internal acyclic acetylenes[11] involves hydrozirconation[12] of the acetylene (Eqn. 5.5). Stability of this complex arises through back-bonding to the acetylene reducing electron density on the metal. The 3-hexyne derivative $Cp_2Zr(PMe_3)(EtC{\equiv}CEt)$ made by this route reacts with alkenes, acetylenes, nitriles and aldehydes and ketones to produce a range of zirconacyclopentenes, as does the cyclohexyne derivative[13] (Fig 5.3).

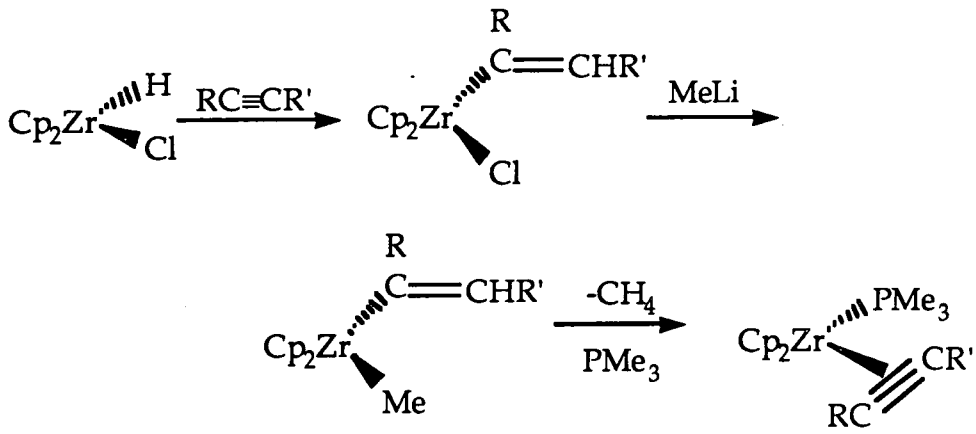

Equation 5.5

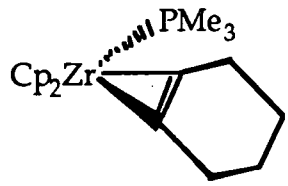

Figure 5.3

Group five half-sandwich imido complexes containing acetylene ligands are uncommon. Two examples have been produced[2] at elevated temperatures in equilibrium mixtures by ligand exchange with propene adducts (Eqn 5.6).

$$\begin{array}{ccc} CpNb(NAr)(\eta^2\text{-}C_3H_6)(PMe_3) & \rightleftharpoons & CpNb(NAr)(\eta^2\text{-}RC{\equiv}CR)(PMe_3) \\ + & & + \\ RC{\equiv}CR & & C_3H_6 \end{array}$$

Equation 5.6

These complexes are present in two forms, whose existence may be explained in terms of steric considerations. The pseudo-metallocene character of the [Cp(NAr)Nb] fragment would favour the coordination of the acetylene to the metal in an orientation in which the acetylenic bond lies coplanar with the phosphine. Molecular models indicate that such a conformation places the phosphine very close to the acetylene substituents; in order to alleviate this situation the acetylene swings slightly out of the plane in two possible directions. Both rotamers exist in equal proportions, indicating that neither form is thermodynamically favoured.

A range of molybdenum bis(imido) diphenylacetylene complexes have been synthesised[14] from the ethylene complexes by a simple ligand exchange reaction (Eqn. 5.7); displacement of ethylene occurs slowly at 70°C, going to completion in ca. 10 days. Structural analysis of $Mo(N\text{-}tBu)_2(PMe_3)(PhC{\equiv}CPh)$ confirms the expected pseudo-tetrahedral

metallocene-like geometry. This section discusses the syntheses and characterisation of a selection of analogous compounds.

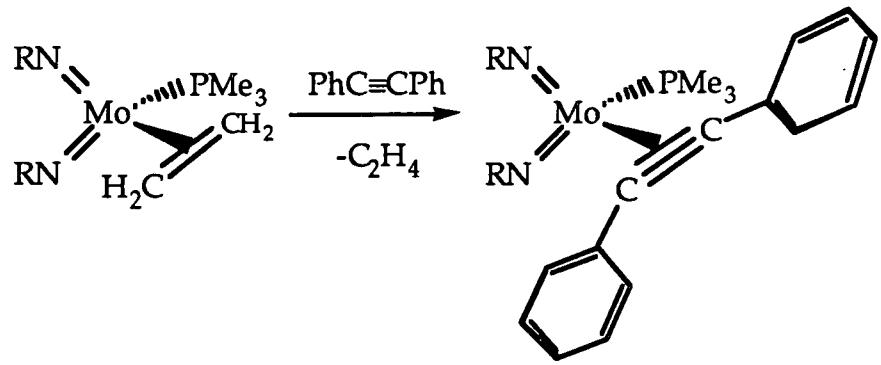

Equation 5.7

In addition to these molybdenum bis(imido) acetylene complexes, other group 6 bis(imido) acetylene complexes have been made by Schrock[15]. $W(NAr)_2(PMe_2Ph)_2$ reacts with acetylenes to give products dependent on the size of the coordinating ligand (Fig. 5.4). Trimethylsilylacetylene gives a four coordinate, pseudotetrahedral metallocene-like complex $W(NAr)_2(PMe_2Ph)(TMSC{\equiv}CH)$; while acetylene itself reacts to give $W(NAr)_2(PMe_2Ph)_2(HC{\equiv}CH)$, a five coordinate, formally 20 electron complex. Its structure is expected to be analogous to that observed[14] in $Mo(NAr)_2(PMe_3)_2(C_2H_4)$. The analogous route to the molybdenum systems using $Mo(NR)_2(PMe_3)_2$ has been investigated[14] but failed to give tractable products.

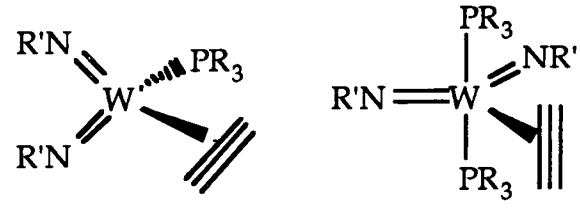

Figure 5.4

A selection of rhenium acetylene complexes have also been made[16]. These are analogous to rhenium tris(imido) complexes and the structurally characterised trigonal planar osmium complex $Os(NAr)_3$. The chloride complex shown in fig. 5.5 may be reduced to give anions of the type $[Re(NAr)_2(\eta^2\text{-}C_2Np_2)]_2Hg$ and $Na(THF)_2[Re(NAr)_2(\eta^2\text{-}C_2Np_2)]$.

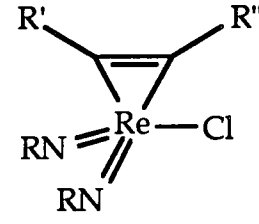

Figure 5.5

5.2 Synthesis of $Mo(NAd)_2(PMe_3)(PhC{\equiv}CPh)$

A preliminary reaction at 60°C between a benzene solution of $Mo(NAd)_2(PMe_3)(C_2H_4)$ and one equivalent of diphenylacetylene was monitored by ^1H NMR; total loss of the bound ethylene signals was observed after 15 hours. It is unclear why ligand exchange should be so facile in this system compared with similar exchange reactions which can take up to two weeks.

Owing to the problems experienced in extracting the ethene adduct $Mo(NAd)_2(PMe_3)(C_2H_4)$ (Section 3.2.2) ligand substitution was attempted *in situ* . After work-up, the resulting brown crystalline solid was recrystallised from heptane. Elemental analysis and ^1H NMR data are consistent with the expected product $Mo(NAd)_2(PMe_3)(PhC{\equiv}CPh)$.

Proton NMR experiments show the imido ligands to be equivalent, and two different phenyl rings are present on the diphenylacetylene. The trimethylphosphine proton resonance shows a strong positive NOE with only one of the resonances designated as a phenyl H_{ortho} resonance; this is then assigned as being on the *"cis"* ring, the remaining protons on this ring are then identifiable by means of a ^1H-^1H COSY experiment.

The carbon spectum was assigned on the basis of a HETCOR experiment; four singlets in the $^{13}C[^1H]$ spectrum are assigned, on the basis of $^2J_{PC}$ and $^3J_{PC}$ values, to the acetylenic and phenyl C_{ipso} in *cis* and *trans* positions relative to the phosphine. Acetylenic carbons are anticipated to show large phosphorus coupling ($^2J_{PC}$), with the greatest coupling on the carbon atom at the more acute angle to the phosphorus, this position is effectively *"cis"* to the phosphine. Precedent for such an assignment comes from $^2J_{PC}$ values observed in NMR experiments on the phenylacetylene complex $Mo(N\text{-}t\text{-}Bu)_2(PMe_3)(\eta\text{-}PhC{\equiv}CH)$[14]. The phenyl C_{ipso} resonances show smaller phosphorus coupling ($^3J_{PC}$ ca. 3 Hz), again the carbon *"cis"* to the phosphine bearing the larger coupling. A comparison of selected NMR data for this complex with that for the other diphenylacetylene adducts produced is made in Table 5.1 at the end of this section.

The observed spectra and couplings are all consistent with the compound having a pseudo-tetrahedral metallocene-like geometry (Fig. 5.6) analogous to that observed in $Mo(N\text{-}tBu)_2(PMe_3)(\eta\text{-}PhC{\equiv}CPh)$[14].

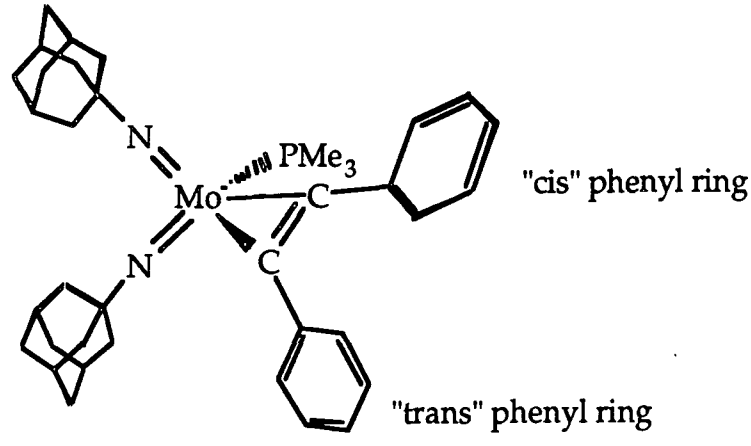

Figure 5.6

5.3 Synthesis of Mo(NAr)(N-t-Bu)(PMe3)(PhC≡CPh)

The reaction between $Mo(NAr)(N\text{-}t\text{-}Bu)(PMe_3)(C_2H_4)$ and diphenylacetylene in benzene was monitored by ^1H NMR spectroscopy and showed that ethylene was exchanged over a period of 14 days at 60°C.

A larger scale reaction (Eqn. 5.7) was carried out in heptane at 70°C for 10 days affording an analytically pure yellow, crystalline solid, which was characterised as $Mo(NAr)(N\text{-}t\text{-}Bu)(PMe_3)(PhC{\equiv}CPh)$. Selected NMR data for this complex are presented for comparison with the data for the other diphenylacetylene adducts in Table 5.1.

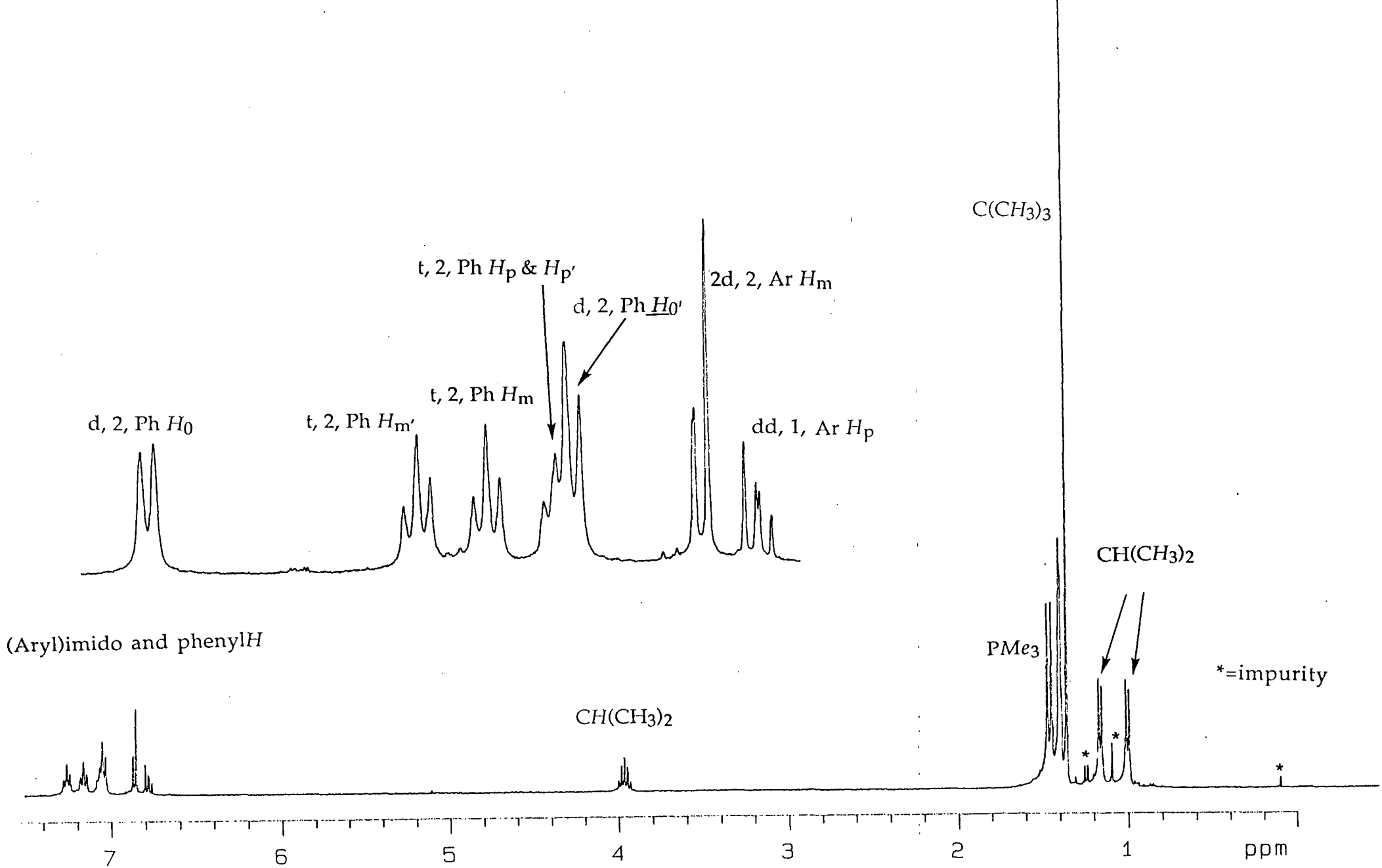

Figure 5.7: ^1H *NMR spectrum of* $Mo(NAr)(N\text{-}t\text{-}Bu)(PMe_3)(PhCCPh)$.

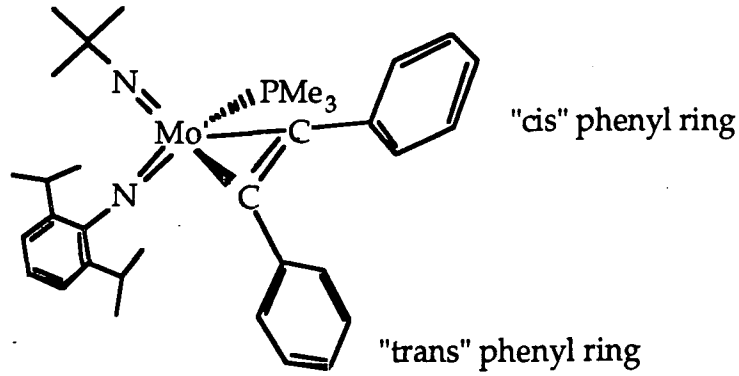

Figure 5.8

Assignment of the proton spectrum (Fig. 5.7) was facilitated by a ^1H-^1H COSY experiment. Those resonances assigned to the phenyl rings indicate two magnetically inequivalent rings. This suggests that the complex exists in a psuedo-tetrahedral metallocene-like geometry with the phosphine and diphenylacetylene ligands lying coplanar (Fig. 5.8). In addition, a pair of doublet resonances assigned to the *iso*propyl groups exist; this is indicative of two sets of diastereotopic protons on the *iso*propyl group since the metal is chiral.

^{13}C NMR spectra in combination with a HETCOR experiment provide further support for this assignment. Since non-protonated carbon atom resonances are of very low intensity, there are insufficient singlet resonances observed in the usual $^{13}C[^1H]$ spectrum to account for the expected total of the imido C_{ipso} and C_{ortho} carbons, the two different phenyl C_{ipso} carbons and the two different acetylenic carbons. However a $^{13}C\{^1H\}$ spectrum (Fig. 5.9) acquired over an extended period in a different solvent (C_6D_6) allowed all of the expected carbon resonances to be located and phosphorus couplings to be resolved; shift differences for the carbon atom resonances between the two solvents are small.

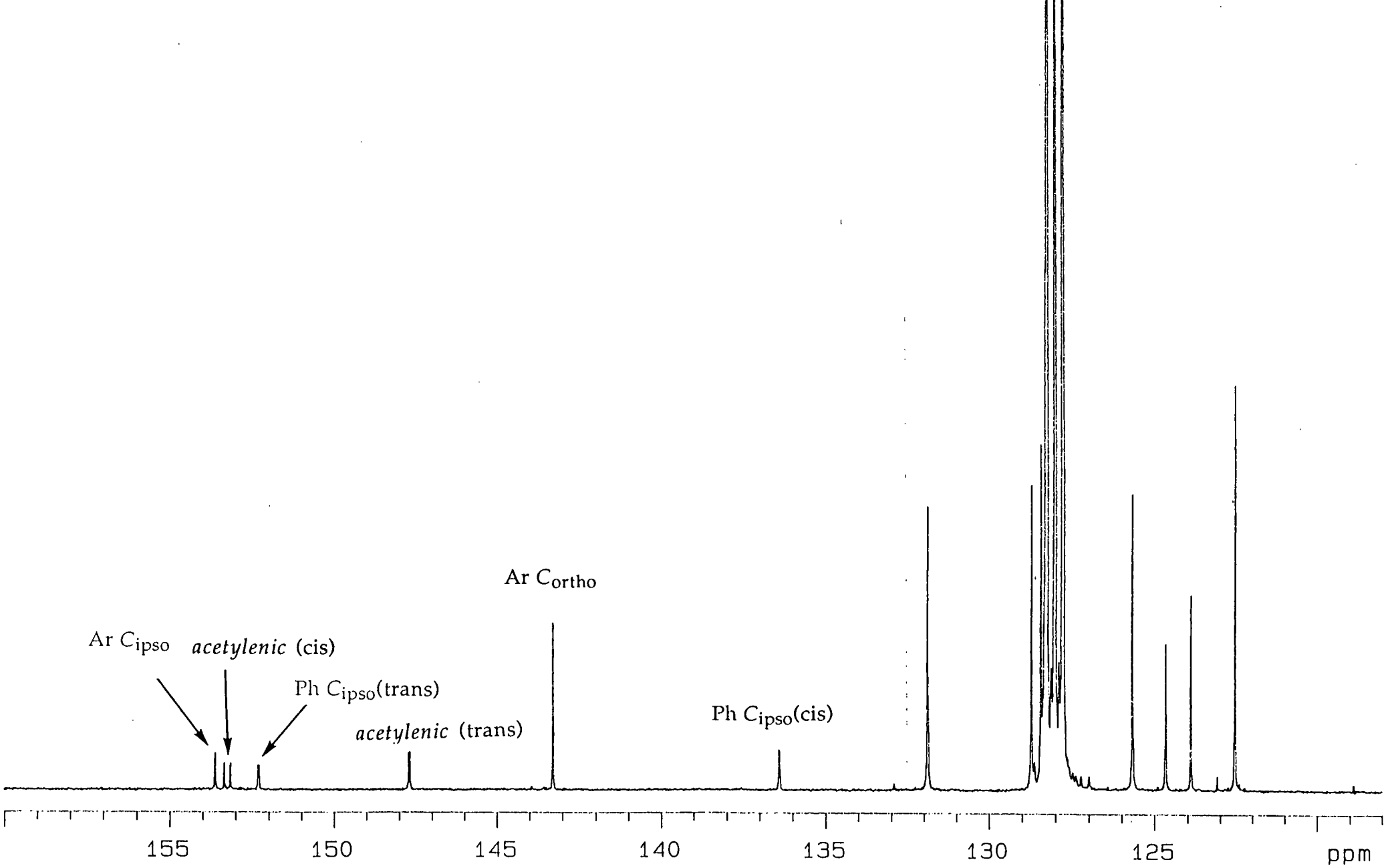

Figure 5.9: ^{13}C *NMR spectrum of the aromatic region of Mo(NAr)(N-t-Bu)(PMe$_3$)(PhCCPh).*

The imido C_{ipso} and C_{ortho} resonances are clearly observable at δ 153.6 and 143.3 ppm respectively and the carbon atoms of the diphenylacetylene ligand without protons attatched are assigned on the basis of phosphorus couplings, as outlined in section 5.2 above, with largest couplings to the C atoms *cis* to the phosphine. Thus, as seen in figure 5.9, the acetylenic carbon atoms are assigned as δ 153.3 ($^2J_{PC}$=18.7 Hz, *cis*) and δ 147.7 ($^2J_{PC}$=4.9 Hz, *trans*) and the phenyl *ipso* carbon atoms are assigned as δ 136.4 ($^3J_{PC}$=3.1 Hz, *cis*) and δ 152.3 ($^3J_{PC}$=2.7 Hz, *trans*).

NOE experiments were carried out in order to assign the proton resonances of the *cis* and *trans* phenyl rings. Irradiation of the trimethylphosphine proton doublet would be expected to give a response with one of the two different phenyl H_{ortho} doublets, which would then allow assignment as the *"cis"* ring, i.e. adjacent to the phosphine. In fact, irradiation of the trimethylphosphine proton doublet gave (Fig. 5.10(a)) a large positive NOE with *both* phenyl H_{ortho} doublets at 7.62 ppm and 7.03 ppm (C_6D_{12}). This suggests that on the timescale of the NOE experiment (ca. 10 s) both rings experience equal proximity to the trimethylphosphine ligand.

In order to probe the origin of this phenomenon, further NOEs with the ortho doublet were investigated. Irradiation of the phenyl H_{ortho} doublet at 7.62 ppm (Fig. 5.10(b)) gave a large negative NOE with the other phenyl H_{ortho} doublet at 7.03 ppm, and positive NOEs with both phenyl H_{meta} triplets.

The size and sign of this effect between these protons is characteristic of their total exchange in the ten seconds of the experiment window. Thus

(b) Irradiation of phenyl H_{ortho} doublet at δ 7.62 ppm.

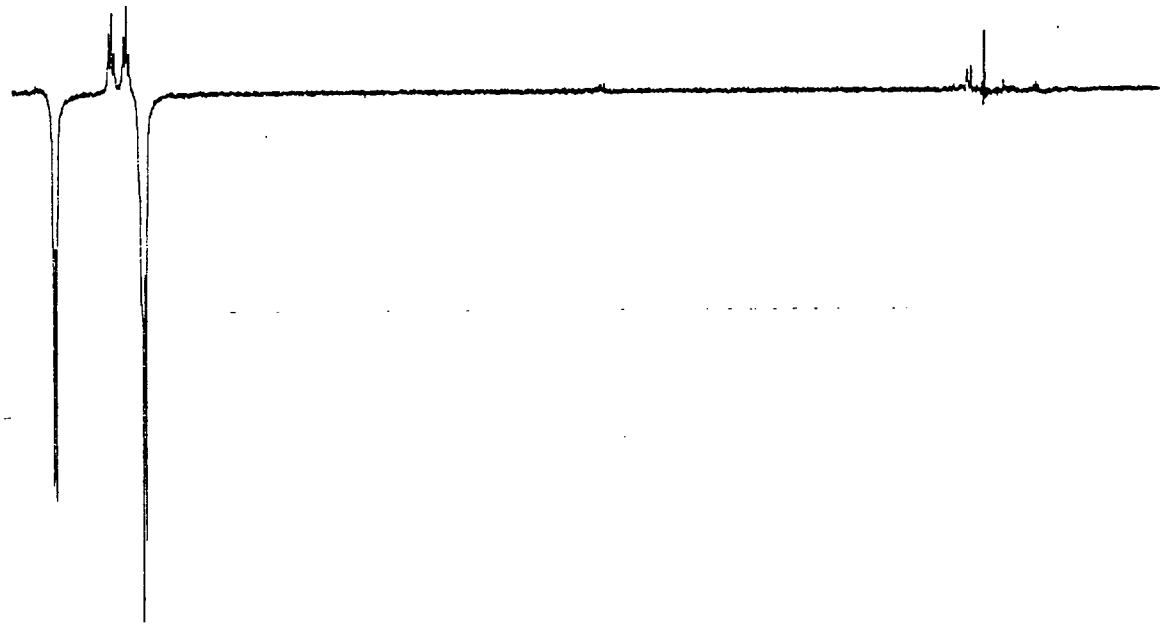

(a) Irradiation of PMe_3 proton doublet at δ 1.44 ppm.

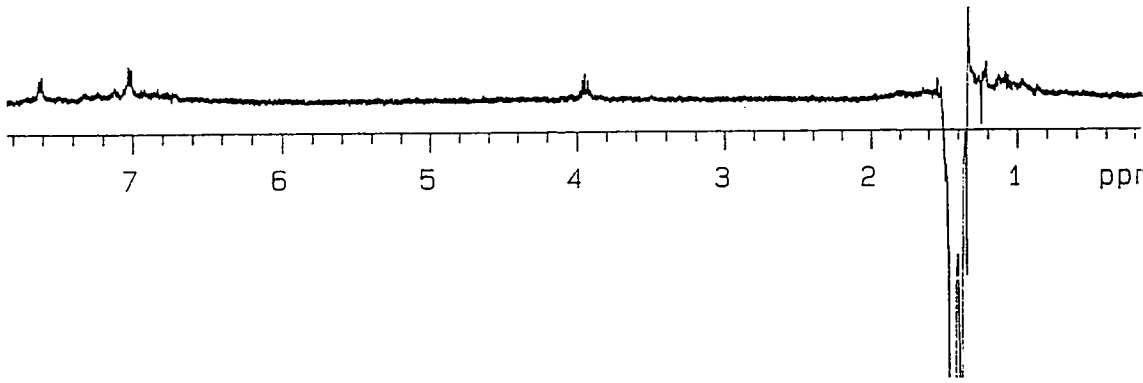

Figure 5.10: *Nuclear Overhauser Enhancement Experiments on Mo(NAr)(N-t-Bu)(PMe3)(PhCCPh).*

irradiating at 7.62 ppm saturated the 7.02 ppm resonance, giving a response from both phenyl H_{meta} triplets. An estimate for the rate of this rotation may be made:

(a) since all H_{ortho} exchange in the 10 s window of the NOE experiment, rotation must be faster than 0.1 Hz.

(b) since both of the H_{meta} triplets are clearly resolved (i.e. there is no signal broadening into the baseline), the rate of rotation must be considerably slower than the difference in their resonant frequencies.

$\Delta\nu = (7.24 - 7.14) \times 400$ Hz = 40 Hz.

Thus, the rate of rotation of the diphenylacetylene is estimated as being between 0.1 Hz and 40 Hz.

Attempts were made to freeze out this motion in order to allow meaningful low temperature NOE experiments. Reaching sufficiently low temperatures necessitated the use of d_8-toluene as a solvent; unfortunately this masked the relevant proton resonances which precluded such a study. Chlorocarbon solvents cannot be employed since the acetylene compounds react to give dichloro products. The observed interchange of the *cis* and *trans* phenyl rings on the diphenylacetylene ligand in this complex is thus attributed to slow rotation about the metal-acetylene bond. This behaviour is unexpected in view of the other analogous acetylene complexes which contain fixed acetylene ligands; it mirrors the unusual behaviour of the ethylene adduct, which also undergoes rotation.

5.4 Synthesis of $Mo(N\text{-}2\text{-}t\text{-}BuC_6H_4)_2(PMe_3)(PhC{\equiv}CPh)$

A preliminary experiment monitoring the reaction between $Mo(N\text{-}2\text{-}t\text{-}BuC_6H_4)_2(PMe_3)_2(C_2H_4)$ and one equivalent of diphenylacetylene in benzene showed that reaction was complete after 12 days at room temperature.

A scaled up version was run in heptane at 65°C for 5 days, producing yellow solid which was identified by ^1H NMR (Fig. 5.11) as $Mo(N\text{-}2\text{-}t\text{-}BuC_6H_4)_2(PMe_3)(PhC{\equiv}CPh)$. Proton NMR resonances were assigned by virtue of a $^1H\text{-}^1H$ cosy experiment and NOE response with the t-butyl singlet. Both imido ligands are equivalent on the NMR timescale. Additionally, both phenyl groups are equivalent and the phenyl H_{ortho} resonance (δ 7.35 ppm) is broadened. This equivalence of the phenyl groups was somewhat surprising in view of the anticipated geometry of this compound based on the other derivatives characterised in this thesis and their analogues (Figs. 5.8, 5.6; Eqn 5.7).

The ^{13}C NMR spectra obtained are also in accordance with equivalent phenyl rings, the phenyl ortho carbon atom resonance (δ 129 ppm) is particularly broad. Selected NMR data for this complex is presented for comparison in Table 5.1. Owing to the low intensity of the signals due to the non-protonated carbons, a very low noise proton decoupled carbon spectrum was obtained. This showed an especially broad resonance at 141 ppm (C_6D_{12}) which was not observed in previous spectra. It has already been noted that the phenyl ortho carbon and proton resonances are particularly broad, this broadened resonance at 141 ppm is assigned to phenyl C_{ipso}. The remaining three singlet resonances observed in the proton coupled carbon

spectrum are assigned as equivalent imido C_{ipso}, imido C-tBu and acetylenic carbons. Unlike the other diphenylacetylene complexes made, no phosphorus coupling is observed on any of these signals, suggesting that there are geometrical differences between this and the other two complexes prepared in this section where phosphorus coupling to the acetylenic and phenyl ipso-carbons is resolved. An unanticipated geometry about the metal may be the reason behind the observed broadening of the phenyl ipso and ortho resonances. However, a more likely reason for the observed equivalence of the imido and phenyl groups is the rotation of the acetylene ligand (Fig. 5.12); this rationalises the observed broadening of resonances attributed to *ortho* protons and carbons and *ipso* carbons of the diphenylacetylene ligand.

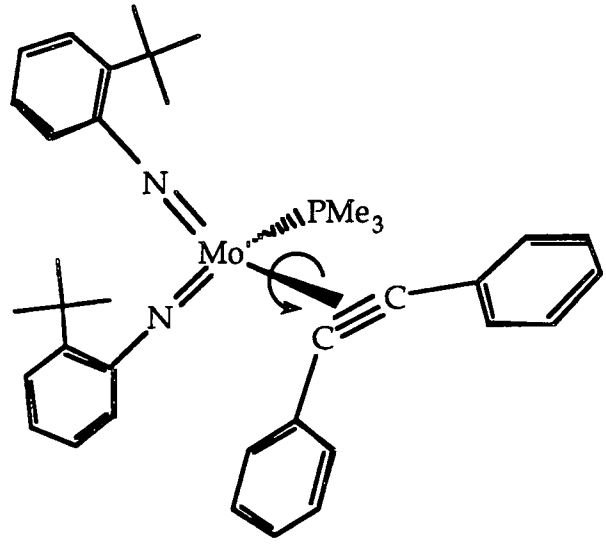

Figure 5.12

These observations contrast with the other diphenylacetylene complexes made, which appear to exhibit ground state metallocene-like geometries in which the alkyne coordinates to the metal with the acetylenic bond and the metal phosphine bond lying in the equatorial binding plane. These are

conformationally rigid like $Mo(NAd)_2(PMe_3)(PhC{\equiv}CPh)$, with the exception of $Mo(NAr)(N\text{-}t\text{-}Bu)(PMe_3)(PhC{\equiv}CPh)$ which exhibits very slow rotation of the diphenylacetylene ligand.

5.5 Summary

Three molybdenum bis(imido) diphenyl acetylene complexes have been synthesised and characterised. $Mo(NAd)_2(PMe_3)(PhC{\equiv}CPh)$ is an eighteen electron complex showing the commonly observed, conformationally rigid, metallocene-like geometry.

$Mo(NAr)(N\text{-}t\text{-}Bu)(PMe_3)(PhC{\equiv}CPh)$ is an eighteen electron complex and on the normal NMR timescale appears to exhibit the anticipated metallocene-like geometry. However, further experiments show that it undergoes slow rotation about the acetylene-metal bond.

$Mo(N\text{-}2\text{-}t\text{-}BuC_6H_4)_2(PMe_3)(PhC{\equiv}CPh)$ is an eighteen electron complex, however, unexpectedly the diphenylacetylene ligand appears to undergo fast rotation on the NMR timescale, averaging the proton and carbon resonances of the diphenylacetylene ligand. This is a further example of the $[Mo(N\text{-}2\text{-}t\text{-}BuC_6H_4)_2]$ fragment deviating from the metallocene-like behaviour observed in other $[Mo(NR)_2]$ fragments.

Table 5.1 below presents selected NMR data for the diphenylacetylene complexes for comparative purposes.

	$Mo(NAd)_2(PMe_3)(PhC{\equiv}CPh)$		$Mo(NAr)(N\text{-}t\text{-}Bu)(PMe_3)(PhC{\equiv}CPh)$		$Mo(N\text{-}2\text{-}t\text{-}BuC_6H_4)_2(PMe_3)(PhCCPh)$	
	^1H (ppm)	^{13}C (ppm)	^1H (ppm)	^{13}C (ppm)	^1H (ppm)	^{13}C (ppm)
<u>Diphenylacetylene</u>						
Acetylinic C*(trans)*		149.3 $^2J_{PC}$ 5 Hz		147.7 $^2J_{PC}$ 4.9 Hz[a]		154.5
Acetylinic C*(cis)*		153.1 $^2J_{PC}$ 19 Hz		153.3 $^2J_{PC}$ 18.7 Hz[a]		
Ph C_{ipso}*(trans)*		148.9 $^3J_{PC}$ 2 Hz		152.3 $^3J_{PC}$ 2.7 Hz[a]		141 broad
Ph C_{ipso}*(cis)*		137.6 $^3J_{PC}$ 3 Hz		136.4 $^3J_{PC}$ 3.1 Hz[a]		
C_{meta} *(cis)*	7.19 t	128.5	7.24 t	128.7	7.20 t	128.6
C_{para} *(cis)*	6.96 t	123.2	7.04 2t (coincident)	124.7 & 127.5	7.06 t	126.5
C_{ortho} *(cis)*	6.93 d	125.6	7.02 d	125.9	7.35 d broad	129 broad
C_{meta} *(trans)*	7.14 t	128.0	7.14 t	128.2		
C_{para} *(trans)*	7.03 t	127.1				
C_{ortho} *(trans)*	7.62 d	132.4	7.62 d	132.1		
<u>Imido</u>						
C_{ipso}				153.6[a]		157.6
$C_{4°}$		66.6		67.8		
<u>Phosphine</u>	1.45	20.45	1.44	18.6	1.39	17.0

[a] Shifts recorded using benzene-d_6 as a solvent.

Table 5.1: *Selected NMR data for the diphenylacetylene complexes synthesised in Chapter 5.*

5.6 References.

1. S.L. Buchwald, R.B. Neilsen, Chem. Rev., 1988, 88, 1047.
2. A.D. Poole, Thesis (1992).
3. R.H. Crabtree, "The Organometallic Chemistry of the Transition Metals.", Wiley, New York, 1988.
4. S.A Cohen, J.E. Bercaw, Organometallics, 1985, 4, 1006.
5. S.L. Buchwald, K.A. Kreutzer, R.A. Fisher, J. Am. Chem. Soc., 1990, 112, 4600.
6. G. Franchinetti, C. Floriani, F. Marchetti, M. Mellini, J. Chem. Soc., Dalton Trans., 1978, 1398.
7. B. Demersemann, P.H. Dixneuf, J. Chem. Soc., Chem. Commun., 1981, 665.
8. L.B. Kool, M.D. Rausch, H.G. Alt, M. Herberhold, U. Thewalt, B. Wolf, Angew. Chem. Int. Ed. Engl., 1985, 24, 394.
9. J.L. Atwood, W.E. Hunter, H. Alt, M.D. Rausch, J. Am. Chem. Soc., 1976, 98, 2454.
10. T. Takahashi, D.R. Swanson, E.-i. Negishi, Chem. Lett., 1987, 623.
11. S.L. Buchwald, B.T. Watson, J.C. Huffmann, J. Am. Chem. Soc., 1987, 109, 2544.
12 D.W. Hart, T.F. Blackburn, J. Schwaartz, J. Am. Chem. Soc., 1975, 97, 679.
13. S.L. Buchwald, R.T. Lum, J. C. Dewan, J. Am. Chem. Soc., 1986, 108, 7441.
14. P.W. Dyer, Thesis (1993).
15. D.S Williams, M.H. Schofield, J.T. Anhaus, R.R. Schrock, J. Am. Chem. Soc., 1990, 112, 6728.
16. D.S Williams, R.R. Schrock, Organometallics, 1993, 12, 1148.

CHAPTER SIX.

Experimental.

6.1 General.

All manipulations of air and moisture sensitive materials were performed on a conventional vacuum/nitrogen line using standard Schlenk and cannula techniques, or in a nitrogen filled dry box.

Elemental Analyses were performed by the departmental microanalytical service.

Infra red specta were recorded on Perkin-Elmer 577 and 457 grating spectrophotometers using CsI windows; absorbances are abbreviated as vs (very strong), s (strong), m (medium), w (weak) , br (broad), sh(shoulder).

Mass spectra were recorded on a VG 7070E Organic Mass Spectrometer. Ionisation modes are abbreviated as CI (chemical ionisation) and EI (electron ionisation).

NMR spectra were recorded on the following instruments at the frequencies listed unless otherwise stated: Bruker AMX500 ^{1}H (500.14 MHz); Varian VXR400 ^{1}H (399.95 MHz), ^{13}C (100.58 MHz); Bruker AC250 ^{1}H (250.13 MHz), ^{13}C (62.90 MHz); Varian Gemini ^{1}H (199.98 MHz), ^{13}C (50.29 MHz); Varian XL200 ^{1}H (200.06 MHz). Chemical shifts are quoted as δ in ppm with respect to the following references: ^{13}C (C_6D_6 128.0ppm, C_7D_8 125.2ppm, C_6D_{12} 26.4 ppm), ^{1}H (C_6D_6, 7.15ppm, C_7D_8, 6.98 & 2.08ppm, C_6D_{12} 1.38 ppm). The following abbreviations are used for band multiplicities: s (singlet), d (doublet), t (triplet), q (quartet), sept (septet), m (multiplet), br (broad).

Solvents and chemicals. NMR solvents were dried by vacuum distillation from a suitable drying agent: d_6-benzene (phosphorus V oxide), d_8-toluene (phosphorus V oxide), d_{12}-cyclohexane (phosphorus V oxide) and were stored under vacuum prior to use.

The following solvents were dried by prolonged reflux over a suitable drying agent (in parenthesis), being freshly distilled and deoxygenated prior to use: toluene (sodium metal), petroleum ether (40-60°C) (lithium aluminium hydride), pentane (lithium aluminium hydride), heptane (sodium metal), tetrahydrofuran (sodium benzophenone ketyl), diethylether ether (lithium aluminium hydride), 1,2-dimethoxyethane (potassium metal).

Chemicals were obtained commercially and used as received unless stated otherwise. Triethylamine and chlorotrimethlysilane were degassed by bubbling dry nitrogen through the liquids. Trimethylphosphine was prepared according to a previously published procedure[1].

6.2 Experimental Details to Chapter 2: Preparation of Six Coordinate Bis(imido) Molybdenum Complexes.

6.2.1 Preparation of Mo(N-Adamantyl)$_2$Cl$_2$.DME.

To a stirred suspension of anhydrous sodium molybdate (5.00g, 24.3 mmol) in ca. 150 mL DME at room temperature were added, sequentially and dropwise, solutions of triethylamine (13.55 mL, 97.1 mmol) in 10 mL DME, chlorotrimethylsilane (34.0 mL, 267 mmol) in 30 mL DME, and a suspension of 1-adamantanamine (7.346, 48.6 mmol) in DME. On addition of the triethylamine the mixture became opaque, and on addition of chlorotrimethysilane white fumes were evolved and the mixture became pale yellow.

The reaction mixture was heated to 75°C with regular venting, and was maintained stirring at this temperature for 44 h. After this time the mixture was golden yellow. Filtration yielded a clear golden solution and

pale yellow precipitate. The precipitate was washed with several portions of dry degassed diethylether, and the solution and washings were combined. Solvent was removed *in vacuo* giving a pale yellow solid. Yield 8.2g, 61% based on sodium molybdate.

^{1}H NMR (293 K, C_6D_6, 400 MHz): 3.53 (s, 6, $(CH_3OCH_2)_2$), 3.30 (s, 4, $(CH_3OCH_2)_2$), 2.24 (s, 12, adamantyl H_β), 1.97 (s, 6, adamantyl H_γ), 1.49 (dd, 12, adamantyl H_δ, $^2J_{HH}$=30Hz, $^2J_{HH}$=12Hz).

^{13}C NMR (293 K, C_6D_6, 100 MHz): 73.1 (s, adamantyl 4°C_α), 70.9 (t, $(CH_3OCH_2)_2$, $^1J_{CH}$=144.2 Hz), 62.5 (q, $(CH_3OCH_2)_2$, $^1J_{CH}$=144.2 Hz), 43.6 (t, adamantyl C_β, $^1J_{CH}$=131.3 Hz), 36.4 (t, adamantyl C_δ, $^1J_{CH}$=125.9 Hz), 29.9 (d, adamantyl C_γ, $^1J_{CH}$=132.0 Hz).

Elemental analysis for $MoN_2O_2Cl_2C_{24}H_{40}$: found 4.95% N, 51.70% C, 7.46% H.(calculated 5.04% N, 51.85% C, 7.27% H)

Infrared data (Nujol, CsI, cm^{-1}): 1350 sh, 1345 w, 1315 sh, 1305 s, 1290 w, 1260 m, 1242 m, 1198 s, 1178 s, 1115 sh, 1100 s, 1065 s, 1050 sh, 1035 w, 1020 m, 990w, 930w, 865 s, 860 sh, 835 w, 818 m, 765 w, 735 sh, 722 w, 570 s, 475 w, 460 w, 450 w, 418 m, 395 wbr, 340 s, 325 s, 310 sh.

Mass spectral data: (EI) m/z 151 ($AdNH_2$), 94, 57.

6.2.2 Preparation of $Mo(N\text{-}2\text{-}t\text{-}BuC_6H_4)_2Cl_2$.DME.

Sodium molybdate (5.00 g, 24.3 mmol) was treated with triethylamine (13.55 mL, 97.1 mmol), chlorotrimethysilane (37.0 mL, 292 mmol, >11 equivalents) and 2-*tert*-butylaniline (7.346 g, 48.6 mmol) according to the procedure described in section 6.2.1 above.

On addition of the 2-*tert*-butylaniline the mixture became yellow and opaque, which changed to dark red on heating to 75°C; no further

change occured over a further 18 h. Filtration afforded a clear deep red solution and orange precipitate. The precipitate was washed with several portions of dry degassed diethylether, and the solution and washings were combined. Solvent was removed *in vacuo* giving a dark red solid. Yield was 13.21 g, 98% based on sodium molybdate.

^{1}H nmr (293 K, C_6D_6, 200 MHz): 8.19 (dd, 1, CH_{ortho}, $^3J_{HH}$=7.9 Hz, $^4J_{HH}$=1.5 Hz), 7.15 (dd, ~1, CH_{meta}, $^3J_{HH}$=8.0 Hz, $^4J_{HH}$=1.5 Hz), 6.95 (td, 1, CH_{meta}, $^3J_{HH}$=7.4 Hz, $^4J_{HH}$=1.5 Hz), 6.75 (td, 1, CH_{para}, $^3J_{HH}$=7.4 Hz, $^4J_{HH}$=1.5 Hz), 3.36 (s, 6, $(CH_3OCH_2)_2$), 3.16 (s, 4, $(CH_3OCH_2)_2$), 1.54 (s, 18, $C(CH_3)_3$).

This analytical data was entirely consistent with that reported in the literature, *(Inorg. Chem. 31, 2287 (1992))*.

Elemental analysis for $MoN_2O_2Cl_2C_{24}H_{36}$: found 4.89% N, 52.42% C, 6.86% H. (calculated 5.08% N, 52.23% C, 6.59% H)

Infrared data (Nujol, CsI, cm^{-1}): 1302 m, 1262 m, 1240 w, 1190 w, 1165 w, 1110 sh, 1085 sbr, 1045 s, 1020 m, 985 w, 960 w, 950 w, 860 s, 820 w, 800 mbr, 765 m, 760 s, 723 m, 665 w, 595 w, 480 w, 390 w, 335 m.

6.2.3 Preparation of Mo(N-2,6-i-$Pr_2C_6H_3$)(N-t-Bu)Cl_2.DME.

The method outlined in Section 6.2.1 was used for the reaction of sodium molybdate (9.00 g, 43.7 mmol) with triethylamine (24.4 mL, 174.8 mmol), chlorotrimethysilane (61.0 mL, 481 mmol, >11 equivalents) and a mixture of 2,6-diisopropylaniline (6.60 mL, 34.96 mmol, 0.8 equiv.) and t-butylamine (5.53 mL, 52,44 mmol, 1.2 equiv.) .

On addition of the triethylamine the mixture became opaque, and on addition of chlorotrimethysilane white fumes were evolved and the mixture became peach coloured. The flask was heated to 75°C with

regular venting. After 2h the mixture had become a red/orange colour and a precipitate formed. The mixture was maintained stirring at this temperature for 24 h, the colour remaining throughout.

On cooling, the red solution was filtered off and the precipitate washed with diethylether. Filtrate and washings were combined and solvent removed *in vacuo* to leave a very oily solid. After prolonged drying, this was washed with three portions of petroleum ether at -78°C with some improvement. ^{1}H nmr at this stage shows the presence of both possible bis imido species and some of the mixed bis imido compound in the following proportions: 56% Mo(N-2,6-i-$Pr_2C_6H_3$)(N-t-Bu)Cl_2.DME, 29% Mo(N-t-Bu)$_2Cl_2$.DME, 15% Mo(N-2,6-i-$Pr_2C_6H_3)_2Cl_2$.DME.

A quantity of this solid was partially dissolved in diethylether, and a dark red solid separated by filtration (^{1}H nmr shows enrichment in Mo(N-*t*-Bu)$_2Cl_2$.DME) the filtrate was placed at -30°C. After some time the solid crystallised out was separated by filtration and was shown by ^{1}H nmr to be Mo(N-2,6-i-$Pr_2C_6H_3$)(N-t-Bu)Cl_2.DME. Further quantities of the product were obtained by continued recrystallisations.

^{1}H nmr (293 K, C_6D_6, 400 MHz): 7.13 (d, 2, Aryl H_{meta}, $^3J_{HH}$ 7.6 Hz), 6.95 (t, 1, Aryl H_{para}, $^3J_{HH}$ 8.0 Hz), 4.33 (sept, 2, $CH(CH_3)_2$, $^3J_{HH}$ 6.8 Hz), 3.41 (s, 6, $(CH_30CH_2)_2$), 3.18 (s, 4, $(CH_30CH_2)_2$), 1.42 (d, 12, $CH(CH_3)_2$, $^3J_{HH}$ 6.8 Hz), 1.27 (s, 9, $C(CH_3)_3$).

^{13}C nmr (293 K, C_6D_6, 100.6 MHz): 24.82 (br, q, $CH(CH_3)_2$, $^1J_{CH}$ 126.0 Hz), 28.10 (d,$CH(CH_3)_2$, $^1J_{CH}$ 134.7 Hz), 29.41 (q, $NC(CH_3)_3$,$^1J_{CH}$ 127.4 Hz), 62.38 (q, $(CH_30CH_2)_2$, $^1J_{CH}$ 145.0 Hz), 70.63 (t, $(CH_30CH_2)_2$, $^1J_{CH}$ 146.1 Hz), 75.42 (s, $NC(CH_3)_3$), 123.27 (d, Aryl C_{meta}, $^1J_{CH}$ 123.8 Hz), 125.89 (d, Aryl C_{para}, $^1J_{CH}$ 160.26 Hz), 143.10 (s, Aryl C_{ortho}), 154.42(s,Aryl C_{ipso}).

Elemental analysis for $MoN_2O_2Cl_2C_{20}H_{36}$: found 5.43% N, 48.11% C, 7.49% H. (calculated 5.57% N, 47.71% C, 7.22% H)

6.2.4 Preparation of Mo(NAd)(O)Cl_2.DME.

Sodium molybdate (0.491 g, 2.39 mmol) was reacted with triethylamine (0.67 mL (4.77 mmol), chlorotrimethysilane (2.75 mL, 21.48 mmol) and 1-adamantanamine (0.361 g, 2.39 mmol) using the procedure described above in Section 6.2.1.

On addition of the triethylamine the mixture became opaque, and on addition of chlorotrimethylsilane a small quantity of white fumes were evolved. The ampoule was sealed and heated to 75°C with regular venting to relieve pressure; during this time the mixture became bright yellow and was unchanged after 24 h stirring at this temperature. After cooling, the mixture was filtered to afford a clear yellow solution and creamy yellow precipitate. The solids were washed with two 10 ml portions of diethylether, leaving a white solid. The washings and filtrate were combined as a yellow solution and volatiles were removed *in vacuo* leaving a golden yellow oily solid. This was washed with petroleum ether (40-60°C) at -78° giving a yellow solid. ^1H nmr shows the solid obtained to be a mixture ca 60 % Mo(NAd)(O)Cl_2.DME & 40 % Mo(NAd)$_2Cl_2$.DME. Yield 0.8g mixed products. Based on sodium molybdate, this calculates to be 70% conversion to the above product ratio. The solid was redissolved in DME to give a green solution, filtered, condensed and cooled to -30°C. After one week, pure crystalline material was apparent; this was isolated.

^1H nmr (293 K, 400 MHz, C_6D_6): 3.47 (s, 6, $(CH_3OCH_2)_2$), 3.07 (s, 4, $(CH_3OCH_2)_2$), 2.20 (s, 6, adamantyl H_β), 1.86 (s, 3, adamantyl H_γ), 1.37 (dd, 6, adamantyl H_δ).

^{13}C nmr (293 K, 100 58 MHz, C_6D_6): 76.3 (s, adamantyl 4°C_α), 70.4 (t, $(CH_30CH_2)_2$, $^1J_{CH}$=145.3 Hz), 63.2 (q, $(CH_30CH_2)_2$, $^1J_{CH}$=156 Hz), 41.0 (t, adamantyl C_β, $^1J_{CH}$=128.9 Hz), 35.7 (t, adamantyl C_δ, $^1J_{CH}$=124.0 Hz), 29.2 (d, adamantyl C_γ, $^1J_{CH}$=136.2 Hz).

Elemental analysis for $MoNO_3Cl_2C_{14}H_{25}$: found 3.13% N, 40.06% C, 6.03% H, 16.14% Cl. (calculated 3.33% N, 40.01% C, 6.01% H, 16.87% Cl)

Infrared data (Nujol, CsI, cm^{-1}): 1345 w, 1312 sh, 1305 m, 1282 w, 165 w, 1245 w, 1230 m, 1190 w, 1185 w, 1115 w, 1102 m, 1095 m, 1048 s, 1025 m, 1008 w, 980 w, 908 s, 860 s, 832 m, 824 m, 810 w, 800 w, 723 wbr, 552 m, 510 m, 450 w, 400w, 352 sh, 345 s, 335 sh.

Mo=O stretch is assigned as the 908 cm^{-1} absorbance.

Mass spectrum: (EI) m/z 113, 99, 85, 71, 57.

6.3 Experimental Details to Chapter 3.

6.3.1 Synthesis of $Mo(NAd)_2(PMe_3)(C_2H_4)$

Mo(N Adamantyl)$_2$Cl$_2$.DME (0.425 g, 0.77 mmol) was placed in an ampoule and diethylether (~150 ml) added to give a yellow solution. The solution was frozen to -196°C and the ampoule evacuated. Trimethylphosphine (0..20 ml, 1.5 mmol) was condensed on. Ethylmagnesium chloride (0.80 ml, 2.0M in Et_2O, 1.6 mmol) was syringed onto the solid.

The ampoule was sealed and warmed to -78°C where the solution was yellow. Stirring was maintained and when warmed to room temperature the mixture became tan and opaque. After 3 h the mixture was unchanged. Solvent was removed *in vacuo* giving a pale yellow solid. The product was extracted into warm pentane (ca. 100 mL) as a

golden brown solution. When this was concentrated, material precipitated on the vessel walls and failed to wash back into solution. The solution was placed at -40°C and after five days dark brown crystalline material was present, this was isolated by filtration. The remaining golden filtrate was further concentrated and replaced at -40°C. Yield was 150mg recrystallised solid.

^{1}H nmr (293 K, C_6D_6, 400 MHz): 2.31 (t, 2, C_2H_4, $^3J_{HH}$=12Hz), 2.02 (s, 6, adamantyl $H\gamma$), 1.93(s, 12, adamantyl H_β), 1.58(dd, 12, adamantyl H_δ, $^2J_{HH}$=21.2Hz, $^2J_{HH}$=12.0Hz), 1.2 (t, 2, C_2H_4, $^3J_{HH}$=12Hz), 1.21 (d, 9, PMe_3, $^2J_{PH}$=9.2 Hz)

^{13}C nmr (293 K, C_6D_6, 100 MHz): 65.7 (s, adamantyl 4°C_α), 48.1 (t, adamantyl C_β, $^1J_{CH}$=130.4 Hz), 36.8 (t, adamantyl C_δ, $^1J_{CH}$=126.2 Hz), 32.14 (td, C_2H_4, $^1J_{CH}$=150.2Hz $^2J_{PC}$=9.5 Hz), 30.5 (d, adamantyl C_γ, $^1J_{CH}$=131.7Hz), 21.22 (t, C_2H_4, $^1J_{CH}$=152.6Hz), 20.1 (qd, PMe_3, $^1J_{PC}$=28.3 Hz $^1J_{CH}$=129.3 Hz).

Elemental analysis for $MoN_2PC_{25}H_{43}$): found 5.1% N, 60.3% C, 9.1% H. (calculated 5.6% N, 60.2% C, 8.7% H)

Infrared data (Nujol, CsI, cm^{-1}): 1570 m, 1341 m, 1310 m, 1300 s, 1288 m, 1284 m, 1240 mbr, 1195 s, 1175 m, 1140 s, 1098 m, 1025 wbr, 1020 sh, 960 s, 942 s, 896 w, 850 w, 812 m, 810 w, 805 w, 760 w, 740 w, 730 w, 675 m, 650 w, 565 w, 520 w, 490 w, 440 wbr, 370m.

Mass spectrum: (EI) envelope centred at m/z 499 [M$^+$], m/z 471 [M$^+$]-C_2H_4.

6.3.2 $Mo(N\text{-}2\text{-}C_6H_4\text{-}t\text{-}Bu)_2(PMe_3)_2(C_2H_4)$.

The method described in section 6.3.1 was employed for the reaction of $Mo(N\text{-}2\text{-}t\text{-}BuC_6H_4)_2Cl_2.DME$ (0.9647g, 1.749 mmol) with trimethylphosphine (0.36 ml, 3.5 mmol) and ethylmagnesium chloride (1.75 ml, 2.0M in Et_2O, 3.5 mmol). On warming to -78°C the reaction mixture was dark red; the ampoule was then allowed to warm to room temperature with stirring After 3 h the mixture was a deep purple with the apparent formation of a pecipitate.

Filtration afforded a deep purple filtrate and dark precipitate; this precipitate was washed with diethylether until the washings filtered off colourless. The washings were combined with the filtrate and solvent removed *in vacuo* to give a dark red solid. Yield was 0.73g (73%).

Large purple crystals were obtained from a saturated solution of the compound in pentane at -40°C.

^1H nmr (293 K, C_6D_6, 400 MHz): 7.22 (dd, 2, NR H_{meta} adjacent to t-Bu, $^3J_{HH}$=6.4 Hz, $^4J_{HH}$=1.4 Hz), 7.15 (td, NR H_{para}, $^3J_{HH}$=6.8 Hz, $^4J_{HH}$=1.67 Hz), 7.02 (dd, 2, NR H_{ortho}, $^3J_{HH}$=6.4 Hz, $^4J_{HH}$=1.4 Hz), 6.73 (m, NR H_{meta}, $^3J_{HH}$=6.8 Hz, $^4J_{HH}$=1.6 Hz), 3.26 (q, 0.9, $(CH_3CH_2)_2O$), 1.60 (s, 4, C_2H_4), 1.26 (s, 18, $C(CH_3)_3$), 1.11 (t, 1.5, $(CH_3CH_2)_2O$), 1.02 (s, 18, PMe_3).

^{13}C nmr (293 K, C_6D_6, 100.6 MHz): 156.7 (s, C_{ipso}), 134.0 (s, C-t-Bu), 136.7 (dd, C_{ortho}, $^1J_{CH}$=156.8 Hz, $^2J_{CH}$=8.0 Hz), 126.9 (dd, C_{meta}, $^1J_{CH}$=149.1 Hz, $^2J_{CH}$=8.4 Hz), 126.3 (dd, C_{meta} adjacent to t-Bu, $^1J_{CH}$=154.2 Hz, $^2J_{CH}$=8.0 Hz), 119.1 (dd, C_{para}, $^1J_{CH}$=154.2 Hz, $^2J_{CH}$=8.4 Hz), 35.1 (s, $C(CH_3)_3$), 34.5 (td, C_2H_4, $^1J_{CH}$=153 Hz $^2J_{PC}$=4.2 Hz), 30.0(qsept, $C(CH_3)_3$, $^1J_{HH}$=125.5 Hz), 15.9 (q, PMe_3, $^1J_{PC}$=128.9 Hz).

Residual diethylether was not removed by prolonged exposure to vacuum.

Elemental analysis for $Mo(N_2P_2C_{28}H_{48}(Et_2O)_{0.25}$: found 4.66% N, 59.42% C, 8.90% H. (calculated 4.76% N, 59.11% C, 8.65% H)

Infrared data (Nujol, CsI, cm^{-1}): 1585 m, 1415 s, 1355 w, 1320 w, 1295 s, 1275 s, 1260 s, 1234 m, 1205 w, 1162 m, 1155 w, 1120 w, 1080 mbr, 1040 s, 1020 sbr, 948 s, 930 s, 902 w, 885 w, 848 w, 800 sbr, 748 s, 730 w, 665 w, 638 w, 578 w, 502 w, 458 m, 390 w, 375 w.

The strong absorbance at 1415 cm^{-1} was assigned to the C=C stretch.

Mass spectrum: (EI) m/z 149 (RNH_2), 134, 106, 76 (PMe_3), 61, 60.

6.3.3 Synthesis of $Mo(N\text{-}2,6\text{-}C_6H_3\text{-}i\text{-}Pr_2)(N\text{-}t\text{-}Bu)(PMe_3)(C_2H_4)$

$Mo(N\text{-}2,6\text{-}i\text{-}Pr_2C_6H_3)(N\text{-}t\text{-}Bu)Cl_2.DME$ (0.499g, 0.99 mmol) was treated with ethylmagnesium chloride (1.0 mL, 2.0M in Et_2O, 2.0 mmol) and trimethylphosphine (0.25 ml, xs 2.4 mmol) according to the method described in Section 6.3.1.

When warmed to -78°C, the solution was clear orange, and on reaching room temperature the mixture had become an opaque green. After 30 minutes at room temperature the mixture became red. The reaction was left stirring for a further 3 h with no further changes apparent.

Filtration yielded a red filtrate and pale precipitate, this was washed with diethylether until the washings filtered off colourless; these were combined with the filtrate and solvent removed *in vacuo* giving an oily red material.

The material was redissolved in heptane, filtered, condensed and placed at -78°C. After 30 h solid was apparent. This was isolated by filtration and dried *in vacuo* giving an orange-red solid. Yield was 350 mg of recrystallised solid.

^{1}H nmr (293 K, C_7D_8, 400 MHz): 7.1-6.9 (m N-aryl), 3.97 (sept, 2, $CH(CH_3)_2$, 2.0-1.4 (br, 4, C_2H_4), 1.30 (s, 9, $C(CH_3)_3$), 1.26 (d, $CH(CH_3)_2$ $^3J_{HH}$= 6.9 Hz), 1.09 (d, 9, PMe_3, $^2J_{PH}$=9.2 Hz).

^{13}C nmr (293 K, C_7D_8, 100 MHz): 154.0 (s, C_{ipso}), 142.4 (s, C_{ortho}), 122.7 (d, C_{para}, $^1J_{CH}$=158.3 Hz), 122.3 (dddd, C_{meta}, $^1J_{CH}$=154.0 Hz $^3J_{CHmeta}$=5.6 Hz $^3J_{CH\text{-}i\text{-}Pr}$=12.4 Hz $^2J_{CH}$=1.1 Hz), 66.6 (s, $C(CH_3)_3$), 33.2 (qsept, $C(CH_3)_3$, $^1J_{CH}$=126.2 Hz $^3J_{CH}$=4.2 Hz), 28.0 (dm, $CH(CH_3)_2$, $^1J_{CH}$=130.8 Hz),23.6 (qm, $CH(CH_3)_2$, $^1J_{CH}$=125,1 Hz), 18.22 (qd, PMe_3, $^1J_{CH}$=129.7 Hz $^1J_{PC}$=29.0 Hz).

^{1}H nmr (213 K, C_7D_8, 400 MHz): 7.1- 6.9 (m N-aryl), 4.03 (sept, 2, $CH(CH_3)_2$,.2.66 (br t, 1, C_2H_4), 2.27 (br t, 1, C_2H_4), 1.50 (m, C_2H_4), 1.36 (s, 9, $C(CH_3)_3$), 1.32 (d, $CH(CH_3)_2$ $^3J_{HH}$= 6.4 Hz), 0.92 ((d, 9, PMe_3, $^2J_{PH}$=9.2 Hz). In addition there is a signal at ca. 1.3 ppm which may be the fourth ethylene proton; a low temperature homonuclear decoupling experiment with the triplet at 2.66 ppm affected the signal at 1.50 ppm, verifying their coupling, however a similar experiment with the 2.27 ppm signal gave no significant effect at 1.3 ppm owing to masking by the t-butyl resonance.

^{1}H nmr (363 K, C_7D_8, 400 MHz): 7.10- 6.9 (m N-aryl), 4.03 (sept, 2, $CH(CH_3)_2$), 1.70 (broad C_2H_4)1.28 (s, 9, $C(CH_3)_3$), 1.22 (d, $CH(CH_3)_2$ $^3J_{HH}$= 6.4 Hz), 1.16 (d, 9, PMe_3, $^2J_{PH}$=9.2 Hz).

A high temperature proton decoupled carbon spectrum was run in an attempt to see one ethylene carbon resonance, however none was observable at +60°C.

$^{13}C\{^1H\}$ NMR (223 K, C_7D_8, 125.8 MHz, -70°C): 153.6 (C_{ipso}), 142.81 (C_{ortho}), 122.8 (C_{para}), 122.5 (C_{meta}), 66.7 ($C(CH_3)_3$), 35.6 (C_2H_4, $^2J_{PC}$~10 Hz), 33.1 ($C(CH_3)_3$), 27.9 ($CH(CH_3)_2$), 27.3 (C_2H_4), 24.0 ($CH(CH_3)_2$), 23.4 ($CH(CH_3)_2$), 17.58 (P*Me*$_3$, $^1J_{PC}$=29.0 Hz).

Elemental Analysis: no satisfactory elemental analyses were obtained owing to the lability of the ethylene ligand.

Infrared data (Nujol, CsI, cm^{-1}): 1582 w, 1560 w, 1470 m, 1422 s, 1355 s, 1338 s, 1285 s, 1260 m, 1230 sbr, 1160 w, 1140 s, 1138s, 1110 s, 1100 s, 1058 m, 1045 m, 1020 w, 965 sh, 950 sbr, 895 m, 870 m, 850 m, 803 s, 761 s, 737 s, 674 s, 625 m, 580 m, 575 m, 548 w, 515 w, 452 s, 440 s, 378 m, 360 s.

6.3.4 Magnesium Reductions.

$Mo(N\text{-}2\text{-}C_6H_4\text{-}t\text{-}Bu)_2Cl_2.DME + Mg + 2\ PMe_3$

An ampoule was charged with oven dried magnesium turnings (0.052g, 2.14 mmol, 10% excess) and $Mo(N\text{-}2\text{-}C_6H_4\text{-}t\text{-}Bu)_2Cl_2.DME$ (1.075g, 1.95 mmol). Subsequently, ca. 50 mL THF solvent and trimethylphosphine (0.45 mL, 4.35 mmol, >2 equiv) were condensed onto the solids at -196°C.

The mixture was warmed to room temperature, the colour changing from dark red to green-brown. The ampoule was filled with nitrogen and left stirring for 20h, after which time the solution had become dark green.

THF was removed *in vacuo* giving a dark green solid which was dried *in vacuo* for 5h.

The product was extracted into pentane (ca. 100 mL) and isolated from insoluble $MgCl_2$ by filtration. Solvent was removed from the filtrate under reduced pressure leaving a dark green solid.

^1H nmr (C_6D_6 250 MHz): 7.32 (d, 2, imido H), 7.1 (d, imido H), 6.74 (2t, 4, imido H), 1.61 (s, 20, $C(CH_3)_3$), 1.10 (s br, 30 PMe_3 $\nu_{1/2}$ =32 Hz).

Impurities in the spectrum were not removed by further recrystallisations, thus no further analysis was carried out on this compound.

Mo(N Adamantyl)$_2$Cl$_2$.DME. + Mg + 2 PMe$_3$

This reaction was attempted using a method analogous to that employed above. On all occasions the product obtained was intractable.

6.4 Experimental Details to Chapter Four.

6.4.1 Preparation of Mo(N-2-t-BuC$_6$H$_4$)$_2$(Ph)$_2$(PMe$_3$)

An ampoule was charged with solid phenylmagnesium chloride (2.7 mL at 2.0M in THF, 5.4 mmol dried *in vacuo* overnight) and Mo(N-2-t-BuC$_6$H$_4$)$_2$Cl$_2$.DME (1.50 g, 2.72 mmol). Diethylether was added at room temperature giving an orange opaque solution. The solution was frozen to -196°C and the ampoule evacuated, trimethylphosphine (0.60 mL, 5.8 mmol) was condensed onto the solid. The ampoule was sealed and warmed to -78°C with stirring giving a dark opaque solution. On warming to room temperature, the solution became dark green, with some solid material present. After 20h at room temperature the mixture was dark green with a pale precipitate.

Filtration afforded a dark green filtrate and solids which were washed with 2x10 mL portions of diethylether. Washings and filtrate were combined and solvent removed under reduced pressure affording a dark green solid. Yield was 1.396 g (83%).

Red cubic crystals were obtained from a dark green saturated pentane solution at -40°C over 2 days.

^{1}H nmr (293 K, C_6D_6, 400 MHz): 7.77 (d, 4, PhH_{ortho}, $^3J_{HH}$=7.6 Hz), 7.76 (d, 2, NR H_{ortho} $^3J_{HH}$=7.2 Hz), 7.21 (t, 4, PhH_{meta}, $^3J_{HH}$=7.6 Hz), 7.18 (dd, NR H_{meta} $^3J_{HH}$=7.6 Hz, $^4J_{HH}$=1.6 Hz), 7.09 (t, PhH_{para}, $^3J_{HH}$=7.6 Hz), 6.83 (t, NR $H_{meta'}$, $^3J_{HH}$=7.2 Hz), 6.78 (td, NR H_{para}, $^3J_{HH}$=7.4 Hz, $^4J_{HH}$=1.4 Hz), 1.47 (s, 18, C(CH_3)$_3$), 0.60 (d, 9, PMe_3, $^1J_{PH}$= 7.4 Hz).

^{13}C nmr (293 K, C_6D_6, 100.6 MHz): 174.3 (s, Ph C_{ipso}), 155.7 (s, NR C_{ipso}), 139.5 (s, NR C_{ortho}), 136.7 (s, C-t-Bu), 136.7 (dm, $^1J_{CH}$=156 Hz), 129.7 (dd, $^1J_{CH}$=168 Hz), 127.8 (dd, $^1J_{CH}$=161 Hz $^3J_{CH}$=7.2 Hz), 127.0 (dd, $^1J_{CH}$=~150 Hz $^3J_{CH}$=8.4 Hz), 125.7 (d, $^1J_{CH}$=160 Hz), 124.8 (dd, $^1J_{CH}$=160 Hz), 35.7 (s, imido C(CH_3)$_3$, 30.5 (q, imido C(CH_3)$_3$, $^1J_{CH}$=125.7 Hz), 12.6 (qd, P(CH_3)$_3$, $^1J_{PC}$=18.3 Hz $^1J_{CH}$=131 Hz)

Elemental analysis for $MoN_2PC_{35}H_{45}$: found 4.31% N, 67.97% C, 7.67% H. (calculated 4.51% N, 67.72% C, 7.32% H)

Infrared data (Nujol, CsI, cm^{-1}): 1582 w, 1570 w, 1565 w, 1310 s, 1305 sh, 1287 w, 1280 w, 1265 m, 1240 m, 1165 w, 1155 w, 1130 sh, 1090 m, 1060 w, 1050 m, 1015 m, 1010 sh, 995 w, 975 sh, 965 s, 955 s, 940 sh, 895 w, 865 w, 850 w, 815 sh, 800 brm, 755 s, 750 w, 730s, 725 s, 700s, 695 sh, 665 w, 600 w, 565 w, 535 w, 520 w, 485 w, 475 w, 450 w.

Mass spectrum: (EI) m/z 154, 150, 134, 106, 94, 77 (PMe_3H^+ or C_6H_5), 65.

6.4.2 Preparation of $Mo(N\text{-}2,6\text{-}i\text{-}Pr_2C_6H_3)(N\text{-}t\text{-}Bu)(Ph)_2(PMe_3)$

$Mo(N\text{-}2,6\text{-}i\text{-}Pr_2C_6H_3)(N\text{-}t\text{-}Bu)Cl_2$.DME (0.503 g, 1.00 mmol) was reacted with solid phenylmagnesium chloride (1.0ml at 2.0M in THF, 2.0 mmol dried *in vacuo* overnight) and trimethylphosphine (0.2 mL, 2.0 mmol) using the method described in Section 6.4.1.

On warming to -78°C the solution was clear deep red and on reaching room temperature the mixture became opaque green. No further change occurred in 20h.

Solvent was removed *in vacuo* giving dark brown and yellow solids. The product was extracted into pentane as a dark brown-red solution, leaving yellow solids behind. Solvent was removed *in vacuo* giving a dark brown solid. This solid was recrystallised from pentane at -40°C in 2 days as tan-pink crystals.

^1H nmr (293 K, C_6D_{12}, 400 MHz): 7.55 (d, 4, PhH_{ortho}, $^3J_{HH}$=6.80 Hz), 7.10 (t, 4, PhH_{meta}, $^3J_{HH}$=7.60 Hz), 6.98 (t, 2, PhH_{para}, $^3J_{HH}$=7.60 Hz), 6.74 (d, 2, aryl H_{meta}, $^3J_{HH}$=7.60 Hz), 6.64 (t, 1, aryl H_{para}, $^3J_{HH}$=7.60 Hz), 3.29 (sept, 2, $CH(CH_3)_2$, $^3J_{HH}$=6.40 Hz), 1.42 (s, 9, $C(CH_3)_3$), 0.80 (d, 9, PMe_3, $^1J_{PH}$= 7.60 Hz), 0.68 (d, 12, $CH(CH_3)_2$, $^3J_{HH}$=6.80 Hz).

^{13}C nmr (293 K, C_6D_{12}, 100.6 MHz): 174.5 (s, Ph C_{ipso}), 153.7 (s, Naryl C_{ipso}), 142.3(s, Naryl C_{ortho}), 138.3 (d, Ph C_{ortho}, $^1J_{CH}$=155.6 Hz), 127.4 (dd, Ph C_{meta}, $^1J_{CH}$=156.4 Hz $^2J_{CH}$=6.8 Hz), 125 4 (dt, Ph C_{para}, $^1J_{CH}$=159.0 Hz $^2J_{CH}$=7.2 Hz), 123.1 (d, Ar C_{meta}, $^1J_{CH}$=158 7 Hz), 122 4 (ddd, Ar C_{para}, $^1J_{CH}$=154.5 Hz $^2J_{CH}$=6.1 Hz $^4J_{CH}$=4.9 Hz), 72.0 (s, $C(CH_3)_3$), 31.8 (qsept, $C(CH_3)_3$, $^1J_{CH}$=127.2 Hz, $^4J_{CH}$=4.1 Hz), 28.2 (dm, $CH(CH_3)_2$, $^1J_{CH}$=122.8 Hz), 23.9 (qm, $CH(CH_3)_2$, $^1J_{CH}$=125.5 Hz $^3J_{CH}$=4.9 Hz), 14.5 (qd, PMe_3, $^1J_{PC}$=16.8 Hz, $^1J_{CH}$=129.6 Hz).

Elemental analysis for $MoN_2PC_{31}H_{45}$: found 4.75% N, 64.60% C, 7.89% H. (calculated 4.89% N, 65.00% C, 7.94% H)

Infrared data (Nujol, CsI, cm^{-1}): 1565 w, 1360 m, 1340 s, 1315 w, 1290 sh, 1280 m ,1260 w, 1245 w, 1210 s, 1200 sh, 1175 w, 1155 w, 1120 m, 1110 sh, 1100 w, 1060 w, 1055 w, 1040 w, 1015 m ,990 m, 970 m, 950 s, 895 w, 845 w, 805 m, 790 w, 750 s, 730 sh, 725 s, 700 s, 610 m, 515 w.

Mass spec.: (CI) envelope centred at m/z 499 $[M^+]$-PMe_3 m/z 77 $[HPMe_3]^+$ or C_6H_5.

6.5 Experimental Details to Chapter Five.

6.5.1 Preparation of $Mo(NAd)_2(PMe_3)(PhC{\equiv}CPh)$.

Owing to difficulties in extracting the ethylene adduct (Section 6.3.3), this synthesis involves carrying out the ligand substitution step *in situ*.

Yellow solid $Mo(NAd)_2Cl_2$.DME (0.521 g, 0.94 mmol) was placed in an ampoule with ca. 150 mL diethyl ether, giving a yellow solution; this was frozen to -196°C and evacuated. Trimethylphosphine (0.20 mL; 1.88 mmol) was condensed on, and the ampoule filled with nitrogen. A solution of ethylmagnesium chloride (0.94 mL; 2.0 M in Et_2O) was syringed onto the frozen mixture, and the nitrogen pressure adjusted to 1 atomsphere.

On warming to room temperature with stirring the mixture became opaque and tan in colour. After 4 hours the mixture was unchanged and volatiles were removed *in vacuo* to yield pale yellow solids.

UNIV DUNELM

A solution of diphenylacetylene (0.167 g, 0.94 mmol) in ca. 150 mL heptane was added via cannula. The ampoule was sealed and heated to 70°C with stirring for 3 days; during this time the mixture became opaque brown. Filtration yielded pale brown solids and clear red filtrate; this was concentrated and placed at -40°C. A quantity of brown crystalline material was isloated by filtration after 2 days. The filtrate was concentrated and placed at -40°C, affording further crystalline material.

^{1}H nmr (C_6D_{12}, 400 MHz): 7.62 (d, 2, Ph H_{ortho}, $^3J_{HH}$=6.8 Hz), 7.19 (t, 2, Ph $H_{meta'}$, $^3J_{HH}$=8.0 Hz), 7.14 (t, 2, Ph H_{meta}, $^3J_{HH}$=7.6 Hz), 7.03 (t, 1, Ph H_{para}, $^3J_{HH}$=7.6 Hz), 6.96 (t, 1, Ph $H_{para'}$, $^3J_{HH}$=8.0 Hz), 6.93 (d, 2, Ph $H_{ortho'}$, $^3J_{HH}$=6.8 Hz), 2.00 (s, 6, Ad H_γ), 1.77 (s, 12, Ad H_β), 1.61 (dd, 12, Ad H_δ), 1.45 (d, 9, P*Me*$_3$, $^2J_{PH}$=9.60 Hz).

^{13}C nmr (C_6D_{12}, 100.6 MHz): 153.1 (s, *acetylenic cis*, $^2J_{PC}$=19 Hz), 149.3 (s, *acetylenic trans* , $^2J_{PC}$=5 Hz), 148.9 (s, Ph C_{ipso} *trans*, $^3J_{PC}$=2 Hz), 137.6 (s, Ph C_{ipso} *cis*, $^3J_{PC}$=3 Hz), 132.4 (dd, Ph C_{ortho}, $^1J_{CH}$=158.9 Hz $^3J_{CH}$=6.8 Hz), 128.5 (dd, Ph $C_{meta'}$, $^1J_{CH}$=154.9 Hz $^3J_{CH}$=7.24 Hz), 128.0 (dd, Ph C_{meta}, $^1J_{CH}$=158.9 Hz $^3J_{CH}$=7.64 Hz), 127.1 (d, Ph C_{para}, $^1J_{CH}$=155.6 Hz), 125.6 (d, Ph $C_{ortho'}$, $^1J_{CH}$=157.1 Hz), 123.2 (d, Ph $C_{para'}$, $^1J_{CH}$=160.9 Hz), 66.57 (s, Ad C_α), 48.4 (t, Ad C_β, $^1J_{CH}$=128.9 Hz), 37.4 (t, Ad C_δ, $^1J_{CH}$=127.8 Hz), 31.2 (d, Ad C_γ, $^1J_{CH}$=131.3 Hz), 20.3 (qd, P*Me*$_3$, $^1J_{CH}$=129.7 Hz, $^1J_{PC}$=27.5 Hz).

Elemental analysis for $MoN_2PC_{37}H_{49}$: found 4.48% N, 68.31% C, 7.48% H (calculated 4.32% N, 68.51% C, 7.61% H).

Infrared data (Nujol, CsI, cm^{-1}): 1725 m, 1590 w, 1340 m, 1305 s, 1300 sh, 1282 m, 1255 s, 1245 sh, 1210 sh, 1200 s, 1172 w, 1130 w, 1090 s, 1060 w, 1020 m, 950 s, 940 sh, 920 w, 910 w, 880 w, 840 w, 810 m, 800 w, 790 sh, 760 m, 755 m, 730 w, 710 w, 690 w, 682 s, 410 wbr, 360 w.

Mass spectrum: (EI) m/z 178 (PhC≡CPh), 94, 71, 57; (CI) m/z 152 ($AdNH_3^+$), 110, 93, 77(PMe_3H^+).

6.5.2 Preparation of Mo(N-2,6-i-$Pr_2C_6H_3$)(N-t-Bu)(PhC≡CPh)(PMe_3).

An ampoule was charged with Mo(N-2,6-i-$Pr_2C_6H_3$)(N-t-Bu)(C_2H_4)(PMe_3) (138.6 mg, 0.31 mmol) and diphenylacetylene (55.3 mg, 0.31 mmol); heptane (ca. 50 ml) was added giving a clear deep purple solution which was heated to 65°C with stirring for 5 days.

On heating to 60°C with stirring for 10 d the solution became golden in colour, and some golden brown solid sublimed on the walls of the vessel. Cooling to room temperature afforded yellow needles; these were isolated by filtration and vacuum dried. The filtrate was placed at -40°C and yielded further needles.

^1H nmr (293 K, C_6D_{12}, 400 MHz): 7.62 (d, 2, Ph H_{ortho}, $^3J_{HH}$=7.2 Hz), 7.24 (t, 2, Ph $H_{meta'}$, $^3J_{HH}$=8.0 Hz), 7.14 (t, 2, Ph H_{meta}, $^3J_{HH}$=7.6 Hz), 7.04 (t, 2, Ph H_{para} & $H_{para'}$, $^3J_{HH}$=7.2 Hz), 7.02 (d, 2, Ph $H_{ortho'}$, $^3J_{HH}$=8.0 Hz), 6.84 (2d, 2, Ar H_{meta}, $^3J_{HH}$=8.0 & 7.2 Hz), 6.68 (dd, 1, Ar H_{para}, $^3J_{HH}$=8.6 & 6.8 Hz), 3.94 (sept, 2, $CH(CH_3)_2$, $^3J_{HH}$=3.9 Hz), 1.44 (d, 9, PMe_3, $^1J_{PH}$= 9.6 Hz), 1.34 (s, 9, $C(CH)_3$), 1.40 (d, 6, $CH(CH_3)_2$, $^3J_{HH}$=6.8 Hz), 0.94 (d, 6, $CH(CH_3)_2$, $^3J_{HH}$=6.8 Hz).

NOEs observed in proton spectrum:

1.44 ppm (P*Me*$_3$) : 7.62 ppm & 7.03 ppm.

7.62 ppm (Ph*H*$_0$) : large negative response at 7.02 ppm (d, Ph*H*$_{0'}$)

: positive response at 7.24 ppm and 7.14 ppm (two Ph*H*$_m$).

^{13}C nmr (293 K, C_6D_{12}, 100.6 MHz): 153.6 (s, Ar C_{ipso}), 152.3 (s, Ph C_{ipso} cis), 148.3 (s, *acetylenic* cis), 143.5 (s, imido C_{ortho}), 136.6 (s, Ph C_{ipso} trans), 132.1 (d, Ph C_{ortho}, $^1J_{CH}$=159.8 Hz), 128.7 (d, Ph $C_{meta'}$, $^1J_{CH}$=155.2 Hz), 128.2 (d, Ph C_{meta}, $^1J_{CH}$=157.9 Hz), 127.5 (d, Ph C_{para}, $^1J_{CH}$=150.9 Hz), 125.9 (d, Ph $C_{ortho'}$, $^1J_{CH}$=156.8 Hz), 124.7 (d, Ph C_{para}, $^1J_{CH}$=161.3 Hz), 122.3 (d, Ar C_{meta}, $^1J_{CH}$=154.5 Hz), 124.0 (d, Ar C_{para}, $^1J_{CH}$=158.3 Hz), 67.8 (s, $C(CH)_3$), 33.7 (q, $C(CH)_3$ $^1J_{CH}$=125.2 Hz) 28.1 (d, $CH(CH_3)_2$, $^1J_{CH}$=132.0 Hz), 23.8 (q, $CH(CH_3)_2$, $^1J_{CH}$=125.2) Hz, 18.6 (qd, P*Me*$_3$, $^1J_{CH}$=129.7 Hz, $^1J_{PC}$=28.2 Hz).

^{13}C nmr (293 K, C_6D_6, 100.6 MHz): 153.6 (s, Ar C_{ipso}), 153.3 (s, *acetylenic cis*, $^2J_{PC}$=18.7 Hz), 152.3 (s, Ph C_{ipso} *trans*, $^3J_{PC}$=2.7 Hz), 147.7 (s, *acetylenic trans*, $^2J_{PC}$=4.9 Hz), 143.3 (s, imido C_{ortho}), 136.4 (s, Ph C_{ipso} *cis*, $^3J_{PC}$=3.1 Hz), 131.9, 128.7, 128.2, 127.5, 125.9, 124.7, 122.3, 124.0, 67.6 ($C(CH)_3$), 33.5 ($C(CH)_3$), 27.8 ($CH(CH_3)_2$), 23.7 ($CH(CH_3)_2$) Hz, 18.1 (d, P*Me*$_3$).

Elemental analysis for $MoN_2PC_{33}H_{45}$: found 4.32% N, 66.63% C, 7.89% H (calculated 4.70% N, 66.43% C, 7.62% H).

Infrared data (Nujol, CsI, cm^{-1}): 1725 w, 1582 w, 1350 w, 1330 m, 1280 m, 1258 m, 1230 s, 1208 w, 1170 w, 1150 w, 1120 w, 1095 wbr, 1065 w, 1015 mbr, 975 m, 952 s, 908 w, 890 w, 840 w, 800 sbr, 768 s, 760 s, 750 w, 745 w, 738 w, 720w, 700 s, 670 w, 590 w, 540 w, 500 w, 440 w, 400 w.

Mass spectrum: (EI) m/z 178 (PhC≡CPh), 162, 120, 77 (PMe_3H^+), 69.

6.5.3 $Mo(N\text{-}2\text{-}t\text{-}BuC_6H_4)_2(PhC{\equiv}CPh)(PMe_3)$.

$Mo(N\text{-}2\text{-}t\text{-}BuC_6H_4)_2(C_2H_4)(PMe_3)_2$ (150.6 mg, 0.264 mmol) was reacted with diphenylacetylene (47.1 mg, 0.264 mmol) in heptane (ca. 50 ml) using the method described in section 6.5.2.

After 18h at this temperature the initially purple solution became blue-green and yellow solid sublimed on the walls of the vessel. After 5d the reaction mixture was cooled to room temperature, and further yellow solid was apparent in the green-red dichroic solution. Further heptane was added to redissolve the yellow solid, the solution was filtered, and solvent removed *in vacuo* giving a bright yellow solid.

The solid was dissolved in diethylether as a green red dichroic solution, filtered, condensed and placed at -40°C. After 2d yellow needles were present. These were isolated by filtration, the filtrate being further condensed and cooled to yield further solid.

^1H nmr (293 K, C_6D_{12}, 400 MHz): 7.49 (d, 2, imido H_{ortho}, $^3J_{HH}$=7.60 Hz), 7.35 (br d, 4, Ph H_{ortho}, $^3J_{HH}$=6.0 Hz), 7.20 (t, 4, Ph H_{meta}, $^3J_{HH}$=7.6 Hz), 7.12 (d, 2, imido $H_{meta'}$, $^3J_{HH}$=7.6 Hz), 7.06 (t, 2, Ph H_{para}, $^3J_{HH}$=7.6 Hz), 7.01 (t, 2, imido H_{meta}, $^3J_{HH}$=7.6 Hz), 6.82 (t, 2, imido H_{para}, $^3J_{HH}$=7.2 Hz), 1.39 (d, 9, PMe_3, $^1J_{PH}$= 8 Hz), 1.31 (s, 18, $C(CH_3)_3$).

NOE observed between t-butyl resonance and resonance at 7.12 ppm.

^{13}C nmr (293 K, C_6D_{12}, 100.6 MHz): 157.6 (s, imido C_{ipso}), 154.5 (s, *acetylenic*), 142.8 (s, imido $C_{ortho'}$), 141 (s broad Ph C_{ipso}), 133.3 (dd, imido C_{ortho}, $^1J_{CH}$=156.0 Hz), 129 (br d, Ph C_{ortho}, $^1J_{CH}$=150 Hz), 128.6 (dd, Ph C_{meta}, $^1J_{CH}$=158Hz), 126.5 (dd, Ph C_{para}, $^1J_{CH}$=159Hz), 126.4 (dd, imido C_{meta}, $^1J_{CH}$=159 Hz), 126.0 (dd, imido $C_{meta'}$, $^1J_{CH}$=151 Hz), 124.6 (dd,

imido C_{para}, $^1J_{CH}$=151 Hz), 36.1 (s, $C(CH_3)_3$), 30.1 (q, $C(CH_3)_3$, $^1J_{CH}$=130.0 Hz), 17.0 (qd, P*Me*$_3$, $^1J_{PC}$=28.3 Hz, $^1J_{CH}$=125.4Hz).

^{1}H nmr (293 K, C_6D_6, 400 MHz): 7.81 (d), 7.57 (br d), 7.27 (t), 7.17 (t), 7.15 (t), 7.01 (t), 6.93 (t), 1.03 (d), 1.46 (s).

^{13}C nmr (293 K, C_6D_6, 100.6 MHz): 157.1 (s, imido C_{ipso}), 154.6 (s, *acetylinic)*, 142.4 (s, imido C_{ortho}), 133.3 (dd), 131.7 (d), 128.6 (dd), 126.2 (dd), 126.6 (d), 124.5 (d), 35.5 (s), 29.7 (q, $C(CH_3)_3$, $^1J_{CH}$=125.4 Hz), 16.1 (qd, P*Me*$_3$, $^1J_{PC}$=28.7 Hz, $^1J_{CH}$=130.2 Hz).

Elemental analysis for $MoN_2PC_{37}H_{45}$: found 4.14% N, 68.63% C, 7.36% H (calculated 4.35% N, 68.92% C, 7.05% H).

Infrared data (Nujol, CsI, cm^{-1}): 1735 m, 1592 w, 1580 w, 1315 m, 1300 sh, 1292 s, 1265 s, 1250 w, 1155 w, 1085 s br, 1070 m, 1048 s, 1020 sbr, 968 s, 952 s, 920 w, 905 w, 860 w, 840 w, 800 s br, 760 s, 700 s, 695 sh, 580 w, 560 w, 552 w, 525 w, 450 m, 400 w.

Mass spectrum: (EI) envelope centred at m/z 646 [M$^+$], m/z 460-469 [M$^+$] - PhC≡CPh, m/z 388 [M$^+$] - PhC≡CPh - PMe$_3$.

6.6 References.

1. W. Wolfsberg, H. Schmidbaur, *Synth. React. Inorg. Metal-Org. Chem.*, 1974, **4**, 149.

2. H.H. Fox, K.B. Yap, J. Robbins, S. Cai, R.R. Schrock, *Inorg. Chem.*, 1992, **31**, 2287.

APPENDICES.

Appendix One. Crystal Data for $Mo(NAd)(O)Cl_2.DME$.

Crystal data: $C_{14}H_{25}Cl_2MoNO_3$, M=422.19. Monoclinic, space group $P2_1/c$ (14), a=10.357(2), b=12.426(2), c=13.357(2) Å, α=90, β=94.92(1), γ=90°, V=1735.6(6) $Å^3$, D_c=1.616 gcm^{-3}, m(Mo-Ka)=1.07 mm^{-1}, F(000)=864, Z=4, T=150K, Rigaku AFC6S diffractometer, graphite monochromated Mo-Kα X-radiation (λ= 0.71073 Å). Full-matrix least-squares refinement of 190 parameters, using 3391 reflections with $F_0>3s(F_0)$ converged at $R(R_w)$=0.0254 (0.0227)

Atomic coordinates and equivalent isotropic atomic displacement parameters ($Å^2$) for $Mo(NAd)(O)Cl_2.DME$

Atom	x/a	y/b	z/c	U(eq)
Mo(1)	0.21195(1)	0.17599(1)	0.89051(1)	0.0167
Cl(1)	0.34279(4)	0.32183(4)	0.95836(3)	0.0221
Cl(2)	0.12350(4)	0.05058(4)	0.76875(4)	0.0252
O(1)	0.2539(1)	0.0871(1)	0.9840(1)	0.0275
N(1)	0.0647(2)	0.2265(1)	0.9180(1)	0.0228
C(1)	-0.0575(2)	0.2528(1)	0.9547(1)	0.0169
C(2)	-0.1669(2)	0.2291(2)	0.8734(1)	0.0260
C(3)	-0.0571(2)	0.3740(1)	0.9802(1)	0.0190
C(4)	-0.0788(2)	0.1869(2)	1.0484(1)	0.0224
C(5)	-0.2974(2)	0.2602(2)	0.9118(2)	0.0263
C(6)	-0.1879(2)	0.4040(2)	1.0176(2)	0.0235
C(7)	-0.2098(2)	0.2178(2)	1.0854(1)	0.0241
C(8)	-0.2967(2)	0.3804(2)	0.9369(2)	0.0280
C(9)	-0.2088(2)	0.3381(2)	1.1106(2)	0.0278
C(10)	-0.3189(2)	0.1939(2)	1.0044(2)	0.0248
C(11)	0.1740(2)	0.3891(2)	0.7435(1)	0.0258
O(12)	0.2290(1)	0.2819(1)	0.74872(9)	0.0199
C(13)	0.3552(2)	0.2807(2)	0.7116(1)	0.0226
C(14)	0.4027(2)	0.1665(2)	0.7154(1)	0.0235
O(15)	0.4029(1)	0.1311(1)	0.81696(9)	0.0197
C(16)	0.4586(2)	0.0259(2)	0.8314(2)	0.0259

Atomic coordinates and isotropic atomic displacement parameters ($Å^2$)

for the hydrogen atoms in $Mo(NAd)(O)Cl_2.DME$

Atom	x/a	y/b	z/c	U(iso)
H(21)	-0.1671	0.1539	0.8574	0.0319
H(22)	-0.1535	0.2705	0.8153	0.0319
H(31)	0.0111	0.3889	1.0309	0.0233
H(32)	-0.0437	0.4153	0.9221	0.0233
H(41)	-0.0106	0.2021	1.0991	0.0280
H(42)	-0.0785	0.1115	1.0329	0.0280
H(51)	-0.3665	0.2457	0.8617	0.0329
H(61)	-0.1886	0.4793	1.0333	0.0297
H(71)	-0.2243	0.1767	1.1435	0.0303
H(81)	-0.3785	0.3999	0.9603	0.0365
H(82)	-0.2830	0.4214	0.8786	0.0365
H(91)	-0.2901	0.3577	1.1346	0.0370
H(92)	-0.1398	0.3527	1.1608	0.0370
H(101)	-0.4008	0.2127	1.0279	0.0309
H(102)	-0.3186	0.1186	0.9883	0.0309
H(111)	0.0900	0.3879	0.7686	0.0317
H(112)	0.2296	0.4374	0.7827	0.0317
H(113)	0.1658	0.4130	0.6758	0.0317
H(131)	0.4136	0.3256	0.7522	0.0282
H(132)	0.3494	0.3065	0.6445	0.0282
H(141)	0.4889	0.1630	0.6944	0.0297
H(142)	0.3461	0.1219	0.6731	0.0297
H(161)	0.4569	0.0053	0.8997	0.0328
H(162)	0.5466	0.0269	0.8142	0.0328
H(163)	0.4095	-0.0250	0.7901	0.0328

Anisotropic atomic displacement parameters ($Å^2$) for

$Mo(NAd)(O)Cl_2.DME$

Atom	U(11)	U(22)	U(33)	U(23)	U(13)	U(12)
Mo(1)	0.01720(7)	0.01498(7)	0.01938(8)	-0.00067(5)	0.00481(5)	0.00134(5)
Cl(1)	0.0238(2)	0.0217(2)	0.0220(2)	-0.0048(2)	-0.0016(2)	0.0004(2)
Cl(2)	0.0243(2)	0.0215(2)	0.0343(2)	-0.0070(2)	0.0022(2)	-0.0050(2)
O(1)	0.0377(8)	0.0227(7)	0.0257(7)	0.0029(5)	0.0059(6)	0.0036(6)
N(1)	0.0210(7)	0.0209(8)	0.0305(8)	-0.0056(6)	0.0067(6)	-0.0026(6)
C(1)	0.0145(7)	0.0167(8)	0.0208(8)	-0.0014(6)	0.0035(6)	-0.0004(6)
C(2)	0.030(1)	0.029(1)	0.0217(9)	-0.0032(7)	-0.0023(7)	-0.0060(8)
C(3)	0.0183(8)	0.0149(8)	0.0269(9)	-0.0017(7)	0.0049(7)	-0.0024(6)
C(4)	0.0196(8)	0.0229(9)	0.0282(9)	0.0079(7)	0.0020(7)	0.0030(7)
C(5)	0.0193(9)	0.032(1)	0.034(1)	0.0043(8)	-0.0064(7)	-0.0059(8)
C(6)	0.0217(9)	0.0165(8)	0.042(1)	-0.0018(8)	0.0113(8)	0.0011(7)
C(7)	0.0238(9)	0.0268(9)	0.0252(9)	0.0062(7)	0.0068(7)	-0.0004(7)
C(8)	0.0181(9)	0.029(1)	0.053(1)	0.017(1)	0.0024(9)	0.0047(8)
C(9)	0.028(1)	0.034(1)	0.031(1)	-0.0062(9)	0.0145(8)	-0.0015(8)
C(10)	0.0187(8)	0.0213(9)	0.043(1)	0.0044(8)	0.0051(8)	-0.0043(7)
C(11)	0.033(1)	0.0197(9)	0.028(1)	0.0021(7)	-0.0023(8)	0.0063(8)
O(12)	0.0207(6)	0.0174(6)	0.0219(6)	0.0006(5)	0.0011(5)	0.0009(5)
C(13)	0.0251(9)	0.0242(9)	0.0213(9)	0.0015(7)	0.0065(7)	-0.0040(7)
C(14)	0.0263(9)	0.0267(9)	0.0217(8)	-0.0014(7)	0.0092(7)	0.0016(7)
O(15)	0.0190(6)	0.0190(6)	0.0224(6)	-0.0015(5)	0.0038(5)	0.0024(5)
C(16)	0.0273(9)	0.0213(9)	0.035(1)	-0.0024(8)	0.0033(8)	0.0086(7)

Selected bond lengths (Å) and angles (°) for $Mo(NAd)(O)Cl_2.DME$

Bond Lengths (Å)	
Mo(1) - Cl(1)	2.3979(4)
Mo(1) - Cl(2)	2.3928(5)
Mo(1) - O(1)	1.708(1)
Mo(1) - N(1)	1.719(2)
N(1) - C(1)	1.436(2)
C(1) - C(2)	1.539(2)
C(1) - C(3)	1.545(2)
C(1) - C(4)	1.542(2)
C(2) - C(5)	1.538(3)
C(3) - C(6)	1.532(2)
C(4) - C(7)	1.535(3)
C(5) - C(8)	1.532(3)
C(5) - C(10)	1.533(3)
C(6) - C(8)	1.529(3)
C(6) - C(9)	1.533(3)
C(7) - C(9)	1.534(3)
C(7) - C(10)	1.534(3)
Mo(1) - O(12)	2.346(1)
Mo(1) - O(15)	2.356(1)
C(11) - O(12)	1.448(2)
O(12) - C(13)	1.440(2)
C(13) - C(14)	1.502(3)
C(14) - O(15)	1.444(2)
O(15) - C(16)	1.436(2)

Bond Angles (°)	
Cl(1) - Mo(1) - Cl(2)	157.88(2)
Cl(1) - Mo(1) - O(1)	96.04(5)
Cl(1) - Mo(1) - N(1)	97.14(5)
Cl(1) - Mo(1) - O(12)	79.04(3)
Cl(1) - Mo(1) - O(15)	82.74(3)
Cl(2) - Mo(1) - O(1)	98.48(5)
Cl(2) - Mo(1) - N(1)	95.28(5)
Cl(2) - Mo(1) - O(12)	81.54(3)
Cl(2) - Mo(1) - O(15)	80.81(3)
O(1) - Mo(1) - O(12)	159.54(6)
O(1) - Mo(1) - O(15)	89.48(6)
O(1) - Mo(1) - N(1)	104.45(7)
N(1) - Mo(1) - O(12)	95.89(6)
N(1) - Mo(1) - O(15)	165.98(6)
O(12) - Mo(1) - O(15)	70.27(4)
Mo(1) - N(1) - C(1)	169.2(1)
N(1) - C(1) - C(2)	109.0(2)
N(1) - C(1) - C(3)	108.3(1)
N(1) - C(1) - C(4)	110.9(1)
C(2) - C(1) - C(3)	109.5(1)
C(2) - C(1) - C(4)	109.8(1)
C(3) - C(1) - C(4)	109.4(1)
C(1) - C(2) - C(5)	109.0(2)
C(1) - C(3) - C(6)	109.0(1)
C(1) - C(4) - C(7)	109.2(1)
C(2) - C(5) - C(8)	109.4(2)
C(2) - C(5) - C(10)	109.6(2)
C(8) - C(5) - C(10)	109.9(2)
C(3) - C(6) - C(8)	109.6(2)
C(3) - C(6) - C(9)	109.4(2)
C(8) - C(6) - C(9)	109.7(2)
C(4) - C(7) - C(9)	109.1(2)
C(4) - C(7) - C(10)	109.7(2)
C(9) - C(7) - C(10)	109.8(2)
C(5) - C(8) - C(6)	109.6(2)
C(6) - C(9) - C(7)	109.7(2)
C(5) - C(10) - C(7)	109.3(1)
Mo(1) - O(12) - C(11)	119.9(1)
Mo(1) - O(12) - C(13)	114.4(1)
C(11) - O(12) - C(13)	110.9(1)
O(12) - C(13) - C(14)	107.6(1)
C(13) - C(14) - O(15)	107.1(1)
Mo(1) - O(15) - C(14)	113.5(1)
Mo(1) - O(15) - C(16)	120.0(1)
C(14) - O(15) - C(16)	112.0(1)

Selected bond lengths (Å) and angles (°) for $Mo(NAd)(O)Cl_2.DME$

Bond Lengths (Å)	
Mo(1) - Cl(1)	2.3979(4)
Mo(1) - Cl(2)	2.3928(5)
Mo(1) - O(1)	1.708(1)
Mo(1) - N(1)	1.719(2)
N(1) - C(1)	1.436(2)
C(1) - C(2)	1.539(2)
C(1) - C(3)	1.545(2)
C(1) - C(4)	1.542(2)
C(2) - C(5)	1.538(3)
C(3) - C(6)	1.532(2)
C(4) - C(7)	1.535(3)
C(5) - C(8)	1.532(3)
C(5) - C(10)	1.533(3)
C(6) - C(8)	1.529(3)
C(6) - C(9)	1.533(3)
C(7) - C(9)	1.534(3)
C(7) - C(10)	1.534(3)
Mo(1) - O(12)	2.346(1)
Mo(1) - O(15)	2.356(1)
C(11) - O(12)	1.448(2)
O(12) - C(13)	1.440(2)
C(13) - C(14)	1.502(3)
C(14) - O(15)	1.444(2)
O(15) - C(16)	1.436(2)

Bond Angles (°)	
Cl(1) - Mo(1) - Cl(2)	157.88(2)
Cl(1) - Mo(1) - O(1)	96.04(5)
Cl(1) - Mo(1) - N(1)	97.14(5)
Cl(1) - Mo(1) - O(12)	79.04(3)
Cl(1) - Mo(1) - O(15)	82.74(3)
Cl(2) - Mo(1) - O(1)	98.48(5)
Cl(2) - Mo(1) - N(1)	95.28(5)
Cl(2) - Mo(1) - O(12)	81.54(3)
Cl(2) - Mo(1) - O(15)	80.81(3)
O(1) - Mo(1) - O(12)	159.54(6)
O(1) - Mo(1) - O(15)	89.48(6)
O(1) - Mo(1) - N(1)	104.45(7)
N(1) - Mo(1) - O(12)	95.89(6)
N(1) - Mo(1) - O(15)	165.98(6)
O(12) - Mo(1) - O(15)	70.27(4)
Mo(1) - N(1) - C(1)	169.2(1)
N(1) - C(1) - C(2)	109.0(2)
N(1) - C(1) - C(3)	108.3(1)
N(1) - C(1) - C(4)	110.9(1)
C(2) - C(1) - C(3)	109.5(1)
C(2) - C(1) - C(4)	109.8(1)
C(3) - C(1) - C(4)	109.4(1)
C(1) - C(2) - C(5)	109.0(2)
C(1) - C(3) - C(6)	109.0(1)
C(1) - C(4) - C(7)	109.2(1)
C(2) - C(5) - C(8)	109.4(2)
C(2) - C(5) - C(10)	109.6(2)
C(8) - C(5) - C(10)	109.9(2)
C(3) - C(6) - C(8)	109.6(2)
C(3) - C(6) - C(9)	109.4(2)
C(8) - C(6) - C(9)	109.7(2)
C(4) - C(7) - C(9)	109.1(2)
C(4) - C(7) - C(10)	109.7(2)
C(9) - C(7) - C(10)	109.8(2)
C(5) - C(8) - C(6)	109.6(2)
C(6) - C(9) - C(7)	109.7(2)
C(5) - C(10) - C(7)	109.3(1)
Mo(1) - O(12) - C(11)	119.9(1)
Mo(1) - O(12) - C(13)	114.4(1)
C(11) - O(12) - C(13)	110.9(1)
O(12) - C(13) - C(14)	107.6(1)
C(13) - C(14) - O(15)	107.1(1)
Mo(1) - O(15) - C(14)	113.5(1)
Mo(1) - O(15) - C(16)	120.0(1)
C(14) - O(15) - C(16)	112.0(1)

Appendix Two.

First Year Induction Courses

The course consists of a series of lectures on the services available in the Department of Chemistry.

1. Postgraduate Studies.
2. Safety Matters.
3. Glassblowing Techniques.
4. Electrical Appliances.
5. Departmental Computing.
6. Chromatography and High Pressure Operations.
7. Elemental Analyses.
8. Mass Spectrometry.
9. Nuclear Magnetic Resonance.
10. University Library Guide to Reader Services.

Examined Lecture Courses (1992-93).

Each course consisted of six one hour lectures followed by a written examination.

1. "Synthetic Methodology in Organometallic and Coordination Chemistry." Prof. D Parker and Dr. V.C. Gibson.
2. "Experimental Methods in X-ray Crystallography." Prof. J.A.K. Howard and Dr. R. Richards.
3. "Synthetic Polymers." Prof. W.J. Feast.

Research Colloquia, Seminars and Lectures Organised by the Department of Chemistry During 1992-93.

* - Indicates attendance by the author.

October 15	Dr M. Glazer & Dr. S. Tarling, Oxford University & Birbeck College, London "It Pays to be British! - The Chemist's Role as an Expert Witness in Patent Litigation."
October 20	*Dr. H. E. Bryndza, Du Pont Central Research "Synthesis, Reactions and Thermochemistry of Metal (Alkyl) Cyanide Complexes and Their Impact on Olefin Hydrocyanation Catalysis."
October 22	*Prof. A. Davies, University College London *The Ingold-Albert Lecture* "The Behaviour of Hydrogen as a Pseudometal."
October 28	Dr. J. K . Cockcroft, University of Durham "Recent Developments in Powder Diffraction."
October 29	*Dr. J. Emsley, Imperial College, London "The Shocking History of Phosphorus."
November 4	*Dr. T. P. Kee, University of Leeds "Synthesis and Co-ordination Chemistry of Silylated Phosphites."
November 5	*Dr. C. J. Ludman, University of Durham "Explosions, A Demonstration Lecture."
November 11	Prof. D. Robins, Glasgow University "Pyrrolizidine Alkaloids : Biological Activity, Biosynthesis and Benefits."
November 12	Prof. M. R. Truter, University College, London "Luck and Logic in Host - Guest Chemistry."
November 18	*Dr. R. Nix, Queen Mary College, London "Characterisation of Heterogeneous Catalysts."
November 25	Prof. Y. Vallee. University of Caen "Reactive Thiocarbonyl Compounds."

November 25	Prof. L. D. Quin, University of Massachusetts, Amherst "Fragmentation of Phosphorous Heterocycles as a Route to Phosphoryl Species with Uncommon Bonding."
November 26	Dr. D. Humber, Glaxo, Greenford "AIDS - The Development of a Novel Series of Inhibitors of HIV."
December 2	Prof. A. F. Hegarty, University College, Dublin "Highly Reactive Enols Stabilised by Steric Protection."
December 2	*Dr. R. A. Aitken, University of St. Andrews "The Versatile Cycloaddition Chemistry of $Bu_3P.CS_2$."
December 3	Prof. P. Edwards, Birmingham University "The SCI Lecture - What is Metal?"
December 9	Dr. A. N. Burgess, ICI Runcorn "The Structure of Perfluorinated Ionomer Membranes."
January 20	Dr. D. C. Clary, University of Cambridge "Energy Flow in Chemical Reactions."
January 21	*Prof. L. Hall, Cambridge "NMR - Window to the Human Body."
January 27	*Dr. W. Kerr, University of Strathclyde "Development of the Pauson-Khand Annulation Reaction : Organocobalt Mediated Synthesis of Natural and Unnatural Products."
January 28	*Prof. J. Mann, University of Reading "Murder, Magic and Medicine."
February 3	Prof. S. M. Roberts, University of Exeter "Enzymes in Organic Synthesis."
February 10	Dr. D. Gillies, University of Surrey "NMR and Molecular Motion in Solution."
February 11	*Prof. S. Knox, Bristol University *The Tilden Lecture* "Organic Chemistry at Polynuclear Metal Centres."
February 17	Dr. R. W. Kemmitt, University of Leicester "Oxatrimethylenemethane Metal Complexes."

February 18	Dr. I. Fraser, ICI Wilton "Reactive Processing of Composite Materials."
February 22	Prof. D. M. Grant, University of Utah "Single Crystals, Molecular Structure, and Chemical-Shift Anisotropy."
February 24	Prof. C. J. M. Stirling, University of Sheffield "Chemistry on the Flat-Reactivity of Ordered Systems."
March 10	*Dr. P. K. Baker, University College of North Wales, Bangor "Chemistry of Highly Versatile 7-Coordinate Complexes."
March 11	*Dr. R. A. Y. Jones, University of East Anglia "The Chemistry of Wine Making."
March 17	Dr. R. J. K. Taylor, University of East Anglia "Adventures in Natural Product Synthesis."
March 24	Prof. I. O. Sutherland, University of Liverpool "Chromogenic Reagents for Cations."
May 13	Prof. J. A. Pople, Carnegie-Mellon University, Pittsburgh, USA *The Boys-Rahman Lecture* Applications of Molecular Orbital Theory.'
May 21	*Prof. L. Weber, University of Bielefeld "Metallo-phospha Alkenes as Synthons in Organometallic Chemistry."
June 1	Prof. J. P. Konopelski, University of California, Santa Cruz "Synthetic Adventures with Enantiomerically Pure Acetals."
June 2	*Prof. F. Ciardelli, University of Pisa Chiral Discrimination in the Stereospecific Polymerisation of Alpha Olefins."
June 7	Prof. R. S. Stein, University of Massachusetts "Scattering Studies of Crystalline and Liquid Crystalline Polymers."
June 16	Prof. A. K. Covington, University of Newcastle "Use of Ion Selective Electrodes as Detectors in Ion Chromatography."

June 17 Prof. O. F. Nielsen, H. C. Ørsted Institute, University of Copenhagen
"Low-Frequency IR - and Raman Studies of Hydrogen Bonded Liquids."

UNIV DUNELM